J.D. Woodard
Executive Vice President

Southern Nuclear Operating Company, Inc.
40 Inverness Center Parkway
P.O. Box 1295
Birmingham, Alabama 35201

Tel 205.992.5086

SOUTHERN COMPANY
Energy to Serve Your World℠

April 11, 2003

NL-03-0815

Docket Nos.: 50-348
50-364

U. S. Nuclear Regulatory Commission
ATTN: Document Control Desk
Washington, D. C. 20555-0001

Joseph M. Farley Nuclear Plant
Responses to NRC Questions on
Relaxation Request to Order EA-03-009

Ladies and Gentlemen:

NRC Order EA-03-009, issued February 11, 2003, established interim inspection requirements for reactor pressure vessel (RPV) heads at pressurized water reactors. On March 3, 2003, Southern Nuclear Operating Company (SNC) submitted an Answer to this Order. This SNC submittal included a request for relaxation of item IV.C.(1)(b)(i) of the Order with respect to performing ultrasonic testing (UT) extending to the bottom of each penetration nozzle at the Farley Nuclear Plant (FNP). This request was made because the physical configuration of the lower ends of the 4" diameter nozzles at FNP limits the extent of such examination.

Review of the SNC March 3, 2003 submittal prompted three questions from the NRC staff relating to this relaxation request. These questions and the SNC responses are provided in Enclosure 1. Enclosure 2 contains supporting Westinghouse document WCAP-15925-P, "Structural Integrity Evaluation of Reactor Vessel Upper Head Penetrations to Support Continued Operation: Farley Units 1 and 2" (Proprietary). Enclosure 3 contains the nonproprietary version of this document, WCAP-15925-NP.

As Enclosure 2 contains information proprietary to Westinghouse Electric Company, it is supported by an affidavit signed by Westinghouse, the owner of the information. The affidavit sets forth the basis on which the information may be withheld from public disclosure by the Commission and addresses with specificity the considerations listed in paragraph (b)(4) of 10 CFR 2.790 of the Commission's regulations. Accordingly, it is respectfully requested that the information which is proprietary to Westinghouse be withheld from public disclosure in accordance with 10 CFR 2.790 of the Commission's regulations. This affidavit, along with a Westinghouse authorization letter, CAW-03-1620, Proprietary Information Notice, and Copyright Notice are contained in Enclosure 4.

A101

Correspondence with respect to the copyright or proprietary aspects of the items listed above or the supporting Westinghouse affidavit should reference CAW-03-1620 and should be addressed to H. A. Sepp, Manager of Regulatory and Licensing Engineering, Westinghouse Electric Company, P. O. Box 355, Pittsburgh, Pennsylvania 15230-0355.

SNC requests approval of the subject relaxation by April 21, 2003, the currently scheduled date of completing the Farley Unit 1 reactor head inspections.

Mr. J. D. Woodard states he is an Excecutive Vice President of Southern Nuclear Operating Company, is authorized to execute this oath on behalf of Southern Nuclear Operating Company and to the best of his knowledge and belief, the facts set forth in this letter are true.

This letter contains no new NRC commitments. If you have any questions, please advise.

Respectfully submitted,

SOUTHERN NUCLEAR OPERATING COMPANY

J. D. Woodard

Sworn to and subscribed before me this 11th *day of* April, *2003.*

Notary Public

My commission expires: 9-14-06

JDW/DWD/sdl

Enclosures:
1. SNC Response to NRC Questions on Relaxation Request to Order EA-03-009 Item IV.C.(1)(b)(i)
2. WCAP-15925-P, "Structural Integrity Evaluation of Reactor Vessel Upper Head Penetrations to Support Continued Operation: Farley Units 1 and 2" (Proprietary)
3. WCAP-15925-NP, "Structural Integrity Evaluation of Reactor Vessel Upper Head Penetrations to Support Continued Operation: Farley Units 1 and 2" (Nonproprietary)
4. Westinghouse Authorization Letter, CAW-03-1620, Affidavit, Proprietary Information Notice, and Copyright Notice

cc: Southern Nuclear Operating Company
Mr. J. D. Woodard, Executive Vice President
Mr. D. E. Grissette, General Manager – Plant Farley
Document Services RTYPE: CFA04.054; LC# 13764

U. S. Nuclear Regulatory Commission
Mr. L. A. Reyes, Regional Administrator
Mr. F. Rinaldi, NRR Project Manager – Farley
Mr. T. P. Johnson, Senior Resident Inspector – Farley

Alabama Department of Public Health
Dr. D. E. Williamson, State Health Officer

Enclosure 1

Joseph M. Farley Nuclear Plant

SNC Response to NRC Questions on
Relaxation Request to Order EA-03-009 Item IV.C.(1)(b)(i)

Enclosure 1

Joseph M. Farley Nuclear Plant

SNC Response to NRC Questions on
Relaxation Request to Order EA-03-009 Item IV.C.(1)(b)(i)

1. What is the minimum distance from the bottom of the weld to the point where UT data can not be acquired in the lower portion of the nozzle?

Response to Question 1:

Figure 11 provides a cross-sectional sketch of a typical 4" diameter penetration nozzle at FNP. For the Unit 1 Spring 2003 RPV head penetration nozzle inspection, the lower limit of UT data acquisition (i.e. the lowest position of the midline of the UT transducer array) is anticipated to be approximately 1.35" above the bottom of each nozzle. Dimension "A" in Table 1 gives the distance to this point from the bottom of the weld on the downhill side for all 69 of the 4" nozzles, grouped by head intersection angle. The minimum distance case for the Unit 1 inspection occurs for the 19.8° group (nozzles #14 – 21), where UT data acquisition is expected to slightly exceed 1.0" below the bottom of the lowest point of the weld. Note that while Unit 2 penetration nozzle locations and dimensions are identical to Unit 1 (except that most lack external threads), the UT coverage extent obtainable in a future Unit 2 inspection may vary depending on the design features of the probe to be used, which has not yet been determined.

Consideration was given to performing penetrant testing (PT) and/or eddy current testing (ECT) on the portions of the nozzles not examined by UT, but it was determined that testing of all such areas would create a substantial increase in radiation dose with no significant safety benefit since flaw initiation in the unexamined areas would be of minimal safety significance, as detailed in the response to Question 2 below. ECT of nearly half the inside nozzle surface below the zone of UT examination will be performed, however, since the probe to be used for the FNP Unit 1 Spring 2003 inspection includes an ECT transducer mounted below the UT transducer array. This arrangement will provide ECT data acquisition down to where the internal taper of the nozzle causes transducer contact loss.

Table 1 - FNP Unit 1 Spring 2003 RPV Penetration Nozzle UT Exam Lower Limits

		Distance (inches) from Bottom of Weld to:		
Nozzle Numbers	Head Intersection Angle	**Lower Limit of UT Data Acquisition**	Nozzle Bottom on the:	
			Downhill Side	Uphill Side
		Dimension A	Dimension B	Dimension C
1	0°	3.94	5.29	5.29
2 - 5	8.7°	4.04	5.39	6.00
6 - 9	12.4°	3.58	4.93	5.80
10 - 13	17.6°	2.54	3.89	5.32
14 – 21	19.8°	1.09	2.44	4.33
22 – 25	25.4°	2.45	3.80	5.83
26 – 29	27.0°	2.20	3.55	5.72
30 – 37	28.6°	3.30	4.65	6.82
38 - 45	33.1°	3.09	4.44	7.03
46 – 49	37.3°	2.90	4.25	7.27
50 – 57	38.6°	2.80	4.15	7.33
58 - 61	40.0°	2.75	4.10	7.43
62 - 69	42.6°	1.56	2.91	6.57
NOTE: Above dimensions are calculated; actual values may vary due to manufacturing tolerances.				

2. In your letter dated March 3, 2003, you stated that "UT of the most highly stressed portion of the nozzle is unaffected by this limitation." Please provide the stress profiles from the stress analysis in the J-groove weld region (across the cross-section) from the top of the J-groove weld to areas below the weld.

Response to Question 2:

The hoop stress distributions, as a function of distance from the top of the weld for a range of penetration nozzle locations from the center of the RPV head to the outermost row, are provided in Figures 1 to 9. These stress profiles represent an alternate presentation of results from the analysis performed by Westinghouse for both FNP units as part of WCAP-15925-P, "Structural Integrity Evaluation of Reactor Vessel Upper Head Penetrations to Support Continued Operation: Farley Units 1 and 2." The expected zone of inspection coverage is also identified in each Figure. As shown in Figures 1 to 9, the magnitude of the stresses in the unexamined portion of the nozzles is low. The end data point is based on the stress model and not the physical end of the penetration tube.

Additionally, the hoop stress distributions across the nozzle wall thickness at the top and bottom of the attachment weld were examined to determine if there were any significant mid-wall peaks in stress higher than the stresses plotted for the tube OD & ID in Figures 1-9. The plots in Figures 12 and 13 for the downhill and uphill side, respectively, of the outermost penetration (42.6°) nozzles show only a small mid-wall peak at the bottom of the weld, but it is not significantly greater than the OD or ID stress. The relative magnitude of the hoop stress across the nozzle cross-section shown in Figures 12 and 13 is typical of those for the remaining penetration nozzles.

3. In your letter dated March 3, 2003, you also stated that, "cracks initiating in the unexamined bottom portion of the nozzle would be of minimal safety significance with respect to pressure boundary leakage or nozzle ejection, since this portion of the nozzle is several inches below the pressure boundary and any cracks would have to grow through a significant examined portion of the tube to reach the pressure boundary." Please provide technical basis, such as an analysis or an evaluation, to show that cracks initiated from the unexamined area will not propagate into the pressure boundary within one operating cycle based on conservative crack growth rate from the industry operating experience.

Response to Question 3:

Axial flaws initiated in the unexamined non-pressure boundary portion of the nozzle base material below the weld are of minimal safety significance with respect to pressure boundary leakage or nozzle ejection. The expected examination coverage from the bottom of the J-groove weld towards the bottom of the nozzle is shown in Figures 1 to 9 (See the Response to Question 2). To determine the significance of such an axial flaw located in the unexamined portion of the nozzle below the weld, a flaw tolerance approach is used. A flaw evaluation was performed postulating an axial flaw in the area of missed coverage below the weld based on Farley Unit 1 specific stresses in the nozzle penetrations. The evaluations performed are based on a methodology consistent with the recently approved Section XI flaw evaluation approach, with a Primary Water Stress Corrosion Cracking (PWSCC) crack growth rate that is consistent with the MRP-55 Rev. 1 report. A through-wall axial flaw was postulated in the nozzle material growing upwards towards the bottom of the weld. Since the stresses for the unexamined portion of the nozzle below the weld are too low (See Figures 1 to 9 in the Response to Question 2) to propagate an axial flaw, the flaw evaluations start at 0.5" below the weld and the time to propagate the flaw in the nozzle to the bottom of the weld (start of the pressure boundary portion of the nozzle material or toe of the J-groove weld) was determined. Assuming a through-wall flaw below the weld, with the flaw end located at 0.5" below the weld (which is in the area of complete UT examination coverage), an axial flaw would take approximately 5 years of operation to grow to the point of contact with the weld; and even longer to grow from the bottom of the weld upwards through the pressure boundary. This time period is significantly greater than the current inspection frequency of every refueling cycle (18 months for FNP) identified in NRC Order EA-03-009.

Figure 10 provides a graphical presentation of the above flaw evaluation discussion for the limiting penetration location. Based on the crack growth results shown in Figure 10, there are no concerns with the structural integrity of the RPV head penetration nozzles that could be caused by axial cracking in the unexamined non-pressure boundary portion of the nozzle material below the weld (See Figures 1 to 9 in the Response to Question 2) for a period of approximately 5 years of operation.

Enclosure 1

Joseph M. Farley Nuclear Plant

SNC Response to NRC Questions on
Relaxation Request to Order EA-03-009 Item IV.C.(1)(b)(i)

Figure 1
Hoop Stress Vs Distance from Top of Weld
0° CRDM Center Penetration Nozzle – Uphill and Downhill

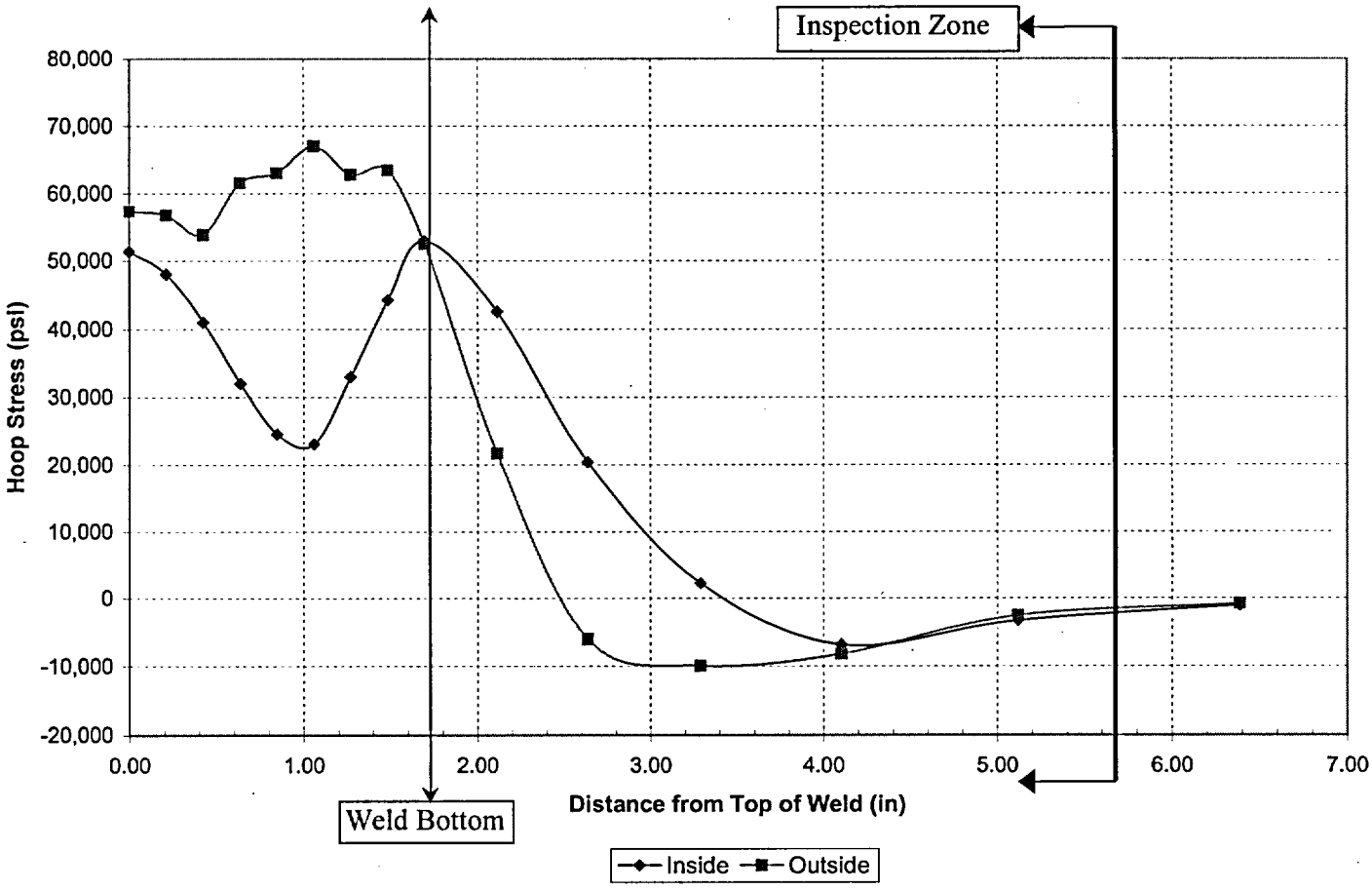

Figure 2
Hoop Stress Vs Distance from Top of Weld
28.6° CRDM Penetration Nozzle – Uphill

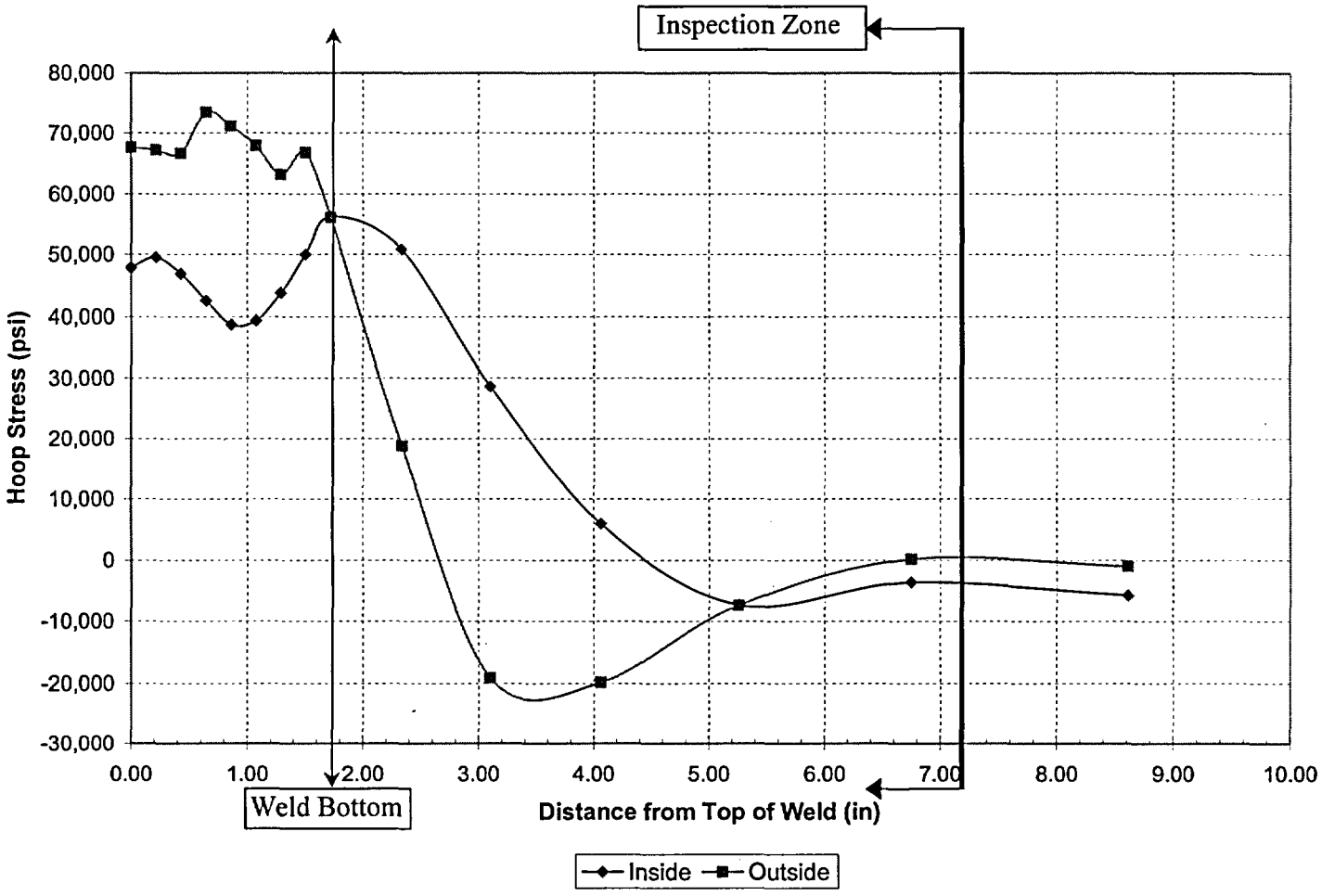

Figure 3
Hoop Stress Vs Distance from Top of Weld
28.6° CRDM Penetration Nozzle – Downhill

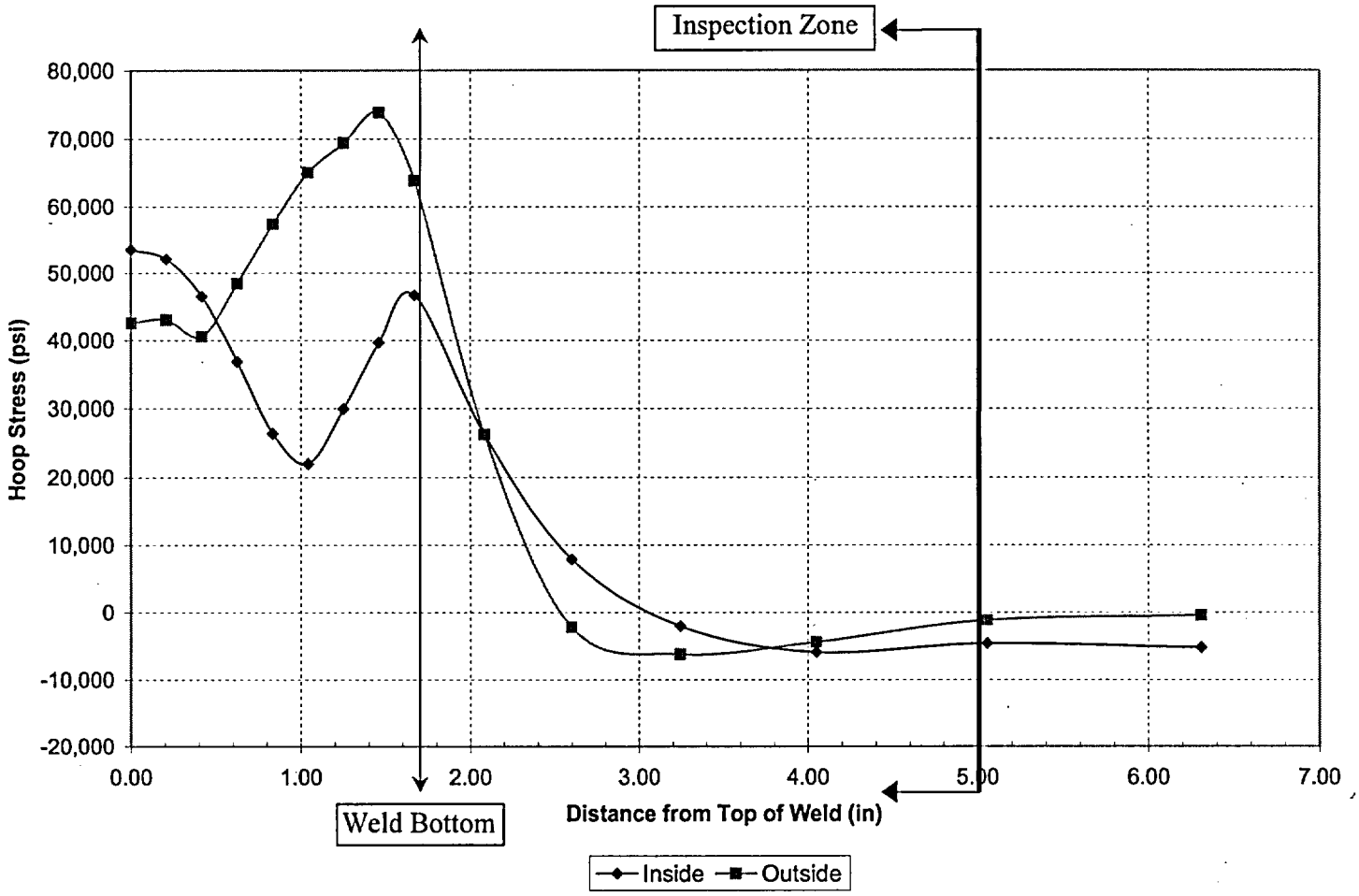

Enclosure 1

Joseph M. Farley Nuclear Plant

SNC Response to NRC Questions on
Relaxation Request to Order EA-03-009 Item IV.C.(1)(b)(i)

Figure 4
Hoop Stress Vs Distance from Top of Weld
38.6° CRDM Penetration Nozzle –Uphill

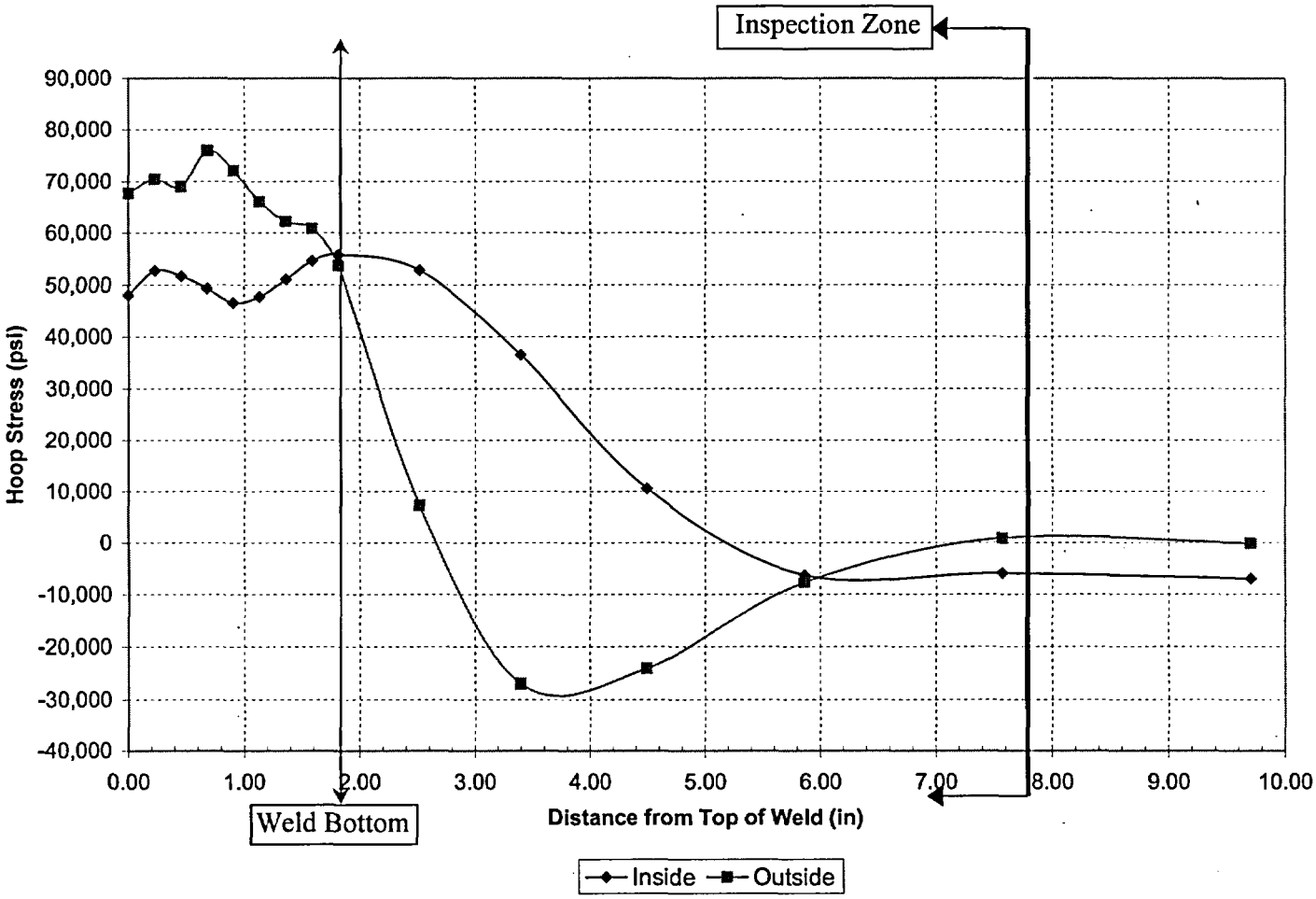

Figure 5
Hoop Stress Vs Distance from Top of Weld
38.6° CRDM Penetration Nozzle – Downhill

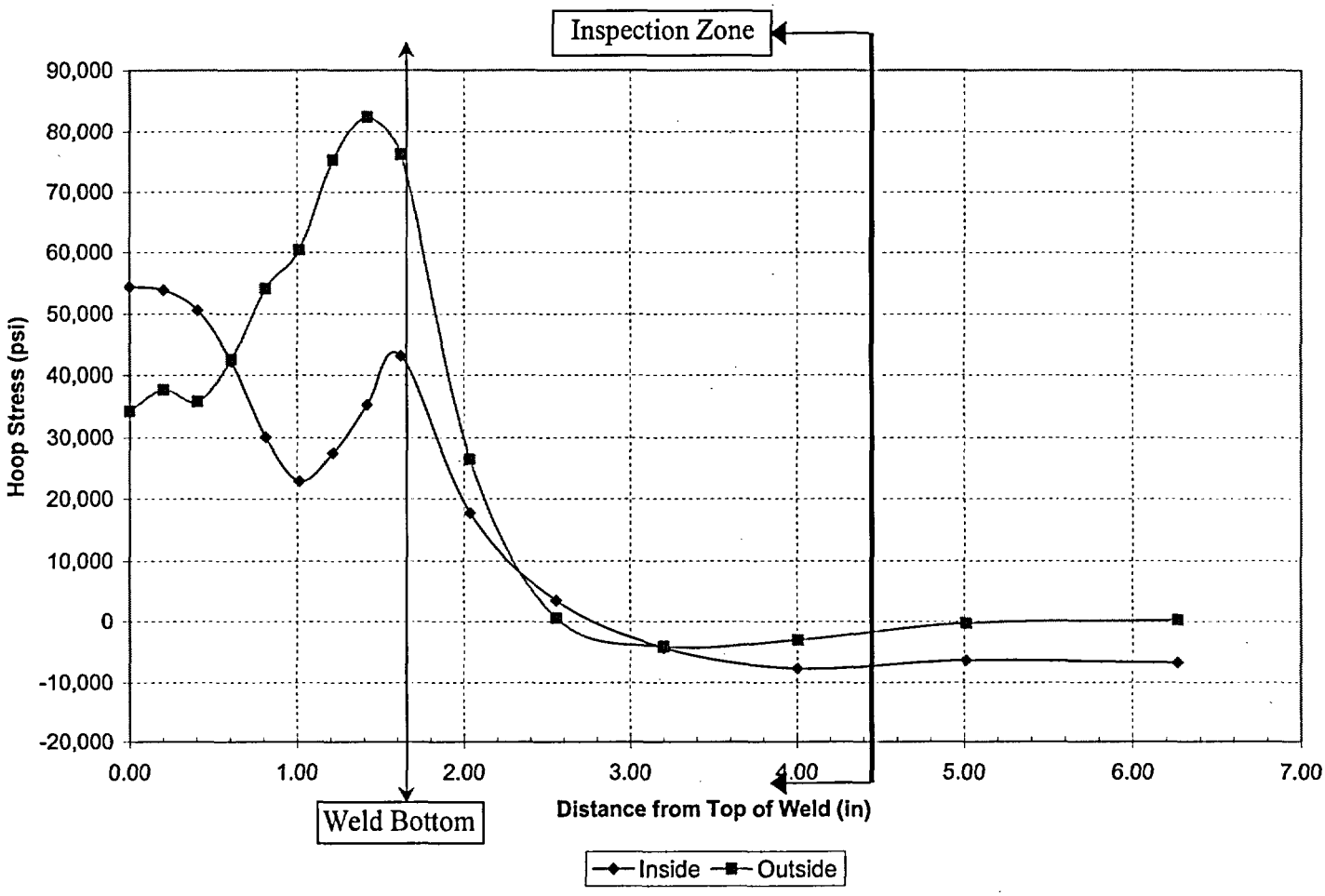

Enclosure 1

Joseph M. Farley Nuclear Plant

SNC Response to NRC Questions on
Relaxation Request to Order EA-03-009 Item IV.C.(1)(b)(i)

Figure 6
Hoop Stress Vs Distance from Top of Weld
40.0° CRDM Penetration Nozzle –Uphill

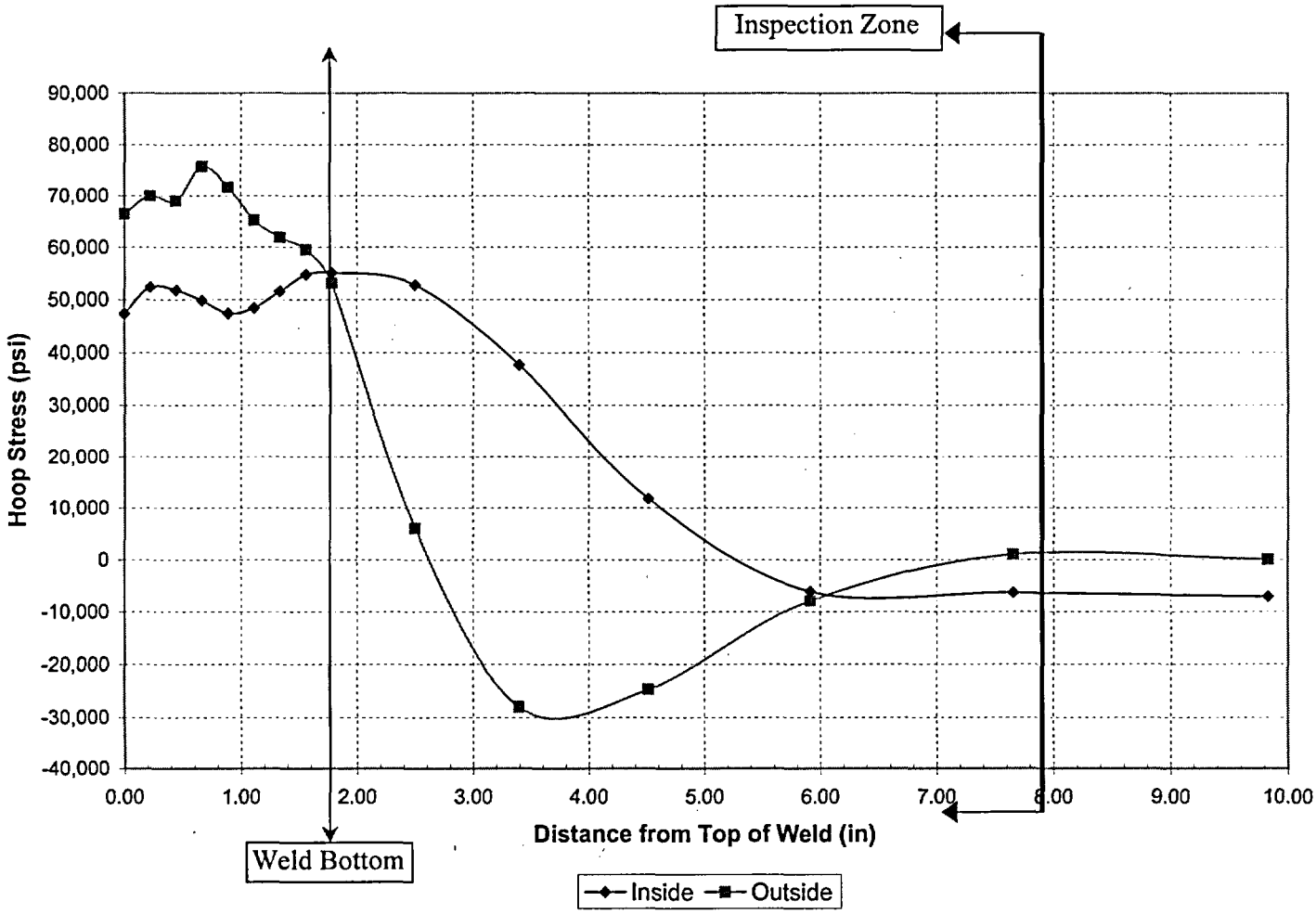

Figure 7
Hoop Stress Vs Distance from Top of Weld
40.0° CRDM Penetration Nozzle –Downhill

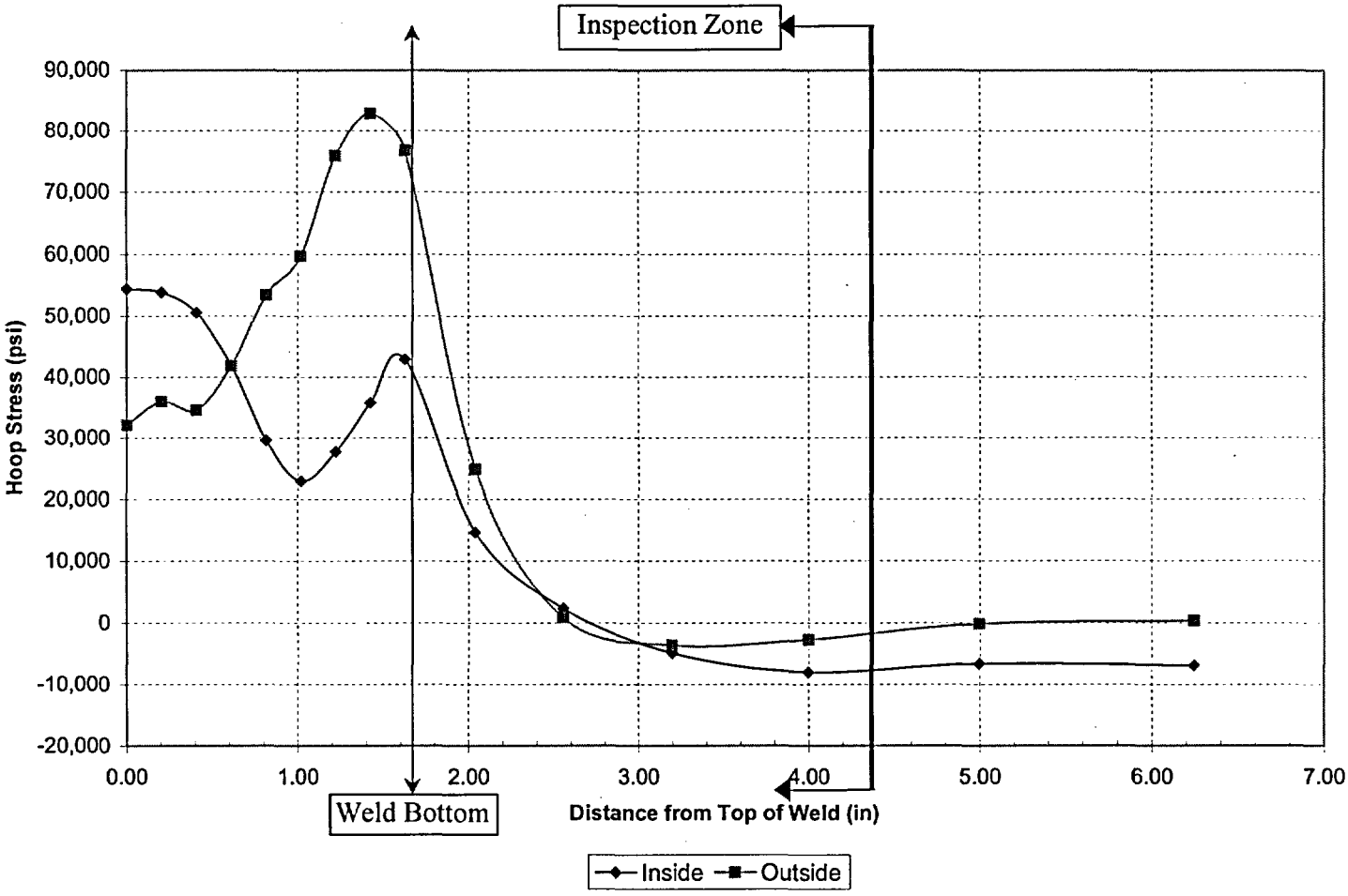

Enclosure 1

Joseph M. Farley Nuclear Plant

SNC Response to NRC Questions on
Relaxation Request to Order EA-03-009 Item IV.C.(1)(b)(i)

Figure 8
Hoop Stress Vs Distance from Top of Weld
42.6° CRDM Penetration Nozzle – Uphill

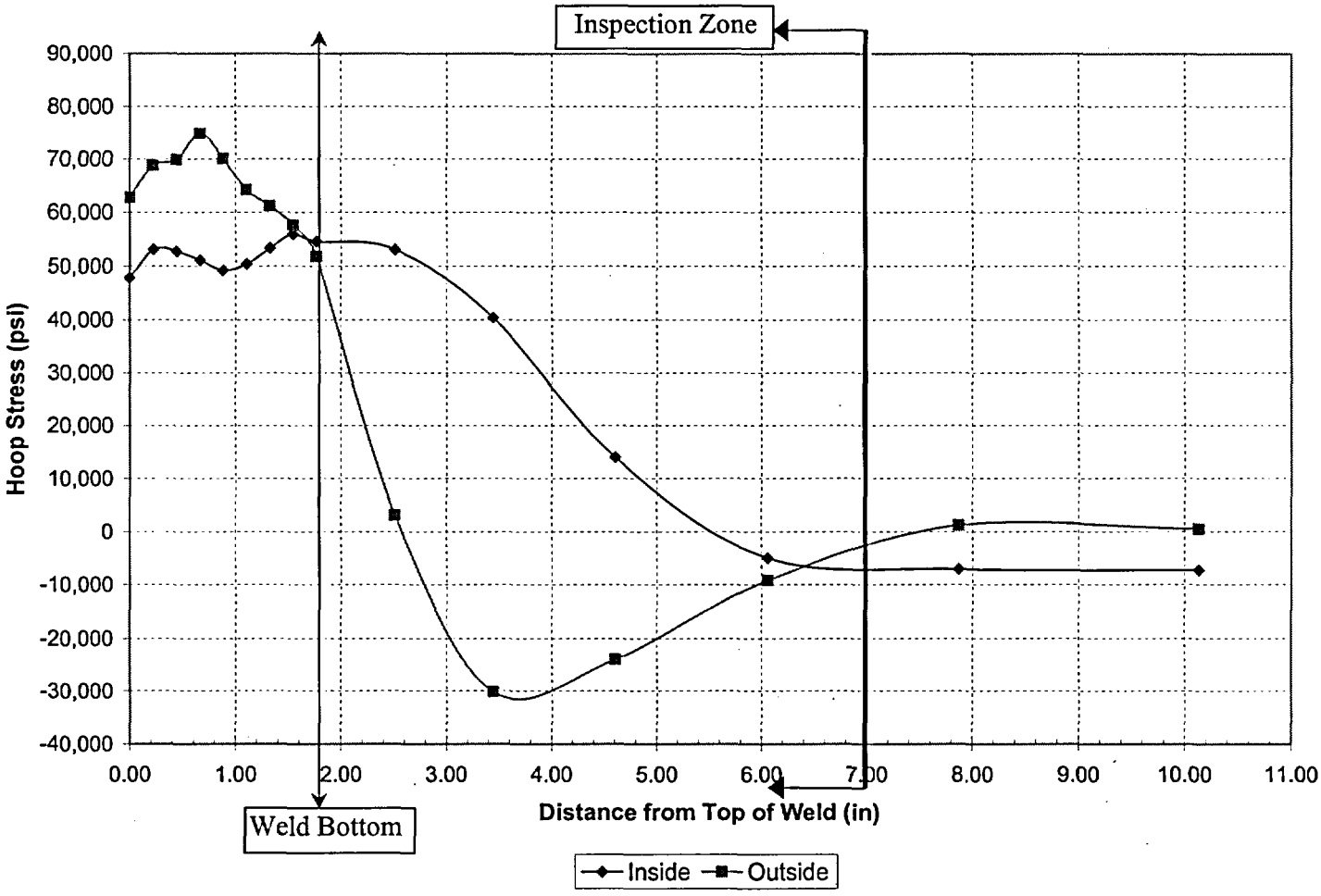

Enclosure 1

Joseph M. Farley Nuclear Plant

SNC Response to NRC Questions on
Relaxation Request to Order EA-03-009 Item IV.C.(1)(b)(i)

Figure 9
Hoop Stress Vs Distance from Top of Weld
42.6° CRDM Penetration Nozzle –Downhill

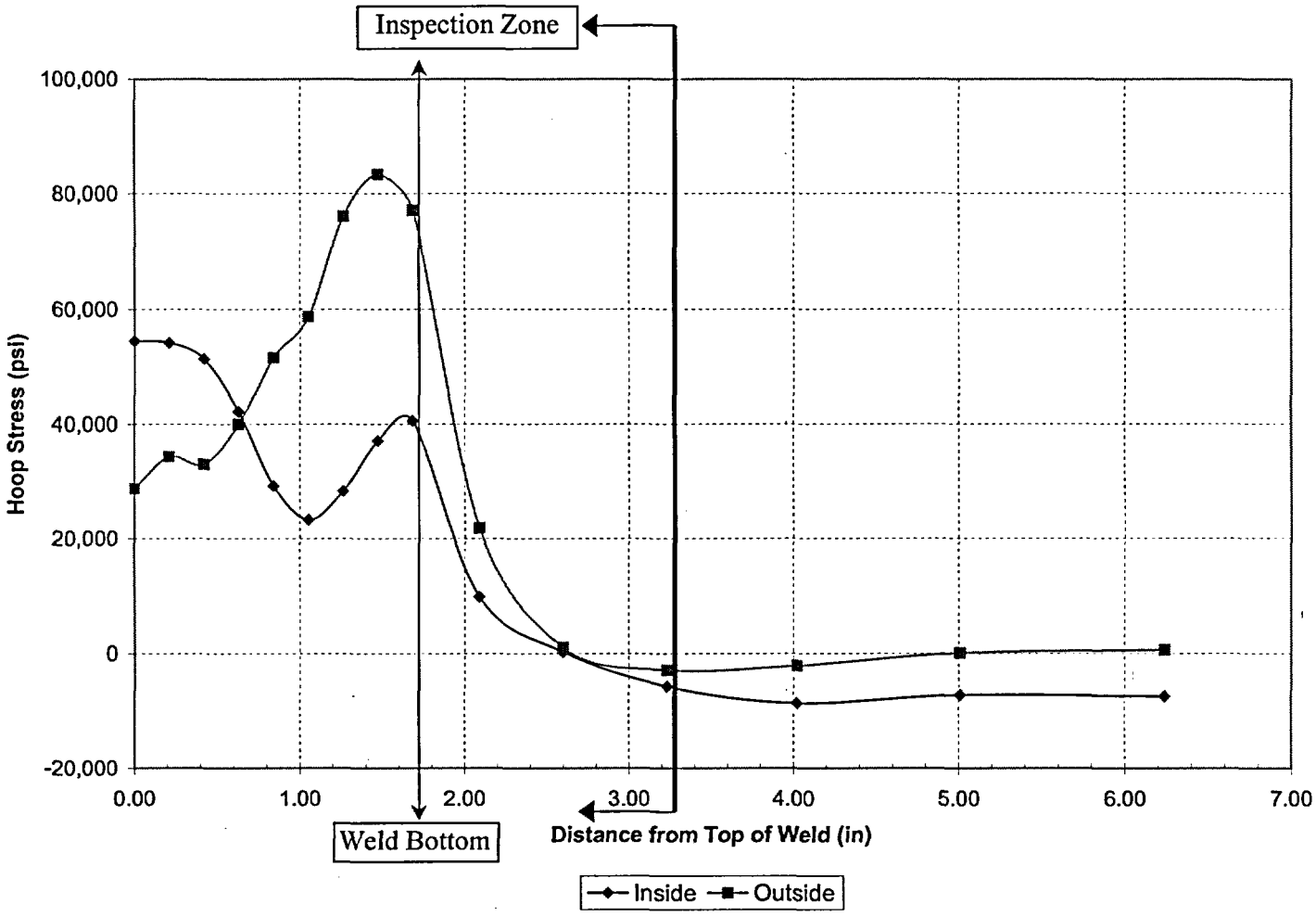

Figure 10
Through-Wall Axial Flaws Located in the 28.6 Degree Row of
Penetrations, Uphill Side - Crack Growth Predictions

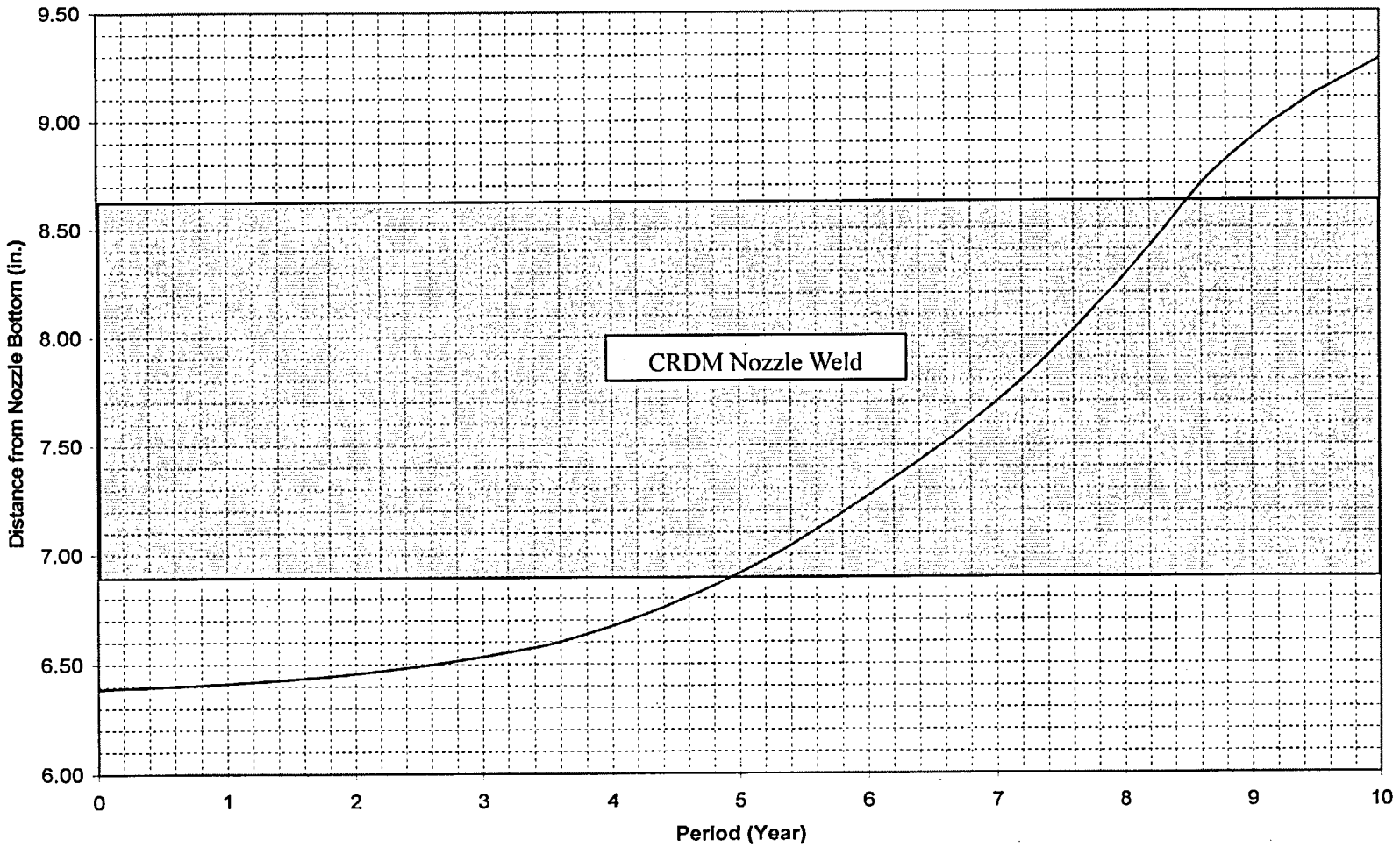

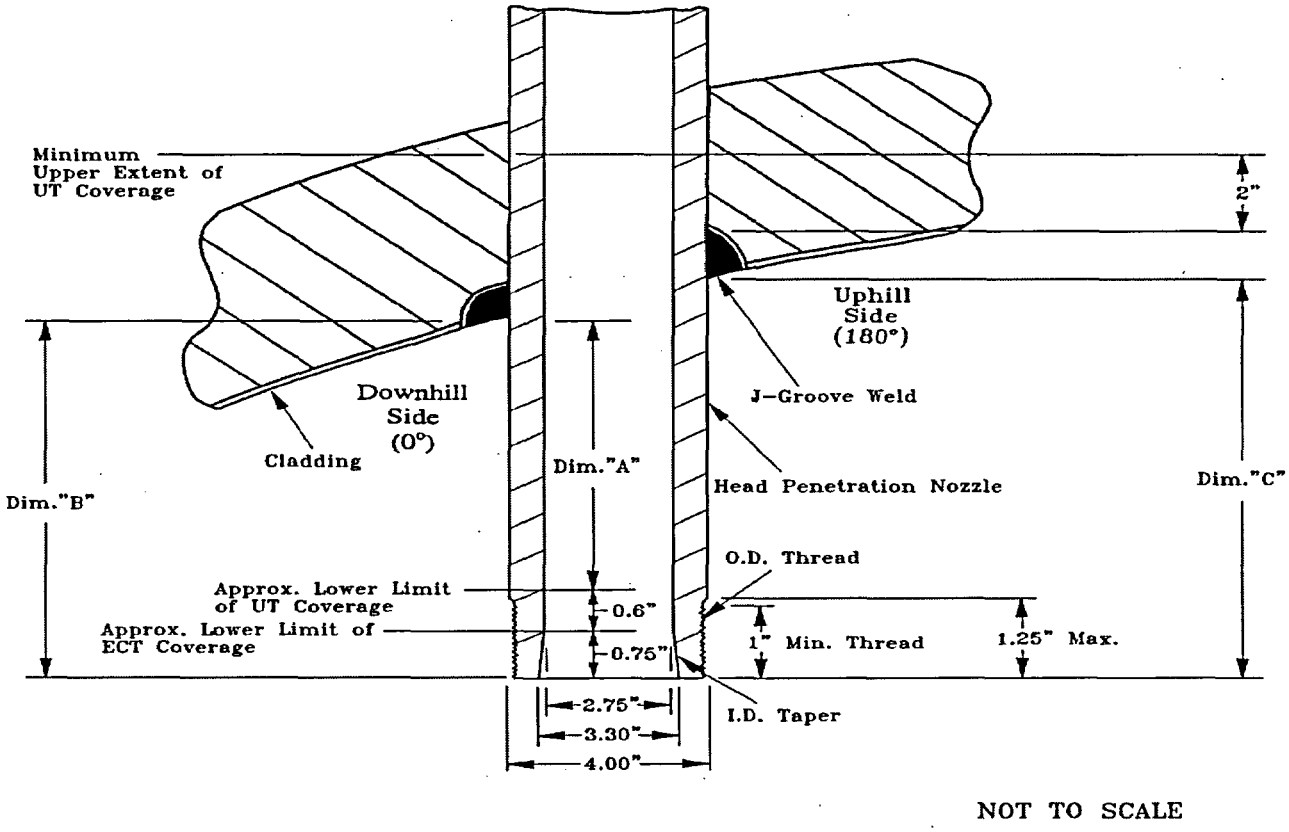

Figure 11

Cross-Section of Typical FNP 4" Diameter RPV Head Penetration Nozzle

Shown with UT Coverage Limits for Unit 1 Spring 2003 Inspection

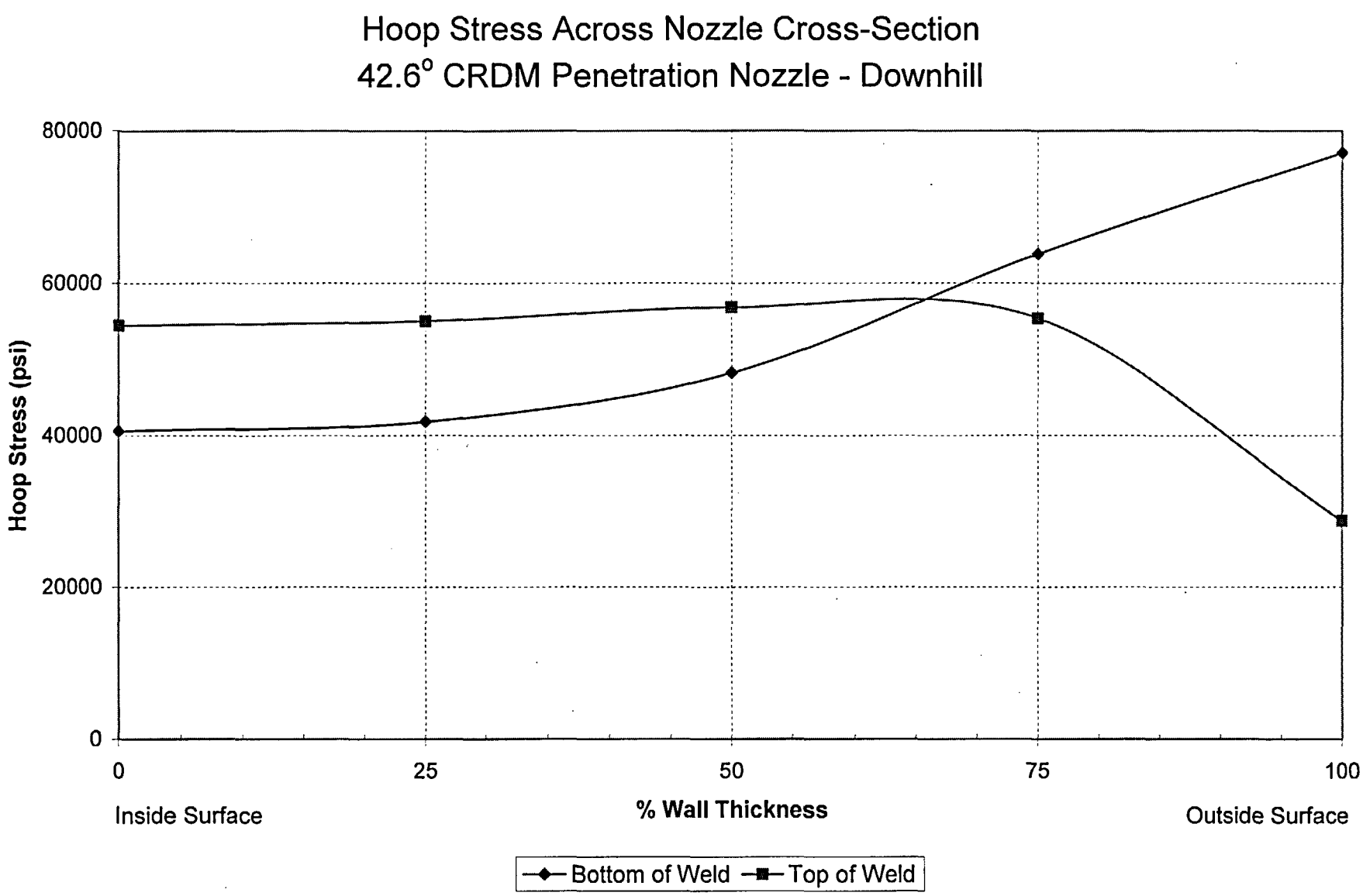
Hoop Stress Across Nozzle Cross-Section
42.6° CRDM Penetration Nozzle - Downhill
80000
60000
40000
20000
0
Hoop Stress (psi)
0
25
50
75
100
Inside Surface
% Wall Thickness
Outside Surface
Bottom of Weld
Top of Weld

Figure 12

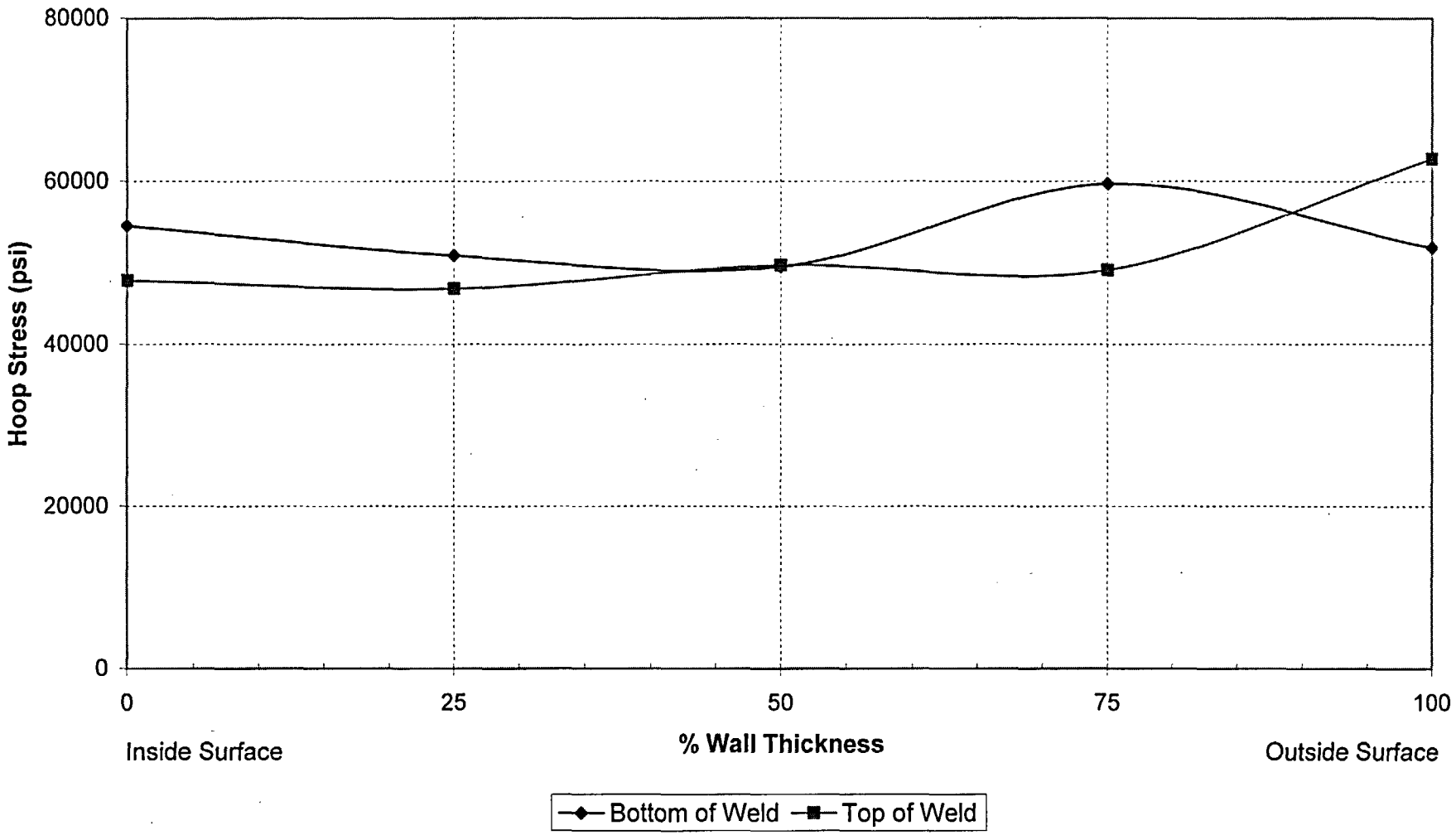
Hoop Stress Across Nozzle Cross-Section
42.6° CRDM Penetration Nozzle - Uphill
80000
60000
40000
20000
0
Hoop Stress (psi)
0
25
50
75
100
Inside Surface
% Wall Thickness
Outside Surface
Bottom of Weld
Top of Weld

Figure 13

Enclosure 3

Joseph M. Farley Nuclear Plant

WCAP-15925-NP, "Structural Integrity Evaluation of Reactor Vessel Upper Head Penetrations to Support Continued Operation: Farley Units 1 and 2" (Nonproprietary)

Westinghouse Non-Proprietary Class 3

WCAP-15925-NP
Revision 0

April 2003

Structural Integrity Evaluation of Reactor Vessel Upper Head Penetrations to Support Continued Operation: Farley Units 1 and 2

Westinghouse

WCAP-15925-NP

Structural Integrity Evaluation of Reactor Vessel Upper Head Penetrations to Support Continued Operation: Farley Units 1 and 2

W. H. Bamford
C. K. Ng
S. Jirawongkraisorn

April 2003

Verifier: _____
D. Tang
Structural Mechanics Technology

Approved: _____
S. A. Swamy
Manager, Structural Mechanics Technology

(This document is the non-proprietary version of WCAP-15925, which was published in September 2002)

Westinghouse Electric Company LLC
P.O. Box 355
Pittsburgh, PA 15230-0355

TABLE OF CONTENTS

TABLE OF CONTENTS (Cont.)

LIST OF TABLES

LIST OF FIGURES

1 INTRODUCTION

In September of 1991, a leak was discovered in the Reactor Vessel Control Rod Drive Mechanism (CRDM) head penetration region of an operating plant. This has led to the question of whether such a case could occur at Farley Units 1 and 2. The geometry of interest is shown in Figure 1-1. Throughout this report, the penetration rows have been identified by their angle of intersection with the head. The location of head penetrations for Farley Units 1 and 2 is shown in Figure 1-2 and the calculated angle for each penetration is identified in Table 1-1.

This issue resulted from cracking occurring in the outermost penetrations of a number of operating plants, as discussed in Section 2. This outermost CRDM location, as well as a number of intermediate CRDM penetrations and the head vent penetration were chosen for fracture mechanics analyses to support continued safe operation of Farley Units 1 and 2 if such cracking were to be found. The dimensions of the CRDM penetrations are all identical, with 4.0 inch Outside Diameter (OD) and wall thickness of 0.625 inch. For the head vent, the OD is 1.014 inches, and the wall thickness is 0.122 inch.

The basis of the analyses was a detailed three-dimensional elastic-plastic finite element analysis of several penetration locations, as described in detail in Section 5. Results were obtained at a number of locations in each penetration, and used in the fracture analysis.

The fracture analyses were carried out using reference crack growth rates recommended by the EPRI Materials Reliability Program (MRP), which are consistent with service experience. The results are presented in the form of flaw tolerance charts for both surface and through wall flaws, to determine the allowable service life of safe operation if indications are found. All the service life calculated in the flaw tolerance charts are Effective Full Power Years (EFPY).

Note that there are several locations in this report where proprietary information has been bracketed and deleted. For each of the bracketed locations, the reason for the proprietary classification is given, using a standardized system. The proprietary brackets are labeled with three different letters to provide this information and the explanation for each letter is given below:

a. The information reveals the distinguishing aspects of a process or component, structure, tool, method, etc., and the prevention of its use by Westinghouse's competitors, without license from Westinghouse, gives Westinghouse a competitive economic advantage.

c. The information, if used by a competitor, would reduce the competitor's expenditure of resources or improve the competitor's advantage in the design, manufacture, shipment, installation, assurance of quality, or licensing of a similar product.

e. The information reveals aspects of past, present, or future Westinghouse or customer funded development plans and programs of potential commercial value to Westinghouse.

This flaw tolerance handbook is the latest in a series of reports prepared for many operating plants. Flaw tolerance charts have been prepared for the following plants to date:

- Point Beach Units 1 and 2
- Almaraz Units 1 and 2
- Beznau Units 1 and 2
- R. E. Ginna
- San Onofre Units 2 and 3
- Palo Verde Units 1 and 2
- Millstone Unit 2
- Waterford Unit 3
- ANO Unit 2
- North Anna Units 1 and 2
- Surry Units 1 and 2
- D. C. Cook Units 1 and 2
- Angra Unit 1

The handbooks for D. C. Cook and North Anna have been submitted to the Regulatory Authority and the plants have received approval for restart. The Safety Evaluation Report for D. C. Cook is published, but that for North Anna is still pending.

Table 1-1 Farley Units 1 and 2 Head Penetration Nozzles, with Intersection Angles Identified

Nozzle No.	Type	Angle (Degrees)
1	CRDM	0.0
2	CRDM	8.7
3	CRDM	8.7
4	CRDM	8.7
5	CRDM	8.7
6	CRDM	12.4
7	CRDM	12.4
8	CRDM	12.4
9	CRDM	12.4
10	CRDM	17.6
11	CRDM	17.6
12	CRDM	17.6
13	CRDM	17.6
14	CRDM	19.8
15	CRDM	19.8
16	CRDM	19.8
17	CRDM	19.8
18	CRDM	19.8
19	CRDM	19.8
20	CRDM	19.8
21	CRDM	19.8
22	CRDM	25.4
23	CRDM	25.4
24	CRDM	25.4
25	CRDM	25.4
26	CRDM	27.0
27	CRDM	27.0
28	CRDM	27.0
29	CRDM	27.0
30	CRDM	28.6
31	CRDM	28.6
32	CRDM	28.6
33	CRDM	28.6
34	CRDM	28.6
35	CRDM	28.6
36	CRDM	28.6
37	CRDM	28.6
38	CRDM	33.1
39	CRDM	33.1
40	CRDM	33.1
41	CRDM	33.1
42	CRDM	33.1
43	CRDM	33.1
44	CRDM	33.1
45	CRDM	33.1
46	CRDM	37.3
47	CRDM	37.3
48	CRDM	37.3
49	CRDM	37.3
50	CRDM	38.6
51	CRDM	38.6
52	CRDM	38.6
53	CRDM	38.6
54	CRDM	38.6
55	CRDM	38.6
56	CRDM	38.6
57	CRDM	38.6
58	CRDM	40.0
59	CRDM	40.0
60	CRDM	40.0
61	CRDM	40.0
62	CRDM	42.6
63	CRDM	42.6
64	CRDM	42.6
65	CRDM	42.6
66	CRDM	42.6
67	CRDM	42.6
68	CRDM	42.6
69	CRDM	42.6

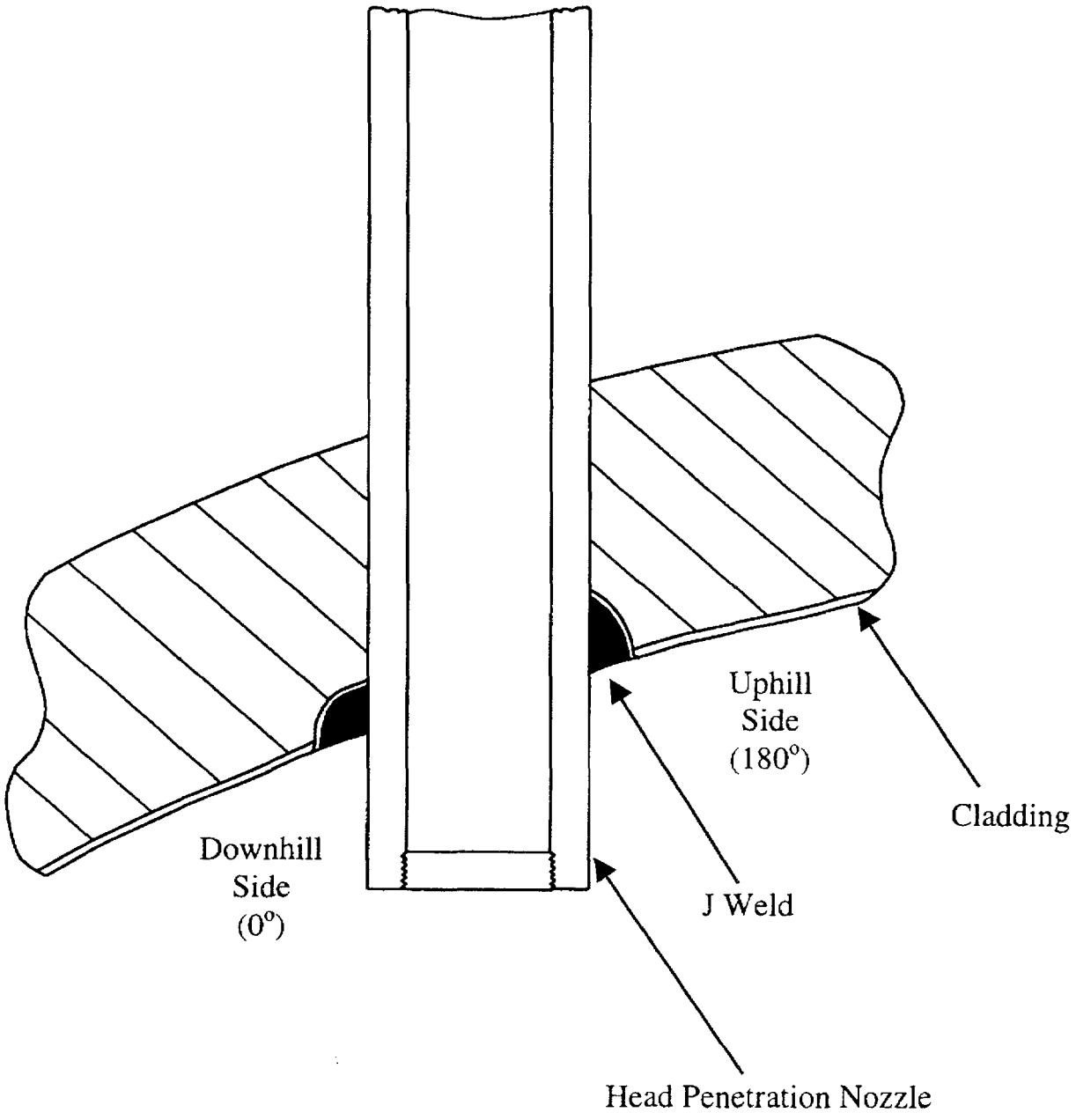

Figure 1-1 Reactor Vessel Control Rod Drive Mechanism (CRDM) Penetration

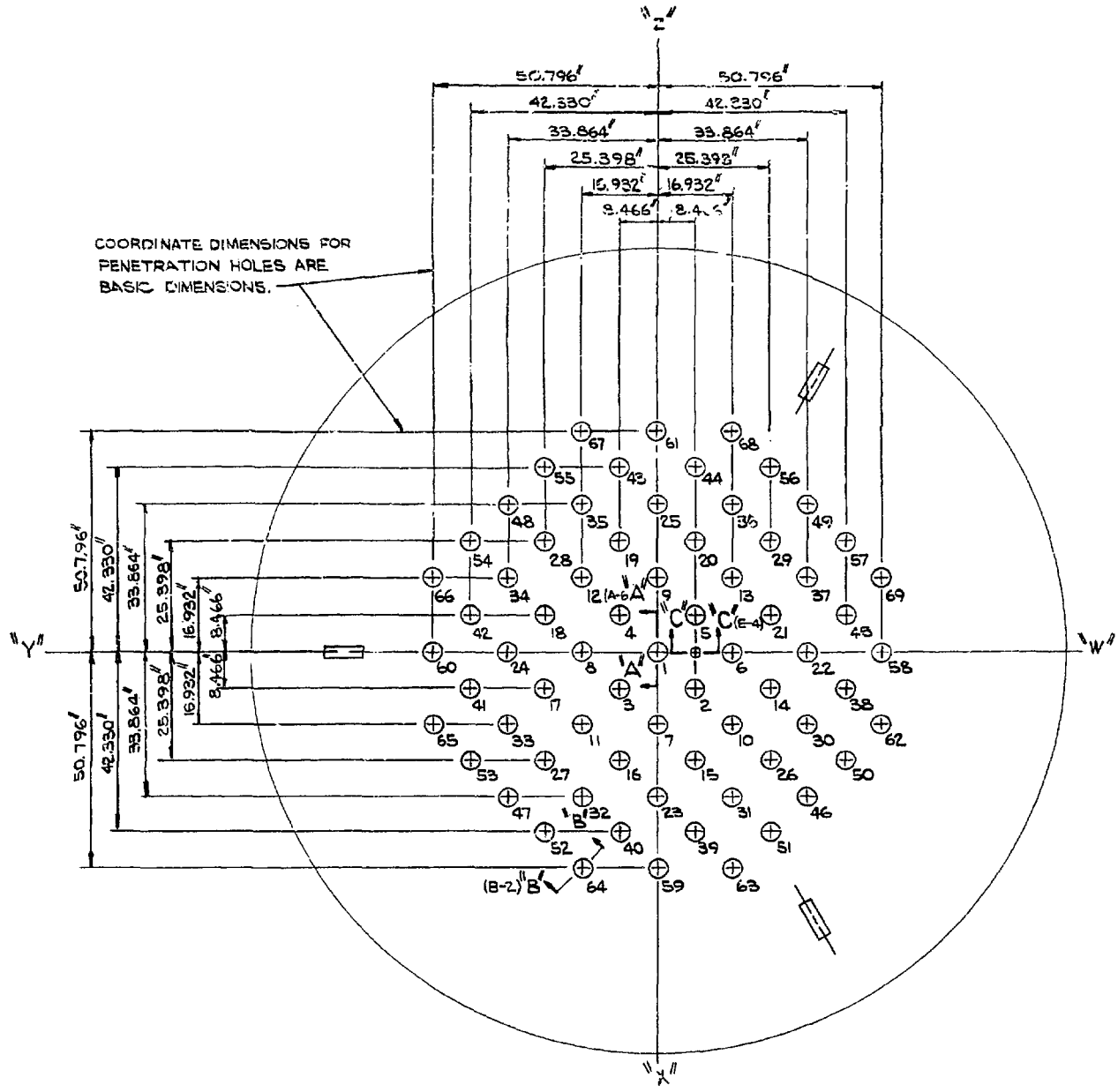

Figure 1-2 Location of Head Penetrations for Farley Units 1 and 2

2 HISTORY OF CRACKING IN HEAD PENETRATIONS

In September of 1991, leakage was reported from the reactor vessel CRDM head penetration region of a French plant, Bugey Unit 3. Bugey 3 is a 920 megawatt three-loop Pressurized Water Reactor (PWR) plant which had just completed its tenth fuel cycle. The leak occurred during a post ten year hydrotest conducted at a pressure of approximately 3000 psi (204 bar) and a temperature of 194°F (90°C). The leak was detected by metal microphones which are located on the top and bottom heads, and the leak rate was estimated to be approximately 0.7 liter/hour. The location of the leak was subsequently established on a peripheral penetration with an active control rod (H-14), as seen in Figure 2-1.

The control rod drive mechanism and thermal sleeve were removed from this location to allow further examination. Further study of the head penetration revealed the presence of longitudinal cracks near the head penetration attachment weld. Penetrant and ultrasonic testing confirmed the cracks. The cracked penetration was fabricated from Alloy 600 bar stock (SB-166), and has an outside diameter of 4 inches (10.16 cm) and an inside diameter of 2.75 inches (7.0 cm).

As a result of this finding, all of the control rod drive mechanisms and thermal sleeves at Bugey 3 were removed for inspection of the head penetrations. Only two penetrations were found to have cracks, as shown in Figure 2-1.

An inspection of a sample of penetrations at three additional plants were planned and conducted during the winter of 1991-92. These plants were Bugey 4 , Fessenheim 1, and Paluel 3. The three outermost rows of penetrations at each of these plants were examined, and further cracking was found in two of the three plants.

At Bugey 4, eight of the 64 penetrations examined were found to contain axial cracks, while only one of the 26 penetrations examined at Fessenheim 1 was cracked. The locations of all the cracked penetrations are shown in Figure 2-1. None of the 17 CRDM penetrations inspected at Paluel 3 showed indications of cracking, at the time, but further inspection of the French plants has confirmed at least one crack in each operating plant.

Thus far, the cracking in reactor vessel heads, not designed by Babcock and Wilcox (B&W), has been consistent in both its location and extent. All cracks discovered by nondestructive examination have been oriented axially, and have been located in the bottom portion of the penetration in the vicinity of the partial penetration attachment weld to the vessel head as shown schematically in Figure 1-1.

[

]^{a,c,e}

[

]^{a,c,e}

Non-destructive examinations of the leaking CRDM nozzles showed that most of the cracks originated on the outside surface of the nozzles below the J-groove weld, were axially oriented, and propagated primarily in the nozzle base material to an elevation above the top of the J-groove weld where leakage could then pass through the annulus to the top of the head where it was detected by visual inspection. In some cases the cracks initiated in the weld metal or propagated into the weld metal, and in a few cases the cracks propagated through the nozzle wall thickness to the inside surface.

[

]^{a,c,e}

The cracking has now been confirmed to be primary water stress corrosion cracking. Relatively high residual stresses are produced in the outermost CRDM penetrations due to the welding process. Other important factors which affect this process are temperature and time, with higher temperatures and longer

times being more detrimental. It is interesting to note that no head vents have been found to have cracks. The inspection findings for the plants examined thus far are summarized in Table 2-1.

Table 2-1 Operational Information and Inspection Results for Units Examined (Results to April 30, 2002)

Country	Plant Type	Units Inspected	K Hours	Head Temp. (°F)	Total Penetrations	Penetrations Inspected	Penetrations With Indications
France	CPO	6	80-107	596-599	390	390	23
	CPY	28	42-97	552	1820	1820	126
	1300MW	20	32-51	558-597	1542	1542	95
Sweden	3 Loop	3	75-115	580-606	195	190	8
Switzerland	2 Loop	2	148-154	575	72	72	2
Japan	2 Loop	7	105-108	590-599	276	243	0
	3 Loop	7	99	610	455	398	0
	4 Loop	3	46	590	229	193	0
Belgium	2 Loop	2	115	588	98	98	0
	3 Loop	5	60-120	554-603	337	337	6
Spain	3 Loop	5	65-70	610	325	102	0
Brazil	2 Loop	1	25	NA	40	40	0
South Africa	3 Loop	1	NA	NA	65	65	6
Slovenia	2 Loop	1	NA	NA	49	49	0
South Korea	2 Loop	3	NA	NA	49	49	3
	3 Loop	2	NA	NA	130	130	2
US	2 Loop	2	170	590	98	98	0
	3 Loop	1	NA	NA	65	20	12
	4 Loop	18	NA	NA	1149	537	35
TOTALS		117	–	–	7384	6373	318

NA = Not Available.

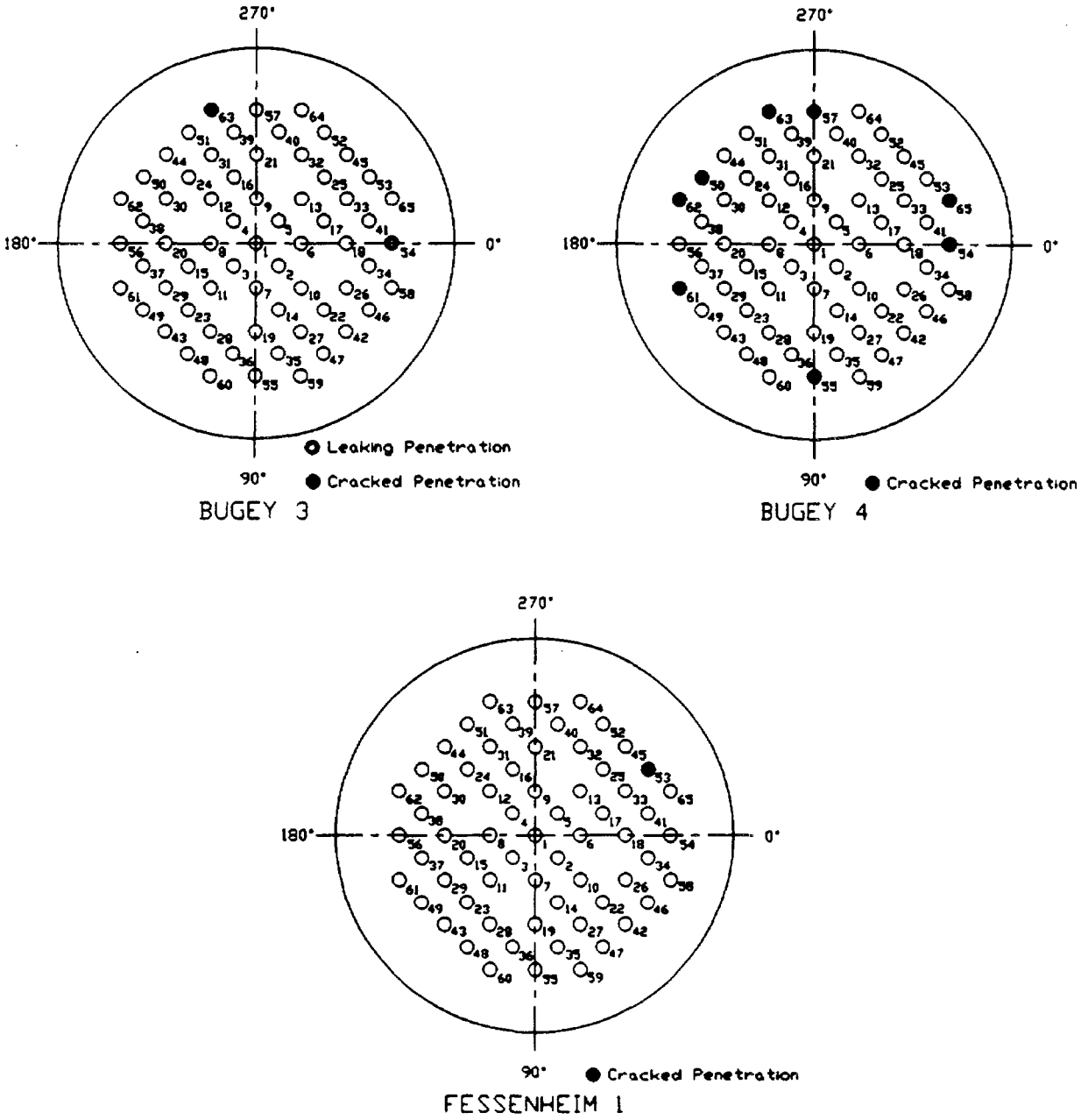

Figure 2-1 French R/V Closure Head CRDM Penetration Cracking EDF Plants – Penetrations with Cracking

3 OVERALL TECHNICAL APPROACH

The primary goal of this work is to provide technical justification for the continued safe operation of Farley Units 1 and 2 in the event that cracking is discovered during in-service inspections of the Alloy 600 reactor vessel upper head penetrations.

3.1 PENETRATION STRESS ANALYSIS

Three-dimensional elastic-plastic finite element stress analyses have been performed to determine the stresses in the head penetration region [6]. These analyses have considered the pressure loads associated with steady state operation, as well as the residual stresses which are produced by the fabrication process.

[

]^{a,c,e}

3.2 FLAW TOLERANCE APPROACH

A flaw tolerance approach has been developed to allow continued safe operation until an appropriate time for repair, or the end of plant life. The approach is based on the prediction of future growth of detected flaws, to ensure that such flaws would remain stable.

If an indication is discovered during in-service inspection, its size can be compared with the flaw size considered as allowable for continued service. This "allowable" flaw size is determined from the actual loadings (including mechanical and residual loads) on the head penetration for Farley Units 1 and 2. Suitable margins to ensure the integrity of the reactor vessel as well as safety from unacceptable leakage rates should also be considered. Acceptance criteria are discussed in Section 6.5.

The time for the observed crack to reach the allowable crack size determines the length of time the plant can remain online before repair, if required. For the crack growth calculation, a best estimate is needed and no additional margins are necessary.

The results of the evaluation are presented in terms of simple flaw tolerance charts. The charts show graphically the time required to reach the allowable length or depth that represents the additional service life before repair. This result is a function of the loadings on the particular head penetration, as well as the circumferential location of the crack in the penetration nozzle.

Schematic drawings of the head penetration flaw tolerance charts are presented as Figures 3-1 and 3-2. These two types of charts can be used to provide estimates of the remaining service life before a leak

would develop from an observed crack. For example, if a part-through flaw was discovered, the user would first refer to Figure 3-1, to determine the time (t_P) which would be remaining before the crack would penetrate the wall or reach the allowable depth (t_a) (eg a/t = 0.75). Once the crack penetrates the wall, the time (t_B) required to reach an allowable crack length would be determined from Figure 3-2. The total time remaining would then be the simple sum:

$$\text{Time remaining} = t_P + t_B$$

Another way to determine the allowable time of operation with a part-through flaw would be to use Figure 3-2 directly, in effect assuming the part-through flaw is a through-wall flaw. This approach would be more conservative than that above, and the time remaining would then be:

$$\text{Time remaining} = t_B$$

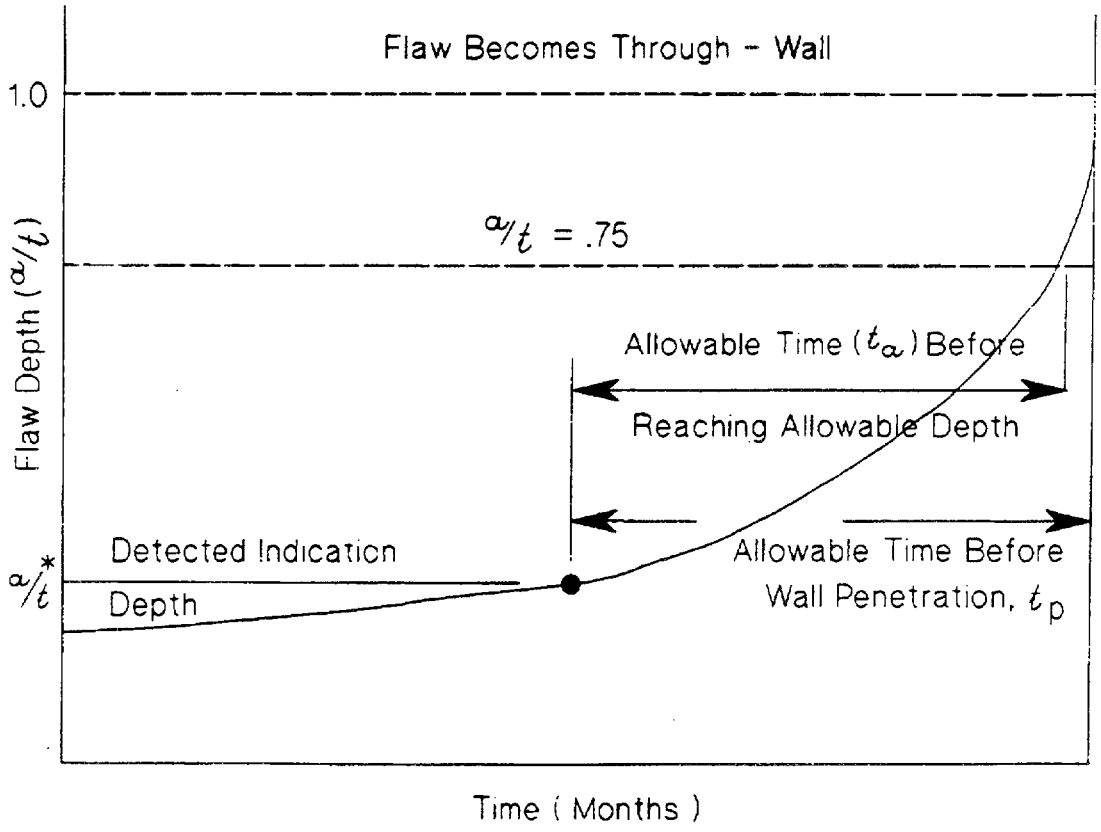

Figure 3-1 Schematic of a Head Penetration Flaw Growth Chart for Part Through Flaws

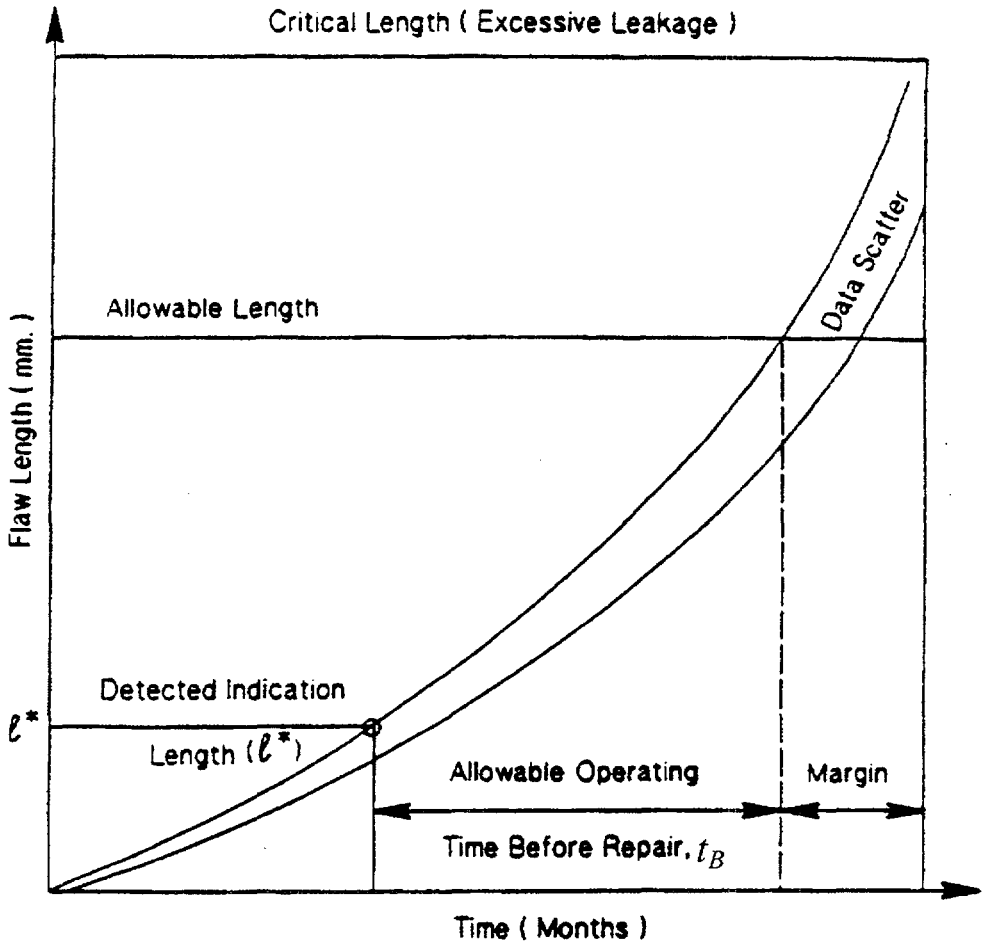

Figure 3-2 Schematic of a Head Penetration Flaw Tolerance Chart for Through-Wall Flaws

4 MATERIAL PROPERTIES, FABRICATION HISTORY AND CRACK GROWTH PREDICTION

4.1 MATERIALS AND FABRICATION

The reactor vessel for Farley Units 1 and 2 were manufactured by Combustion Engineering, with head penetration nozzles from material produced by Babcock and Wilcox Tubular Products, and Huntington in the USA. The carbon content and mechanical properties of the Alloy 600 material used to fabricate the Farley Units 1 and 2 vessel are provided in Table 4-1. The Certified Material Test Reports (CMTRs) were used to obtain the chemistry and mechanical properties for the vessel head penetrations. The Huntington materials were annealed for 1.5 hours at 1725°F and air cooled. The B&W Tubular Products heat treatment was not identified on the CMTRs, but typically B&W heats were annealed at 1800 °F. Figure 4-1 illustrates the yield strengths and carbon contents, based on percent of heats, of the head adapter penetrations in the Farley Units 1 and 2 vessel relative to a sample of the French head penetrations which have experienced cracking. The general trend for the head adapter penetrations in Farley Units 1 and 2 are a higher carbon content, higher mill annealing temperature and lower yield strength relative to those on the French vessels. These factors should all have a beneficial effect on the material resistance to PWSCC in the head penetrations.

4.2 CRACK GROWTH PREDICTION

The cracks in the penetration region have been determined to result from primary water stress corrosion cracking in the Alloy 600 base metal, and in some cases the Alloy 182 weld metal. There are a number of available measurements of static load crack growth rates in primary water environment, and in this section the available results will be compared and a representative growth rate established.

Direct measurements of Stress Corrosion Cracking (SCC) growth rates in Alloy 600 are relatively rare, and care should be used in interpreting the results because the materials may be excessively cold worked, or the loadings applied may be near or exceeding the limit load of the penetration nozzle, meaning there will be an interaction between tearing and crack growth. In these cases the crack growth rates may not be representative of service conditions.

The effort to develop a reliable crack growth rate model for Alloy 600 began in the spring of 1992, when the Westinghouse Owners Group was developing a safety case to support continued operation of plants. At the time, there was no available crack growth rate data for head penetration materials, and only a few publications existed on growth rates of Alloy 600 in any product form.

The best available publication at that time was that of Peter Scott of Framatome, who had developed a growth rate model for PWR steam generator materials [1]. His model was based on a study of results obtained by McIlree, Rebak and Smialowska [2] who had tested short steam generator tubes which had been flattened into thin compact specimens.

An equation was fitted to the data of reference [2] for the results obtained in water chemistries that fell within the standard specification for PWR primary water. Results for chemistries outside the specification were not used. The following equation was fitted to the data at 330°C (626°F):

$$\frac{da}{dt} = 2.8 \times 10^{-11} (K - 9)^{1.16} \text{ m/sec} \quad (4\text{-}1)$$

where K is in MPa$\sqrt{m}$.

The next step was to correct these results for the effects of cold work. Based on work by Cassagne and Gelpi [3], Scott concluded that dividing the above equation by a factor of 10 would be appropriate to account for the effects of cold work. The crack growth law for 330°C (626°F) then becomes:

$$\frac{da}{dt} = 2.8 \times 10^{-12} (K - 9)^{1.16} \text{ m/sec} \quad (4\text{-}2)$$

Scott further corrected this law for the effects of temperature. This forms the basis for the PWR Materials Reliability Program (MRP) recommended crack growth rate (CGR) curve for the evaluation of SCC where a power-law dependence on stress intensity factor was assumed. The MRP recommended CGR curve was used in this report for determining the primary water stress corrosion crack growth rate and a brief discussion on this recommended curve is as follows:

[

]^{a,c,e}

There is a general agreement that crack growth in Alloy 600 materials in the primary water environment can be modeled using a power-law dependence on stress intensity factor with differences in temperature accounted for by an activation energy (Arrhenius) model for thermally controlled processes. Figure 4-3 shows the recommended CGR curve along with the laboratory data from Huntington materials used to develop the curve.

[

]^{a,c,e}

[

]^{a,c,e}

The applicability of the MRP recommended model to head penetrations was recently confirmed by two independent approaches. The first was a collection of all available data from Standard Steel and Huntington Alloys materials tested over the past ten years [4H]. The results are shown in Figure 4-3, along with the Scott model for the test temperature.

The MRP crack growth curve was structured to bound 75 percent of the 26 heats for which test results were available. Fits were done on the results for each heat, and the constant term was determined for each heat. This was done to eliminate the concern that the curve might be biased from a large number of results from a single heat. The 75th percentile was then determined from these results. The MRP expert panel on crack growth endorsed the resulting curve unanimously in a meeting on March 6th and 7th 2002. This approach is consistent with the Section XI flaw evaluation philosophy, which is to make a best estimate prediction of future growth of a flaw. Margins are incorporated in the allowable flaw sizes. The entire data set is shown in Figure 4-3, where the data have been adjusted to a single temperature of 325°C.

A second independent set of data were used to validate the model, and these data were obtained from the two inspections carried out on penetration no. 75 of D.C. Cook Unit 2, which was first found to be cracked in 1994 [4G]. The plant operated for one fuel cycle before the penetration was repaired in 1996 and the flaw was measured again before being repaired. These results were used to estimate the PWSCC growth rate for both the length of the flaw and its depth. These two points are also shown in Figure 4-4, and are consistent with the laboratory data for Huntington materials. In fact, Figure 4-4 demonstrates that the MRP model is nearly an upper bound for these materials. The D.C. Cook Unit 2 penetrations were made from Huntington materials.

Since Farley Units 1 and 2 operate at a temperature of 314°C (597°F) in the head region [9], and the crack growth rate is strongly affected by temperature, a temperature adjustment is necessary. This temperature correction was obtained from study of both laboratory and field data for stress corrosion crack growth rates for Alloy 600 in primary water environments. The available data showing the effect of temperature are summarized in Figure 4-5. Most of the results shown here are from steam generator tube materials, with several sets of data from operating plants, and results from two heats of materials tested in a laboratory [4A].

Study of the data shown in Figure 4-5 results in an activation energy of 31-33 Kcal/mole, which can then be used to adjust for the lower operating temperature. This value is slightly lower than the generally accepted activation energy of 44-50 Kcal/mole used to characterize the effect of temperature on crack initiation, but the trend of the actual data for many different sources is unmistakable.

[

]^{a,c,e}

[

]a,c,e

Therefore the following crack growth rate model was used for the Farley Units 1 and 2 head penetrations for crack growth in all the cases analyzed.

$$\frac{da}{dt} = 1.63 \times 10^{-12} (K - 9)^{1.16} \text{ m/sec}$$

where K = applied stress intensity factor, in $MPa\sqrt{m}$. This equation implies a threshold for cracking susceptibility, $K_{ISCC} = 9$ $MPa\sqrt{m}$. The crack growth rate is applicable to propagation in both axial and circumferential directions.

An in-plant vessel upper head region fluid temperature measurement program was developed in 1978 with the objectives that should lead to a basis for reducing the penalty imposed on LOCA analysis (i.e. the head region fluid is assumed to be at T_{hot}); and also improve the confidence that the head region fluid could be returned to the reactor inlet temperature with the flow rate calculated by the Westinghouse analytical model. The program included plans for measurements in three 15x15 3-loop plants, one 17x17 3-loop plant, two 17x17 UHI plants and one 14x14 2-loop plant. Farley Unit 1 was one of the plants included in the program.

Since Farley Unit 1 was still in the construction phase at the initiation of the program, the instrumentation was designed with concurrence from the utility to address both radial and axial variations in the fluid temperature of the upper head region. Twelve core monitoring thermocouples were removed and replaced by 12 thermocouples to monitor fluid temperature in the reactor vessel head. The 12 thermocouples were removed from their core monitoring positions and the runs (several from each thermocouple port column) were modified to terminate in various locations in the vessel head region. Sufficient in-core thermocouples remain to preserve the ability to measure major and minor core tilts.

The recent fluid temperature measurements [10,11] from these thermocouples in the Farley Unit 1 vessel head region are listed below:

	Hot No Load	Begin of Cycle	8 Months into 18 Months Cycle
	(11-14-01)	(11-25-01)	(7-24-02)
Location	Fluid Temp (° F)	Fluid Temp (° F)	Fluid Temp (° F)
I - 7B	551.0	593.9	597.0
H - 6B	551.0	596.4	592.0
L - 10B	551.0	599.8	597.0
G - 5B	549.0	589.1	589.0
X - 22B	549.0	587.4	588.0
W - 21B	551.1	596.9	599.0
O - 13B	549.0	592.7	593.0
Y - 23B	547.0	587.4	593.0
V - 20B	549.0	589.7	591.0
AJ - 34B	551.0	591.2	586.0
AX - 48B	547.6	587.2	595.0
Total Avg.	549.6	592.0	592.7

The upper head region temperature of 314°C (597°F) for Farley Units 1 and 2 used in this report is based on the information provided as the utility responses to NRC Bulletin 2001-01 [9]. Based on the above data. the temperature used for the head region in this report is consistent with the plant operation data.

(a,c,e)

Table 4-1 Farley Units 1 and 2 Head Penetration Material Information

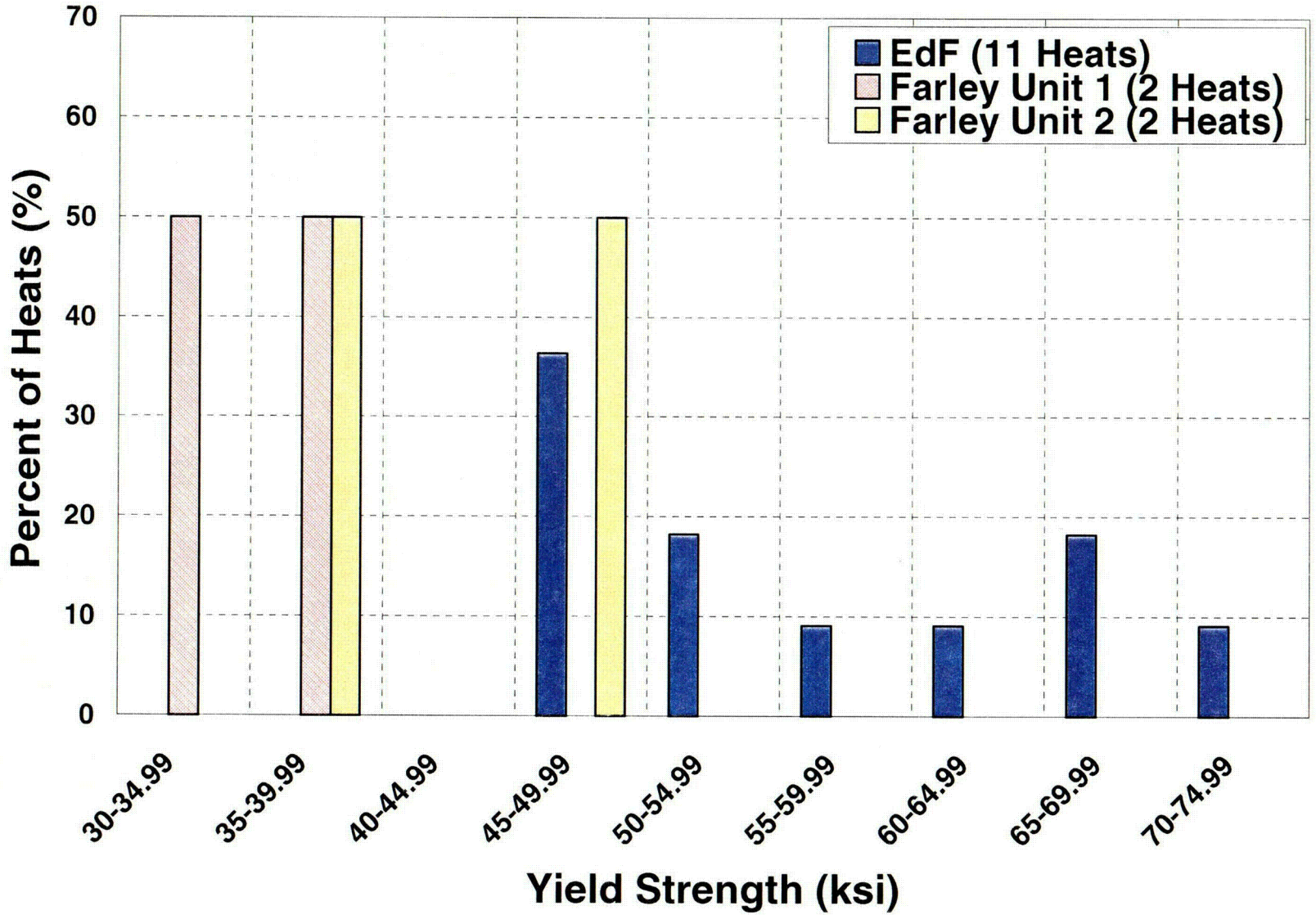

Figure 4-1 Yield Strength of the Various Heats of Alloy 600 Used in Fabricating the Farley Units 1 and 2 and French Head Penetrations

C01

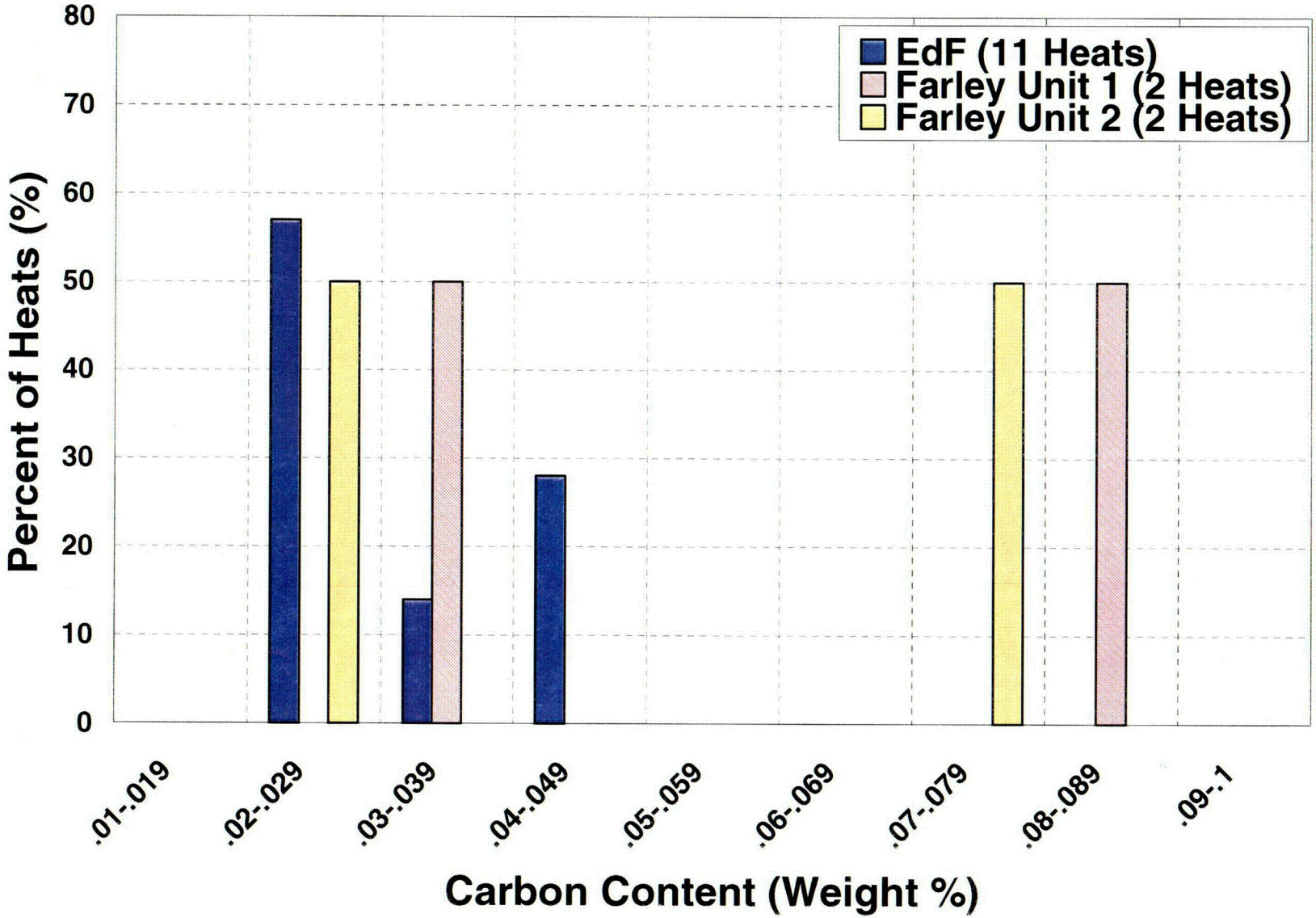

Figure 4-2 **Carbon Content of the Various Heats of Alloy 600 Used in Fabricating the Farley Units 1 and 2 and French Head Penetration**

C02

(a,c,e)

Figure 4-3 Screened Laboratory Data for Alloy 600, with the MRP Recommended Curve. Note that the Modified Scott Model is also Shown [4H]

(a,c,e)

Figure 4-4 Model for PWSCC Growth Rates in Alloy 600 in Primary Water Environments (325°C), With Supporting Data from Standard Steel, Huntington, and Sandvik Materials [4H]

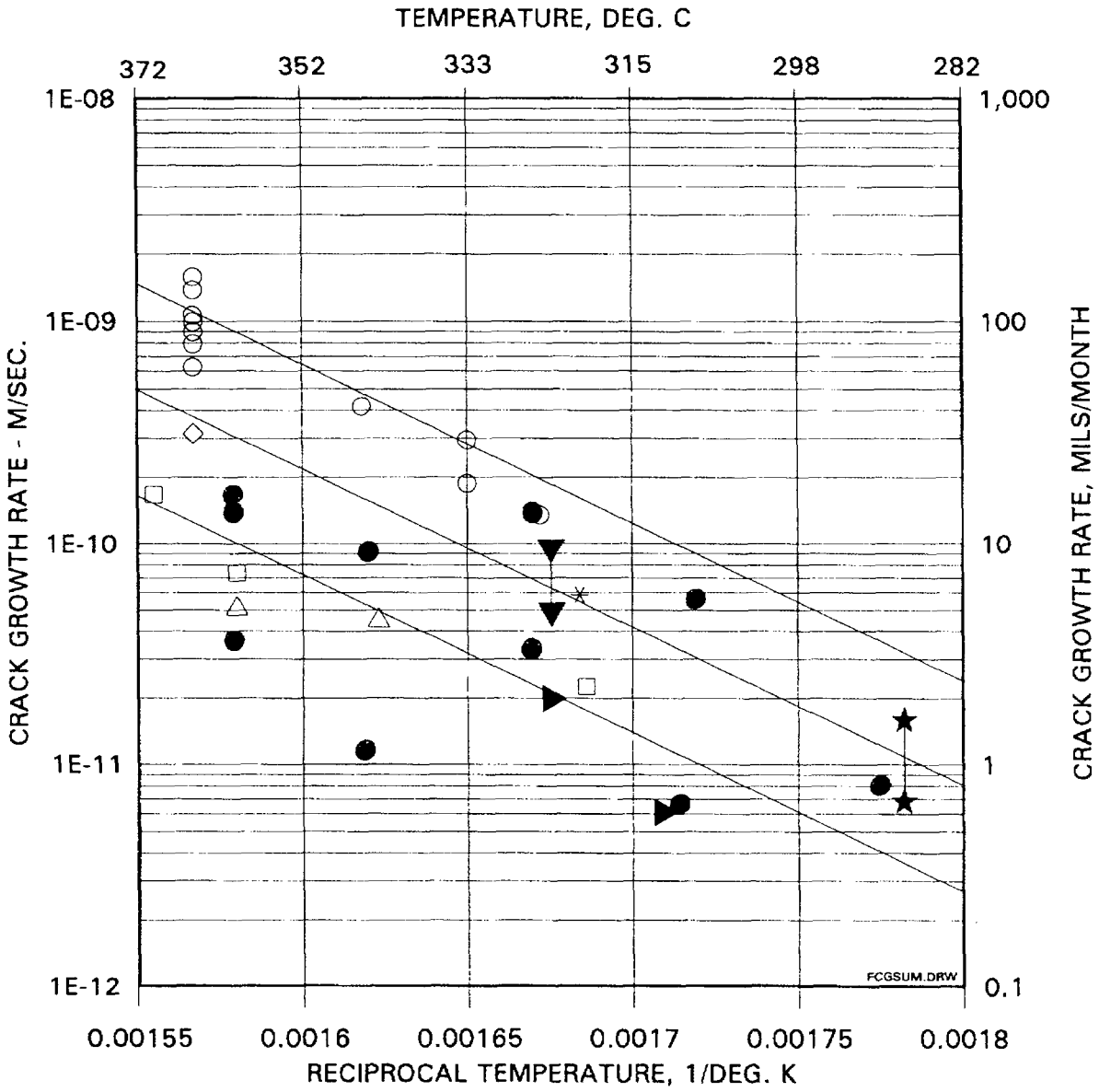

Note: All symbols are for steam generator materials, except the solid circles, which are head penetration laboratory data.

Figure 4-5 Summary of Temperature Effects on PWSCC Growth Rates for Alloy 600 in Primary Water [4A]

5 STRESS ANALYSIS

5.1 OBJECTIVES OF THE ANALYSIS

The objective of this analysis was to obtain accurate stresses in each CRDM, head vent and its immediate vicinity. To do so requires a three-dimensional finite element analysis which considers all the pertinent loadings on the penetration [6]. An investigation of deformations at the lower end of the housing was also performed using the same model. Five CRDM locations were considered: the outermost row (42.6°), rows at 40.0°, 38.6°, 28.6° and the center location (0°), which bound the CRDM penetration angles in the Farley Units 1 and 2 reactor vessel head. In addition, the head vent was analyzed.

The analyses were used to provide information for the flaw tolerance evaluation in Section 6. Also, the results of the stress analysis were compared to the findings from service experience to help assess the causes of the observed cracking.

5.2 MODEL

A three-dimensional finite element model comprised of isoparametric brick and wedge elements with midside nodes on each face was used to obtain the stresses and deflections. A view of the outermost CRDM model is shown in Figure 5-1. Taking advantage of symmetry through the vessel and penetration centerlines, only half of the penetration geometry plus the surrounding vessel were modeled. The difference between the hillside penetrations and the center penetration was that there was no differential height across the weld for the center penetration.

In the models, the lower portion of the Control Rod Drive Mechanism (CRDM) penetration nozzle, head vent, the adjacent section of the vessel closure head, and the joining weld were modeled. The vessel to penetration nozzle weld was simulated with two layers of elements. The penetration nozzle, weld metal and cladding were modeled as Alloy 600 and the vessel head shell as carbon steel.

The only loads used in the analysis are the steady state operating loads. External loads such as seismic loads have been studied and have no impact, because the penetration nozzles are captured by the full thickness of the reactor vessel head (over six inches of steel) into which the penetrations are shrunk fit during construction. The area of interest is in the penetration near the attachment weld, which is unaffected by these external loads.

5.3 STRESS ANALYSIS RESULTS – OUTERMOST CRDM PENETRATION (42.6 DEGREES)

Figure 5-2 presents the hoop and axial stresses for the steady state condition for the outermost penetration.

[

]^{a,c,e}

[

]a,c,e

5.4 STRESS ANALYSIS RESULTS – INTERMEDIATE CRDM PENETRATIONS

[

]a,c,e

5.5 STRESS ANALYSIS RESULTS – CENTER CRDM PENETRATION

[

]a,c,e

5.6 STRESS ANALYSIS RESULTS – HEAD VENT

[

]a,c,e

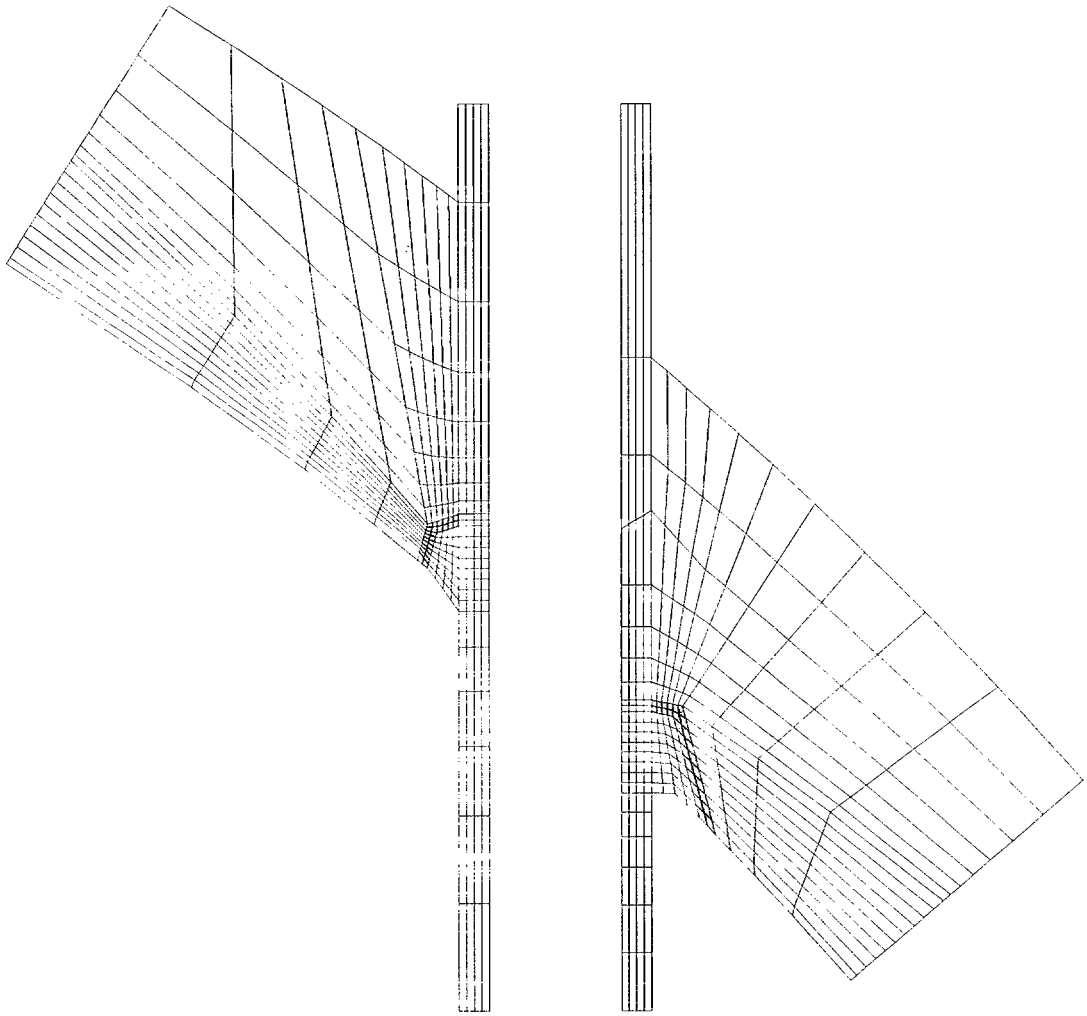

Figure 5-1 Finite Element Model of the Outermost CRDM Penetration (42.6 Degrees) [6]

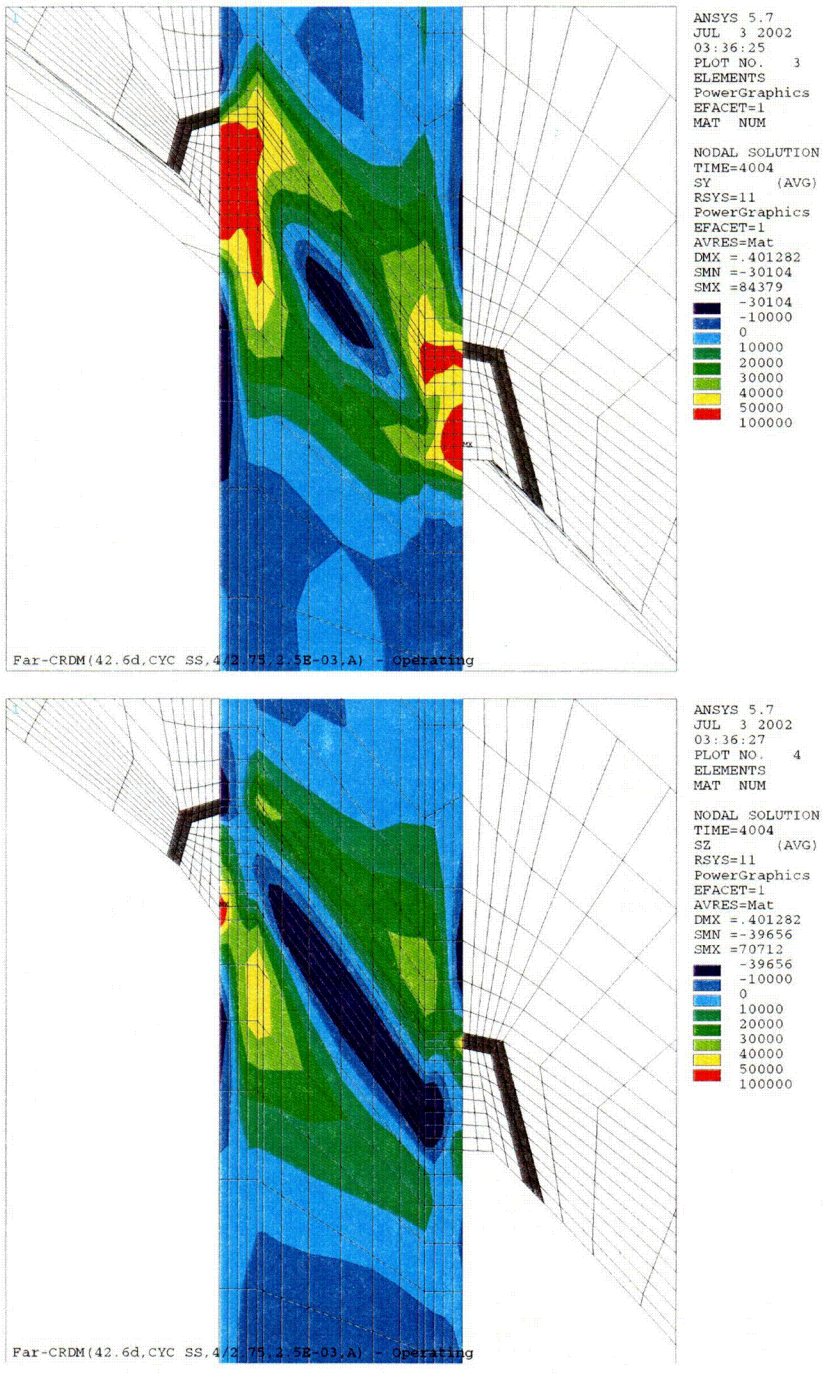

Figure 5-2 Stress Distributions at Steady State Conditions: Outermost CRDM Penetration (42.6 Degrees) (Hoop stress is the top figure; axial stress is the bottom figure) [6]

C03

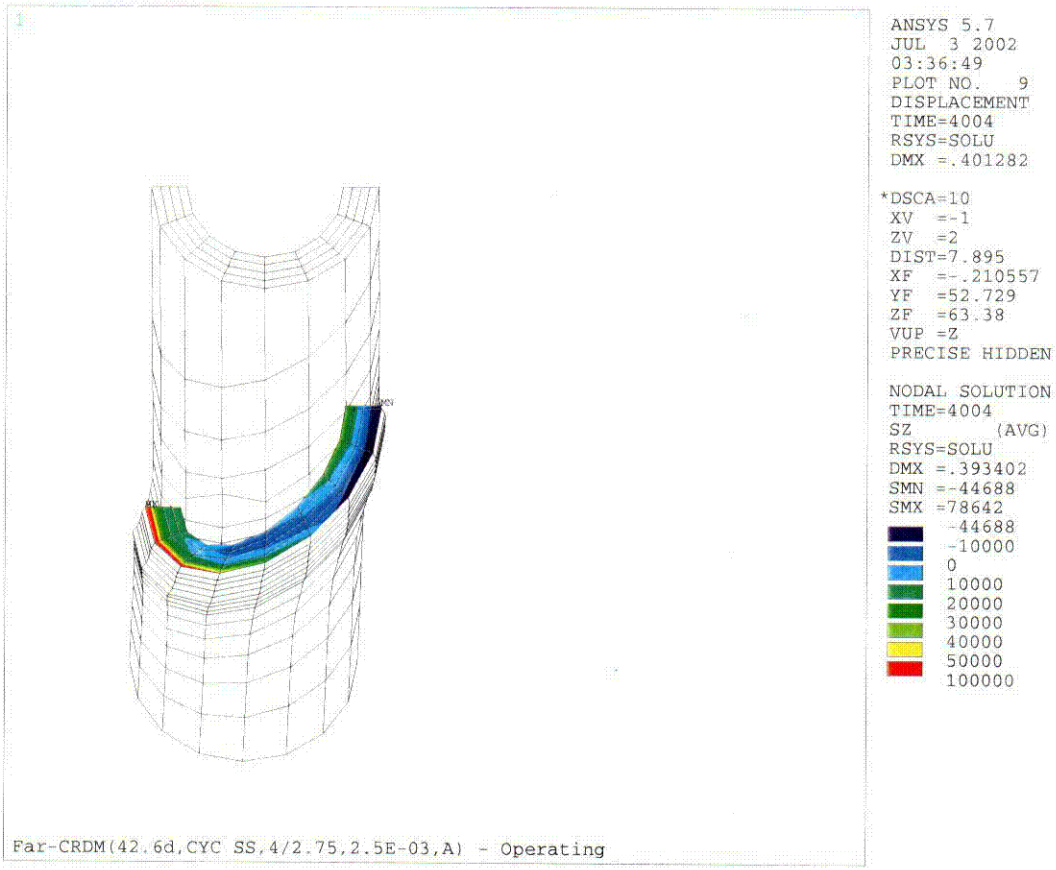

Figure 5-3 **Axial Stress Distribution at Steady State Conditions for the Outermost CRDM (42.6 Degrees) Penetration, Along a Plane Oriented Parallel to, and Just Above, the Attachment Weld [6]**

C04

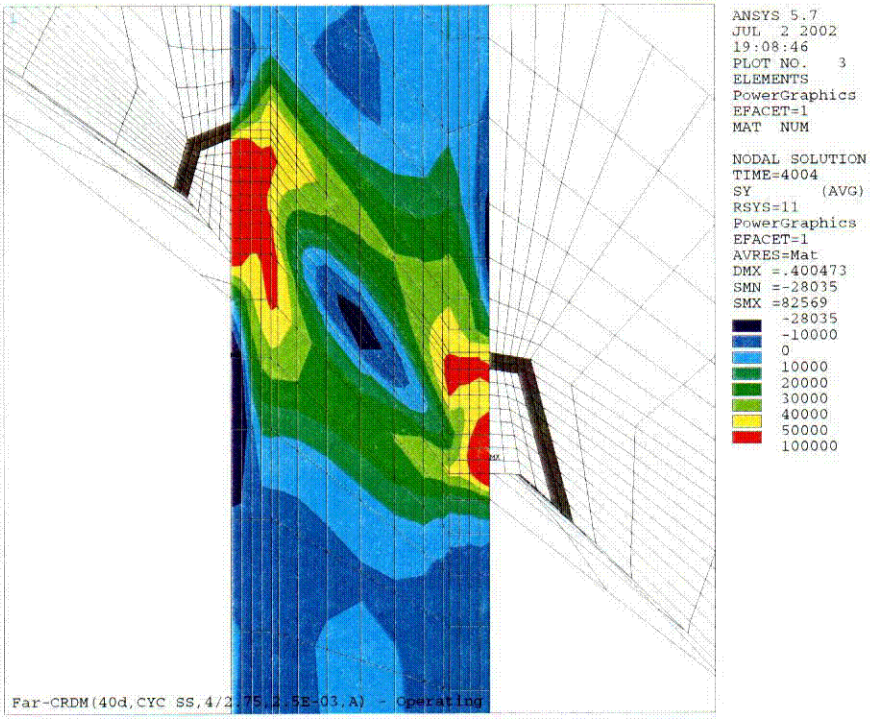

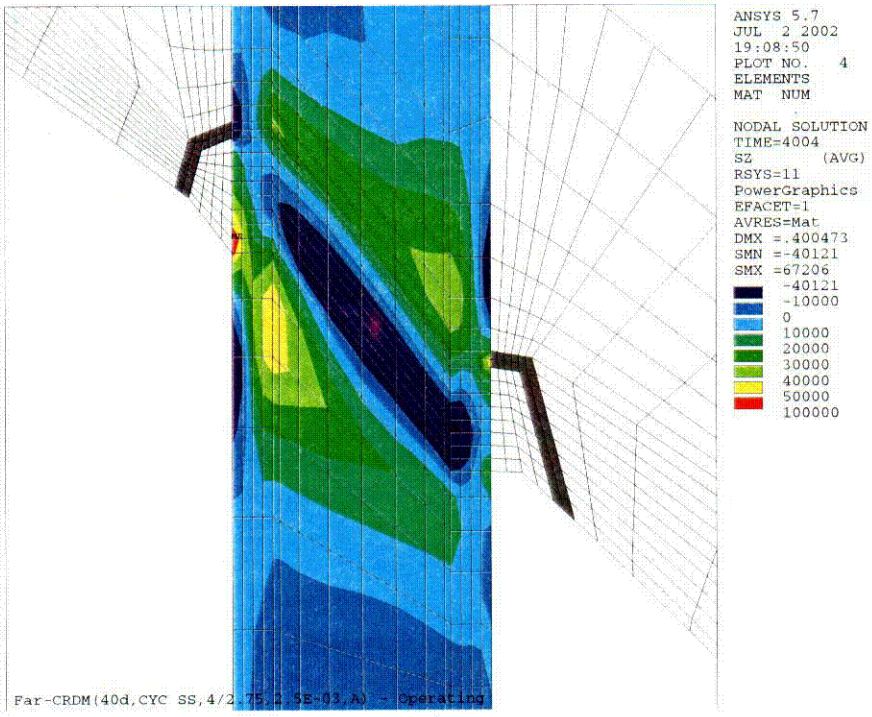

Figure 5-4 Stress Distribution at Steady State Conditions for the 40.0 Degrees CRDM Penetration (Hoop stress is the top figure; axial stress is the bottom figure) [6]

C05

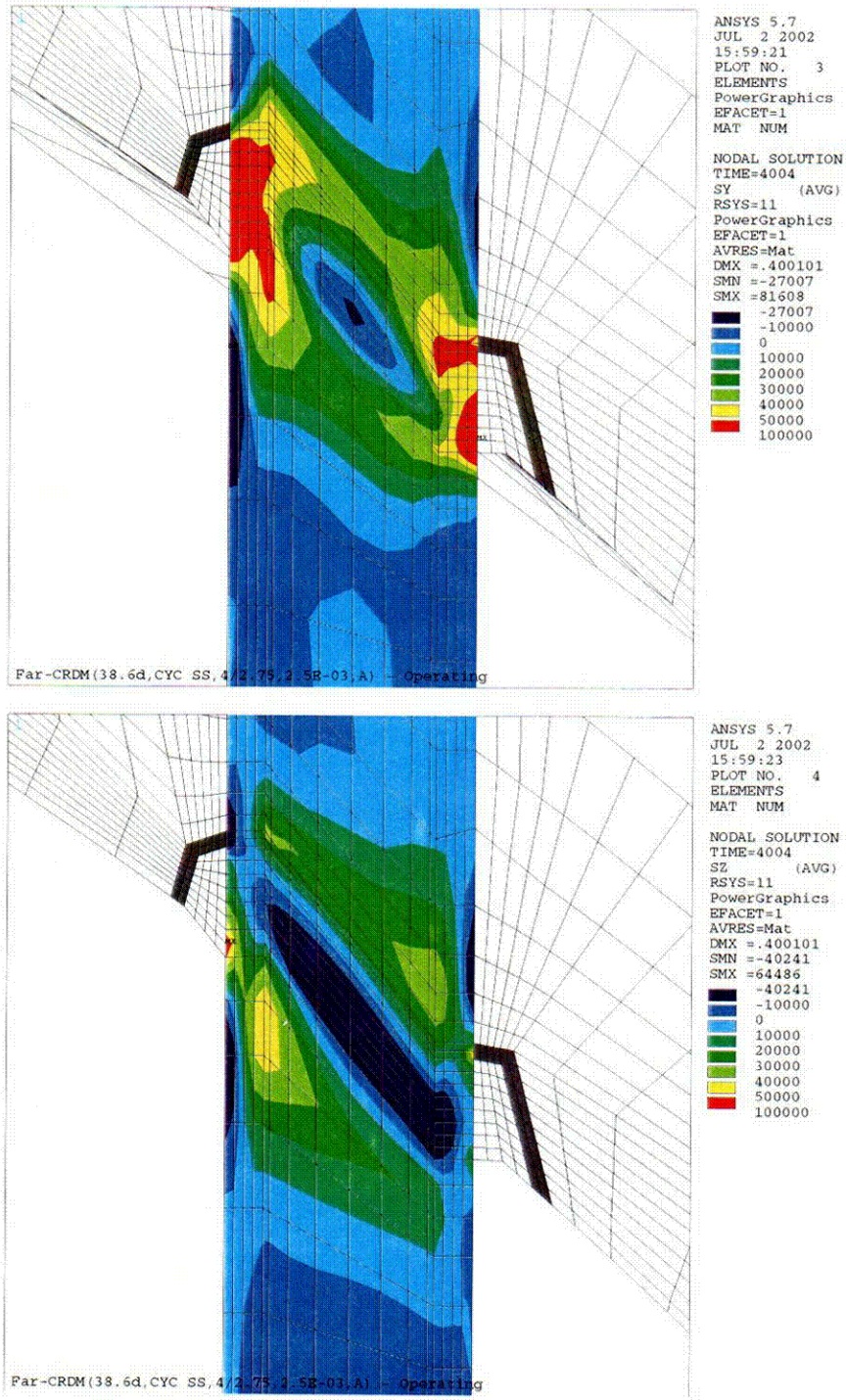

Figure 5-5 Stress Distribution at Steady State Conditions for the 38.6 Degrees CRDM Penetration (Hoop stress is the top figure; axial stress is the bottom figure) [6]

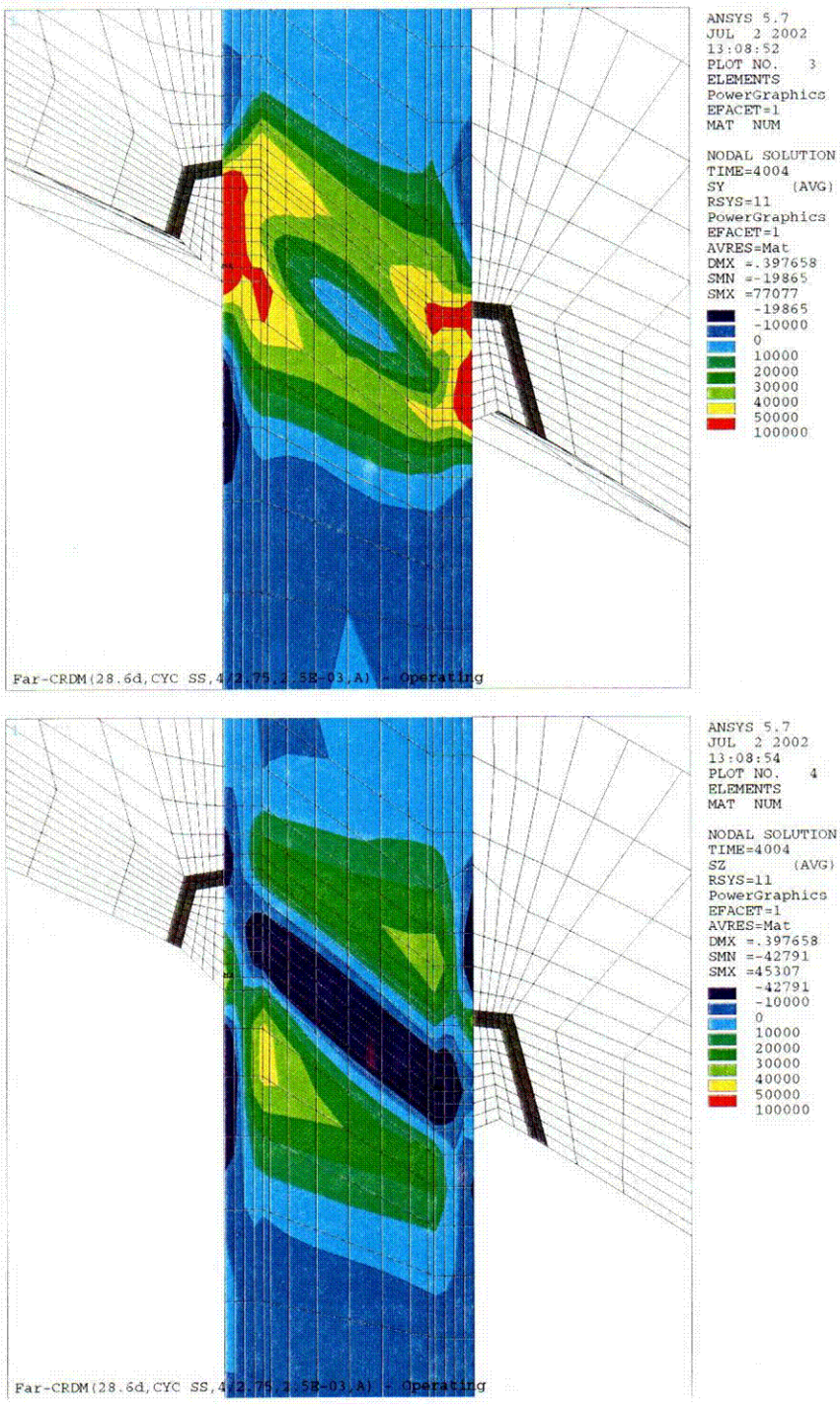

Figure 5-6 Stress Distribution at Steady State Conditions for the 28.6 Degrees CRDM Penetration (Hoop stress is the top figure; axial stress is the bottom figure) [6]

C07

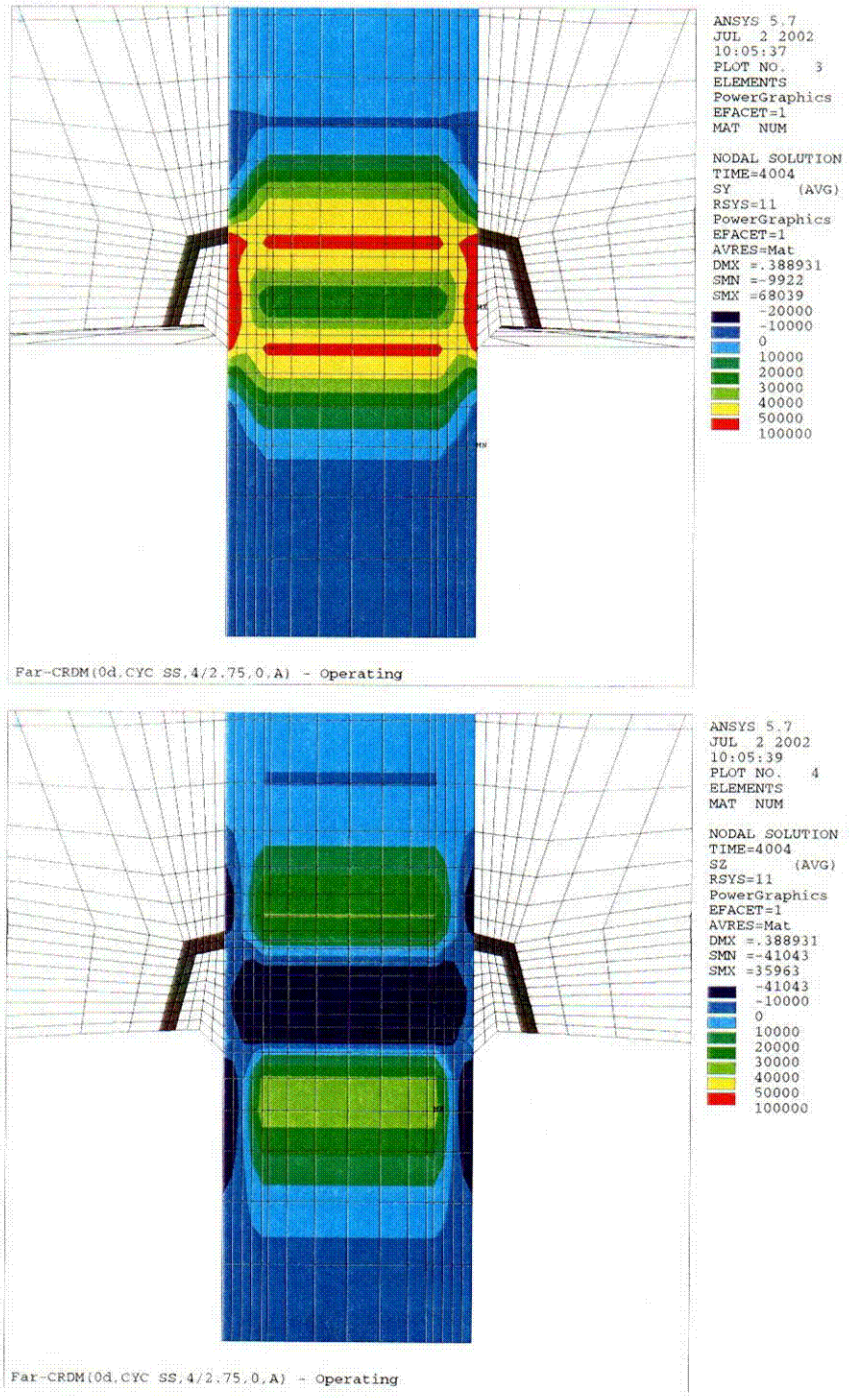

Figure 5-7 Stress Distribution at Steady State Conditions for the Center Penetration (Hoop stress is the top figure; axial stress is the bottom figure) [6]

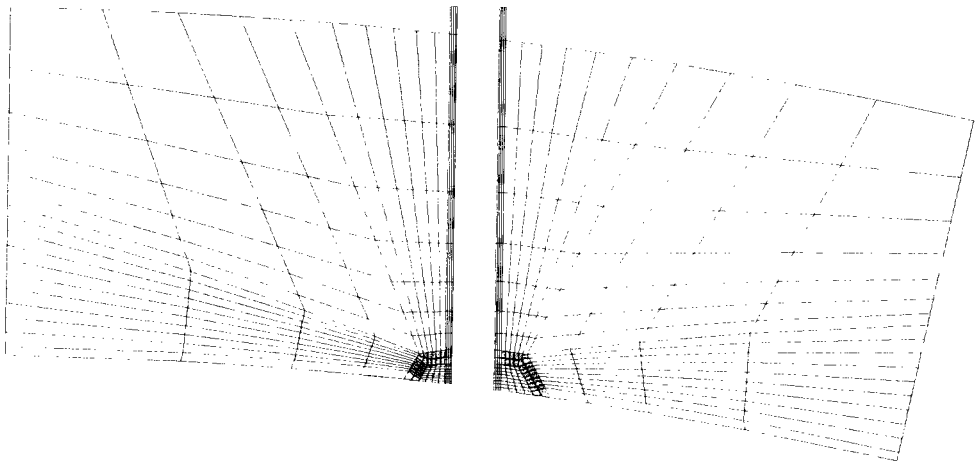

Figure 5-8 Finite Element Model of the Head Vent Penetration [6]

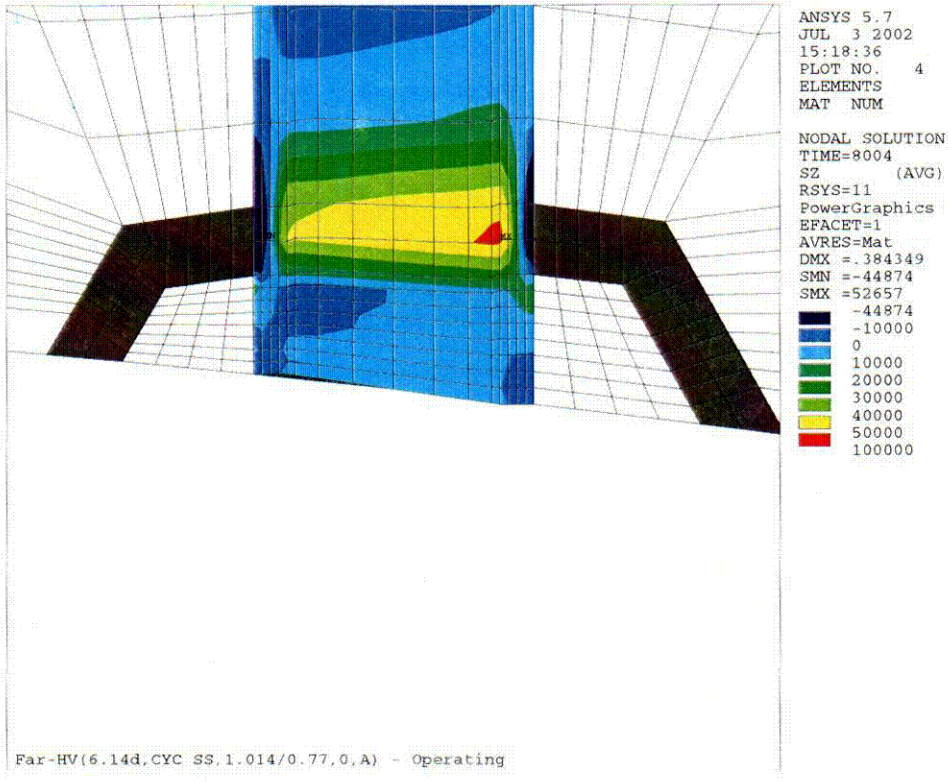

Figure 5-9 Stress Contours in the Head Vent As A Result of Steady State Operation, including Residual Stresses (Hoop stress is the top figure; axial stress is the bottom figure) [6]

C09

6 FLAW TOLERANCE CHARTS

6.1 INTRODUCTION

The flaw tolerance charts were developed using the stress analysis of each of the penetration locations as discussed in Section 5. The crack growth law developed for Farley Units 1 and 2 in Section 4.2 was used for each case, and several flaw tolerance charts were developed for each penetration location. The first series of charts characterizes the growth of a part through flaw, and the second series of charts characterizes the growth of a through-wall flaw in the length direction. The allowable safe operating life of the penetration nozzle may then be directly determined, using the combined results of the two charts. All times resulting from these calculations are effective full power years, since crack growth will only occur at operating temperatures.

6.2 OVERALL APPROACH

The results of the three-dimensional stress analysis of the penetration locations were used directly in the flaw tolerance evaluation.

The crack growth evaluation for the part-through flaws was based on the worst stress distribution through the penetration wall at the location of interest of the penetration. The highest stressed location was found to be in the immediate vicinity of the weld for both the center and outermost penetrations.

The stress profile was represented by a cubic polynomial:

$$\sigma(x) = A_0 + A_1 x + A_2 x^2 + A_3 x^3 \qquad (6\text{-}1)$$

where x = the coordinate distance into the nozzle wall
σ = stress perpendicular to the plane of the crack
A_i = coefficients of the cubic polynomial fit

For the surface flaw with length six times its depth, the stress intensity factor expression of Raju and Newman [5A] was used. The stress intensity factor $K_I(\Phi)$ can be calculated anywhere along the crack front. The point of maximum crack depth is represented by $\Phi = 0$, and this location was also found to be the point of maximum K_I for the cases considered here. The following expression is used for calculating $K_I(\Phi)$, where Φ is the angular location around the crack. The units of $K_I(\Phi)$ are $\text{ksi}\sqrt{\text{in}}$.

$$K_I(\Phi) = \left[\frac{\pi a}{Q}\right]^{0.5} \sum_{j=0}^{3} G_j\left(a/c,\, a/t,\, t/R,\, \Phi\right) A_j\, a^j \qquad (6\text{-}2)$$

The boundary correction factors $G_0(\Phi)$, $G_1(\Phi)$, $G_2(\Phi)$ and $G_3(\Phi)$ are obtained by the procedure outlined in reference [5A]. The dimension "a" is the crack depth, and "c" is the semi crack length, while "t" is the wall thickness. "R" is the inside radius of the tube, and "Q" is the shape factor.

[

]a,c,e

6.3 AXIAL FLAW PROPAGATION

CRDM Surface Flaws

The results of the calculated growth through the wall thickness of the CRDM penetration nozzles for surface flaws are shown in Figures 6-2 through 6-7 for inside surface flaws. For outside surface flaws the results are shown in Figures 6-8 and 6-9. Based on the discussion in MRP-55 report [4H], the use of low crack-tip stress intensity factors less than $15\,MPa\sqrt{m}$ involves assumption not currently substantiated by actual CGR data for CRDM nozzle materials. Therefore, these crack growth curves begin at a flaw depth that results in a stress intensity factor of $15\,MPa\sqrt{m}$ which also exceeds the threshold value of $9\,MPa\sqrt{m}$. This may results in curves with different initial flaw sizes, as seen for example in Figure 6-3. Note that results are only provided for the uphill and downhill sides of each penetration nozzle: the stresses for the regions 90 degrees from these locations are compressive. If flaws are found in such a location, the result for either the uphill or downhill location, whichever is closer, can be used.

Each of these figures allows the future allowable service time to be estimated graphically, as discussed in Section 3. Results are shown for each of the penetration nozzles analyzed in each of these figures. The

stresses are much higher near the attachment weld than at 0.5 inch below or above it, so separate figures have been provided for these three regions. Also, the stresses are different on the downhill side of the penetration as opposed to the uphill side, so these two cross sections have also been treated separately.

Examples have been provided in Section 7 for a range of possible flaw types, so the graphical approach can be completely understood.

CRDM Through-Wall Flaws

The projected crack growth of a through-wall flaw in the CRDM penetration nozzle is the primary concern in evaluating the structural integrity of head penetrations. In some cases, the through-wall flaw may be located sufficiently below the attachment weld that additional time may be required for the flaw to grow up to the attachment weld. To provide a means to evaluate the duration of this additional time, a series of flaw tolerance charts for through-wall flaws were prepared.

Charts were prepared for each of the penetrations evaluated, for both the uphill and downhill locations, as shown in Figures 6-10 through 6-18. In each figure, the through-wall crack length is measured from the bottom of the nozzle itself. Note that in all the cases, the crack slows down significantly as it grows above the weld, due to the decreasing magnitude of the stress field. This provides further assurance that axial flaws will not extend to a critical length which exceeds 15 inches, regardless of the duration of crack growth.

Head Vent

The only flaw tolerance chart that is necessary for the head vent region is for flaws at and above the weld, since there is no portion of the head vent which projects below the weld. Figure 6-21 provides the projected growth of a part through flaw in the head vent just above the attachment weld. The growth through the wall is relatively rapid, because of the thin wall of the head vent.

6.4 CIRCUMFERENTIAL FLAW PROPAGATION

Since circumferentially oriented flaws have been found at five plants (Bugey 3, Oconee 2, Crystal River 3, Davis Besse, and Oconee 3), it is important to consider the possibility of crack extension in the circumferential direction. The first case was discovered as part of the destructive examination of the tube with the most extensive circumferential cracking at Bugey 3, and the crack was found to have extended to a depth of 2.25 mm in a wall thickness of 16 mm. The flaw was found at the outside surface of the penetration (number 54) at the downhill side location, just above the weld.

The circumferential flaws in Oconee Unit 3 were discovered during the process of repairing a number of axial flaws, while the circumferential flaw in Oconee Unit 2 and Crystal River Unit 3 were discovered by UT. Experience gained from these findings has enabled the development of UT procedures capable of detecting circumferential flaws reliably.

To investigate this issue completely, a series of crack growth calculations were carried out for a postulated surface circumferential flaw located just above the head penetration weld, in a plane parallel to the weld itself. This is the only flaw plane which could result in a complete separation of the penetration nozzle,

since all others would result in propagation below the weld, and therefore there is no chance of complete separation because the remaining weld would hold the penetration nozzle in place.

[

]a,c,e

The results of this calculation are shown in Figure 6-20, where it may be seen that the time required for propagation of a circumferential flaw to a point where the integrity of the penetration nozzle would be affected (330-350 degrees) would be at least 45 years. Because of the conservatism in the calculations, where the time period for a surface flaw to become a through-wall flaw was conservatively ignored, it is likely to be even longer.

6.5 FLAW ACCEPTANCE CRITERIA

Now that the projected crack growth curves have been developed, the question remains to be addressed is what flaw size would be acceptable for further service.

Acceptance criteria have been developed for indications found during inspection of reactor vessel upper head penetrations. These criteria were developed as part of an industry program coordinated by NUMARC (now NEI). Such criteria are normally found in Section XI of the ASME Code, but Section XI does not require in-service inspection of these regions and therefore acceptance criteria are not available. In developing the enclosed acceptance criteria, the approach used was very similar to that used

by Section XI, in that an industry consensus was reached using input from both operating utility technical staff and each of the three PWR vendors. The criteria developed are applicable to all PWR plant designs.

Since the discovery of the leaks at Oconee and ANO-1, the acceptance criteria have been revised slightly to cover flaws on the outside diameter of the penetration below the attachment weld, and flaws in the attachment weld. These revised criteria are now in draft form, but they are expected to be acceptable to the NRC, and will be used in these evaluations. The draft portions of the acceptance criteria will be noted below.

The criteria presented herein are limits on flaw sizes which are acceptable. The criteria are to be applied to inspection results. It should be noted that determination of the future service during which the criteria are satisfied is plant-specific and dependent on flaw geometry and loading conditions.

It has been previously demonstrated by each of the owners groups that the penetration nozzles are very tolerant of flaws and there is only a small likelihood of flaw extensions to larger sizes. Therefore, it was concluded that complete fracture of the penetration nozzle is highly unlikely. The approach used here is more conservative than that used in Section XI applications where the acceptable flaw size is calculated by placing a margin on the critical flaw size. For the current application, the critical flaw size would be far too large to allow a practical application of the approach used in Section XI applications, so protection against leakage is the priority.

The acceptance criteria presented herein apply to all the flaw types regardless of orientation and shape. Similar to the approach used in Section XI, flaws are first characterized according to established rules and then compared with acceptance criteria.

Flaw Characterization

Flaws detected must be characterized by the flaw length and preferably flaw depth. The proximity rules of Section XI for considering flaws as separate, may be used directly (Section XI, Figure IWA 3400-1). This figure is reproduced here as Figure 6-22.

When a flaw is detected, its projections in both the axial and circumferential directions must be determined. Note that the axial direction is always the same for each penetration, but the circumferential direction will be different depending on the angle of intersection of the penetration nozzle with the vessel head. The "circumferential" direction of interest here is along the top of the attachment weld, as illustrated in Figure 6-23. It is this angle which will change for each penetration nozzle and the top of the attachment weld is also the plane which could cause separation of the penetration nozzle from the vessel head. The location of the flaw relative to both the top and bottom of the partial penetration attachment weld must also be determined since a potential leak path exists when a flaw propagates through the penetration nozzle wall and up the penetration nozzle past the attachment weld. Schematic of a typical weld geometry is shown in Figure 6-24.

Flaw Acceptance Criteria

The maximum allowable depth (a_f) for axial flaws on the inside surface of the penetration nozzle, at or above the weld is 75 percent of the penetration wall thickness. The term a_f is defined as the maximum

size to which the detected flaw is calculated to grow in a specified time period. This 75 percent limitation was selected to be consistent with the maximum acceptable flaw depth in Section XI and to provide an additional margin against through wall penetration. There is no concern about separation of the penetration nozzle from the vessel head, unless the flaw is above the attachment weld and oriented circumferentially. Calculations have been completed to show that the geometry of all penetrations can support a continuous circumferential flaw with a depth of 75 percent of the wall thickness.

Axial inside surface flaws found below the weld are acceptable regardless of depth as long as their upper extremity does not reach the bottom of the weld during the period of service until the next inspection. Axial flaws which extend above the weld are limited to 75 percent of the wall thickness.

Axial flaws on the outside surface of the penetration nozzle below the attachment weld are acceptable regardless of depth, as long as they do not extend into the attachment weld during the period of service until next inspection. Outside surface flaws above the attachment weld must be evaluated on a case by case basis, and must be discussed with the regulatory authority.

Circumferential flaws located below the weld are acceptable regardless of their depth, provided the length is less than 75 percent of the penetration nozzle circumference for the period of service until the next inspection. Circumferential flaws detected in this area have no structural significance except that loose parts must be avoided. To this end, intersecting axial and circumferential flaws shall be removed or repaired. Circumferential flaws at and above the weld must be discussed with the regulatory authority on a case by case basis.

Surface flaws located in the attachment welds themselves are not acceptable regardless of their depth. This is because the crack growth rate is several times faster than that of the Alloy 600 material, and also because depth sizing capability does not yet exist for indications in the attachment weld.

The flaw acceptance criteria are summarized in Table 6-1. Flaws which exceed these criteria must be repaired unless analytically justified for further service. These criteria have been reviewed and approved by the NRC, as documented in references [7, 8] with the exception of the draft criteria discussed above, for outside surface flaws and flaws in the attachment weld. These criteria are identical with the draft acceptance criteria now being considered for Section XI, for head penetrations.

It is expected that the use of these criteria and crack growth curves will provide conservative predictions of the allowable service time.

Table 6-1 Summary of R.V. Head Penetration Flaw Acceptance Criteria (limits for future growth)

Location	Axial		Circumferential	
	a_f	ℓ	a_f	ℓ
Below Weld (ID)	t	no limit	t	.75 circ.
At and Above Weld (ID)	0.75 t	no limit	*	*
Below Weld (OD)	t	no limit	t	.75 circ.
Above Weld (OD)	*	*	*	*

Note: Surface flaws of any size in the attachment weld are not acceptable.

* Requires case-by-case evaluation and discussion with regulatory authority.

a_f = Flaw Depth as defined in IWB 3600
ℓ = Flaw Length
t = Wall Thickness

Table 6-2 Penetration Geometries

Penetration Type	Wall Thickness (in.)	Penetration OD (in.)
CRDM	0.625	4.000
Head Vent	0.122	1.014

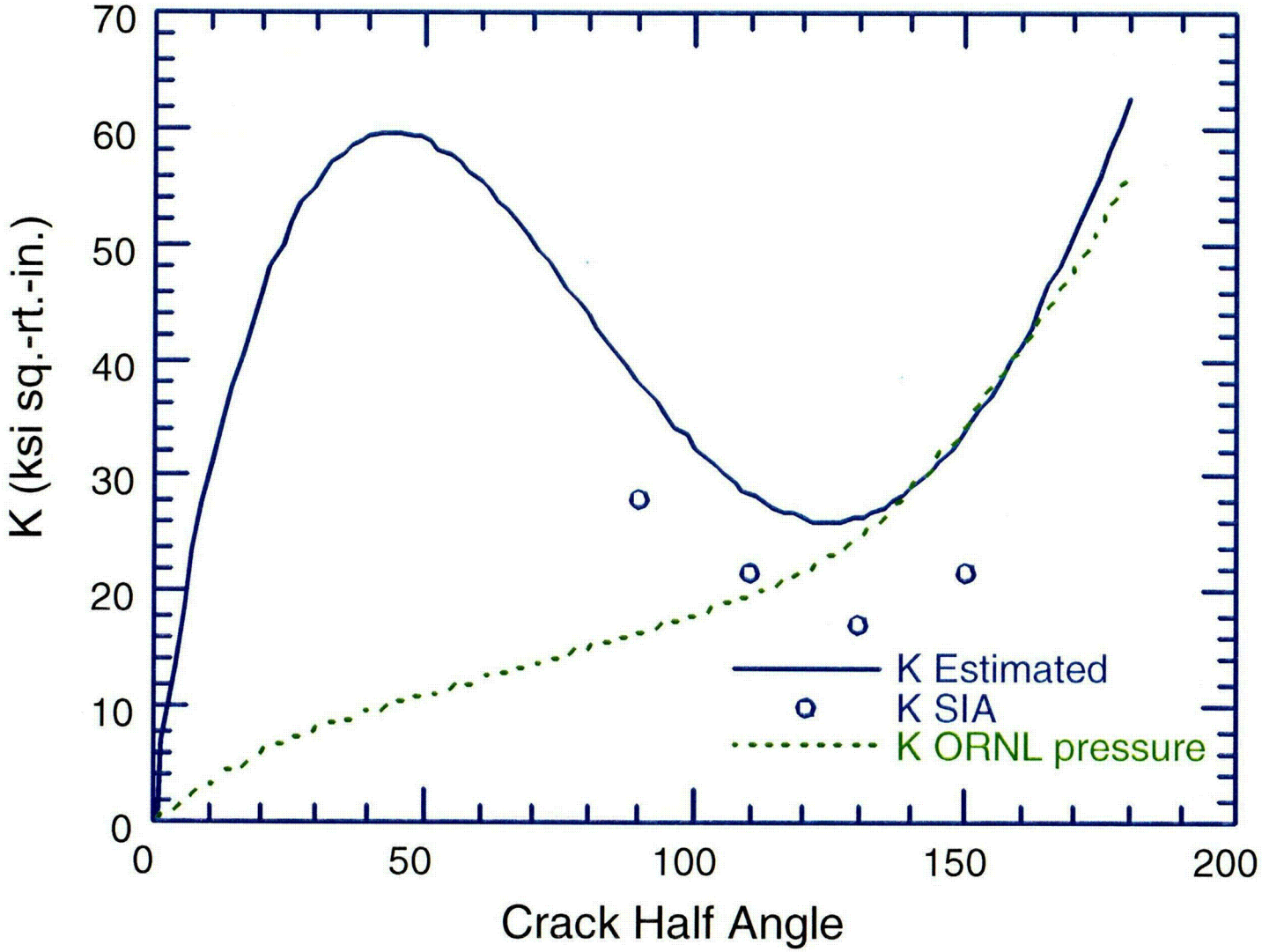

Figure 6-1 Stress Intensity Factor for a Through-Wall Circumferential Flaw in a Head Penetration [5B]

C09A

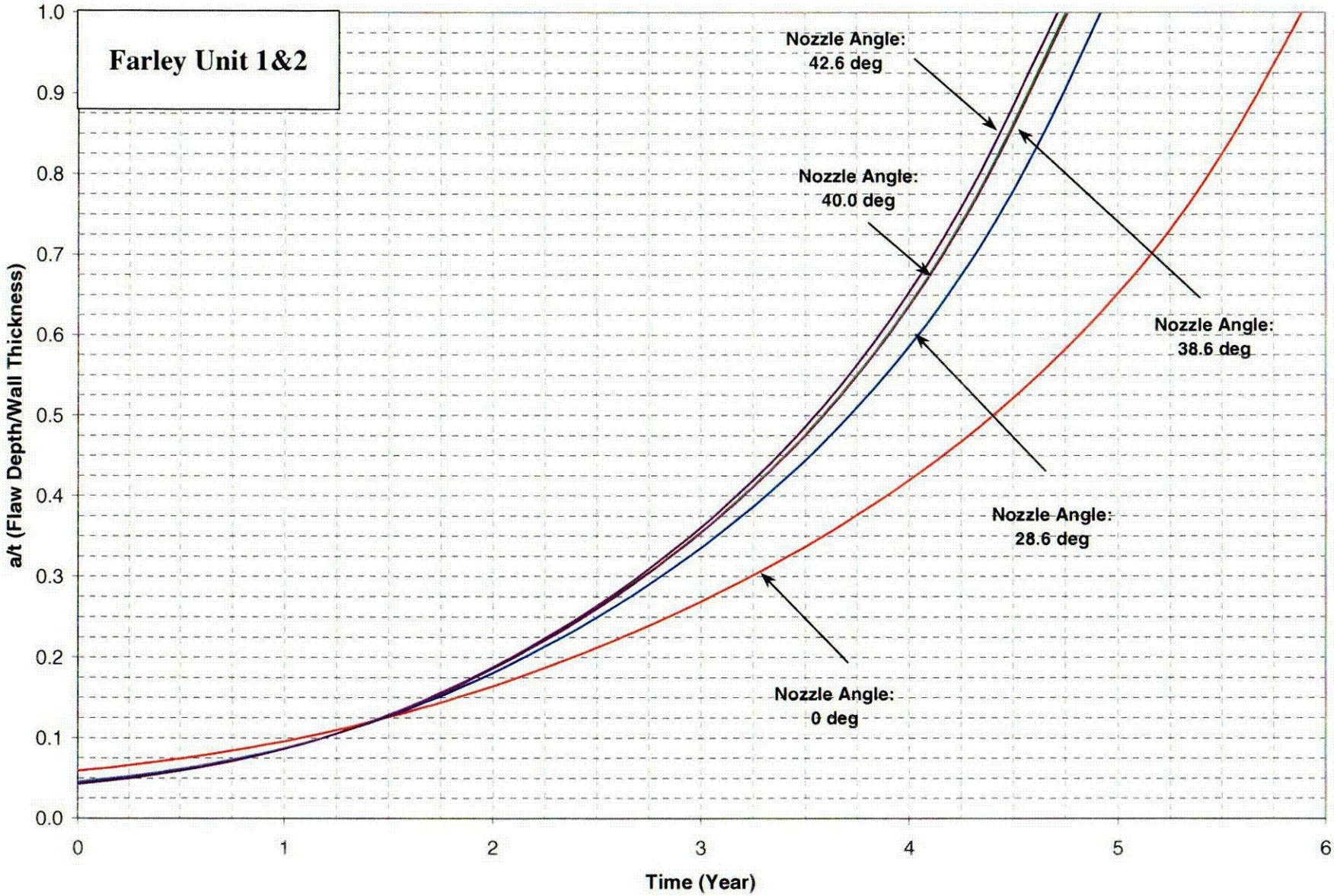

Figure 6-2 **Crack Growth Predictions for Axial Inside Surface Flaws Below the Attachment Weld by More Than 0.5 Inches – Nozzle Uphill Side**

C10

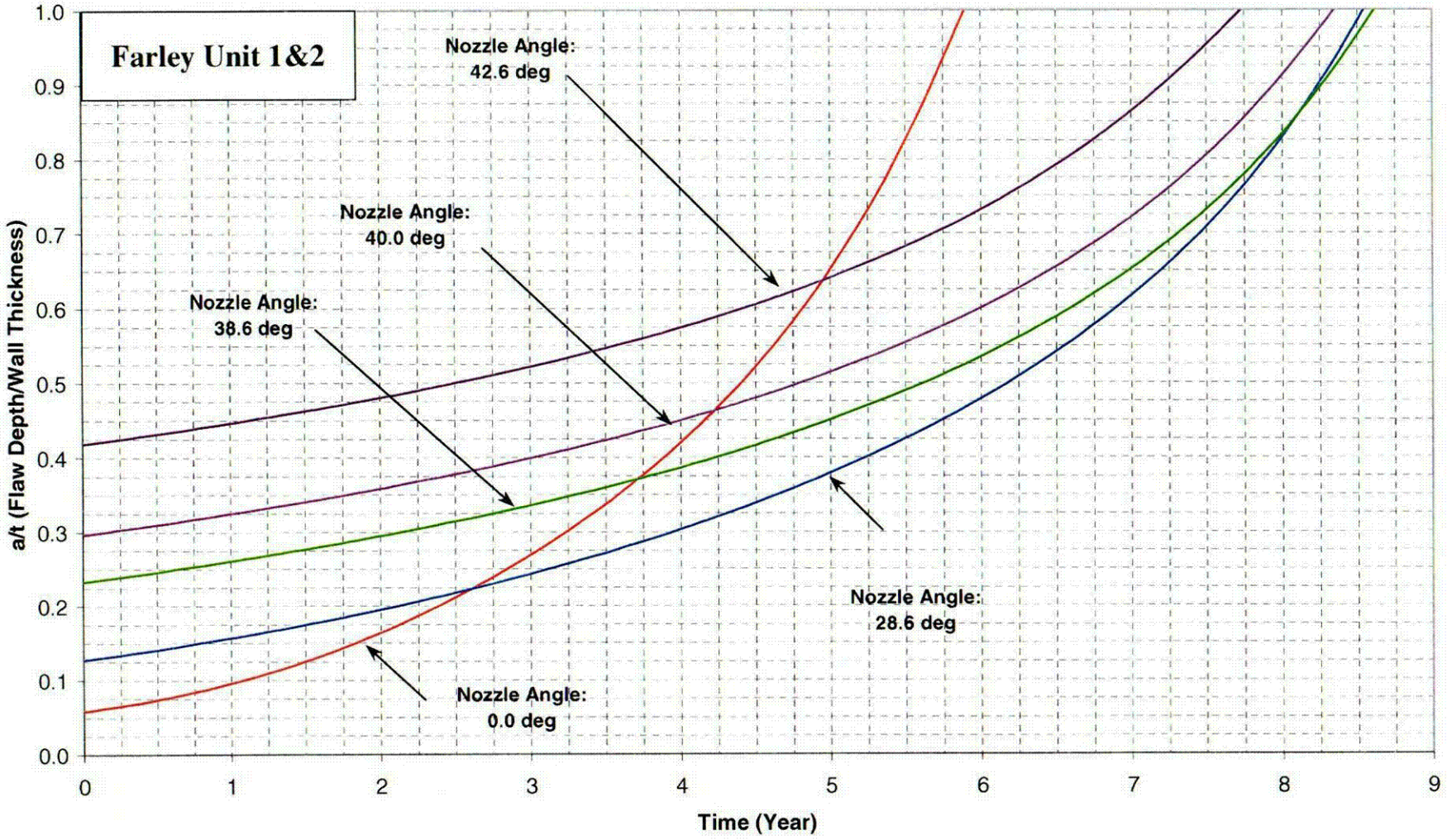

Figure 6-3 **Crack Growth Predictions for Axial Inside Surface Flaws Below the Attachment Weld by More Than 0.5 Inches – Nozzle Downhill Side**

C11

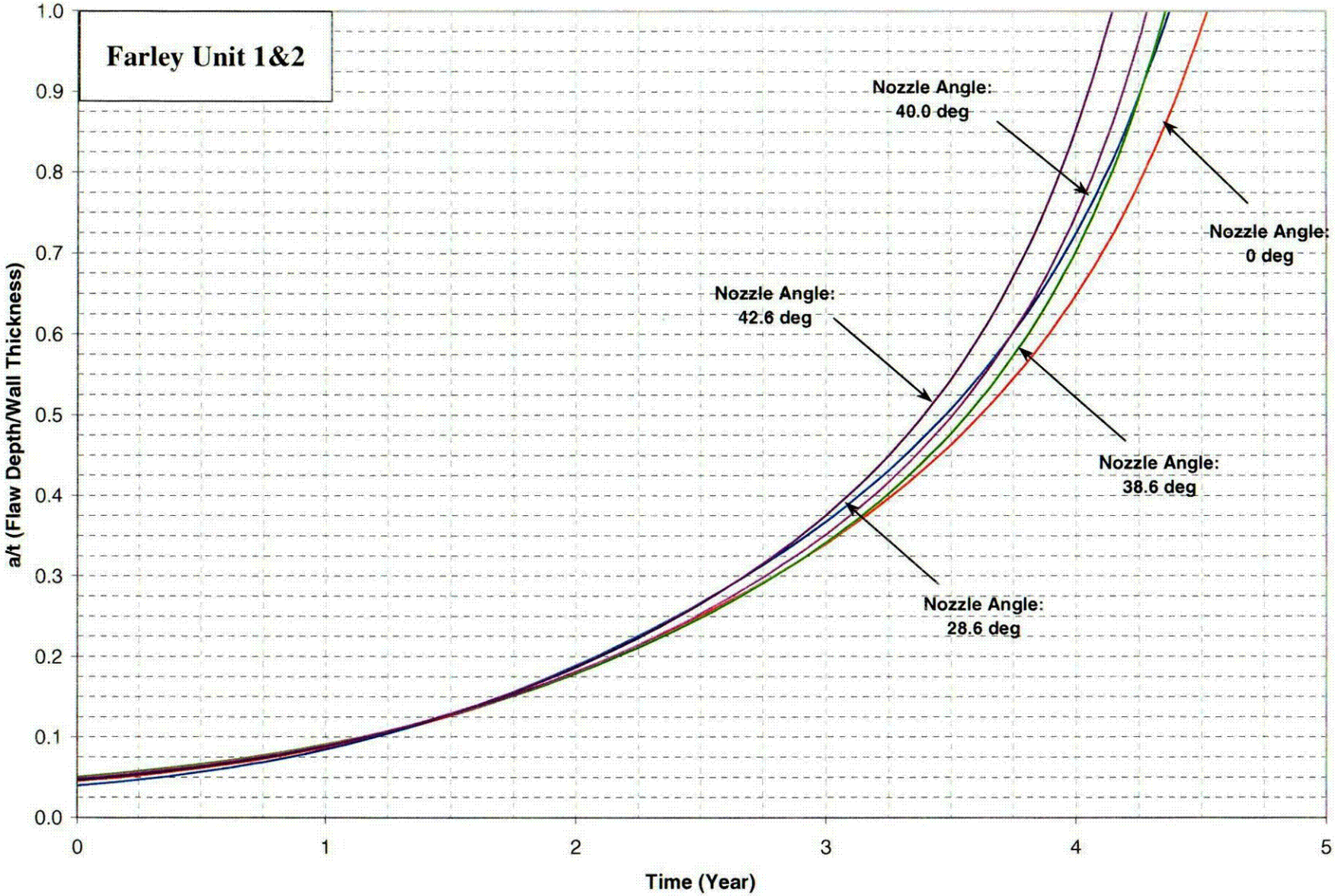

Figure 6-4 Crack Growth Predictions for Axial Inside Surface Flaws Near the Attachment Weld – Nozzle Uphill Side

C12

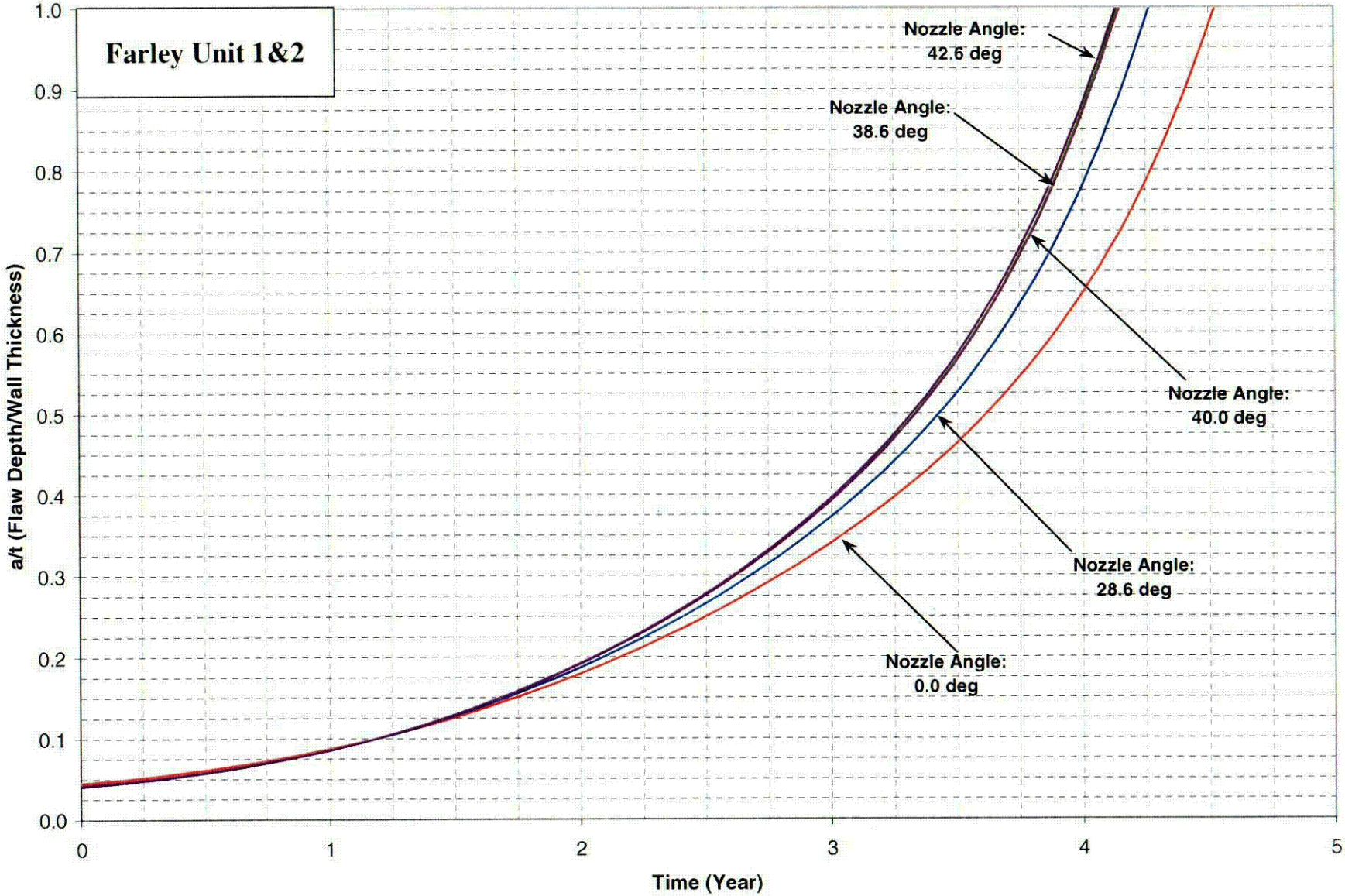

Figure 6-5 Crack Growth Predictions for Axial Inside Surface Flaws Near the Attachment Weld – Nozzle Downhill Side

C13

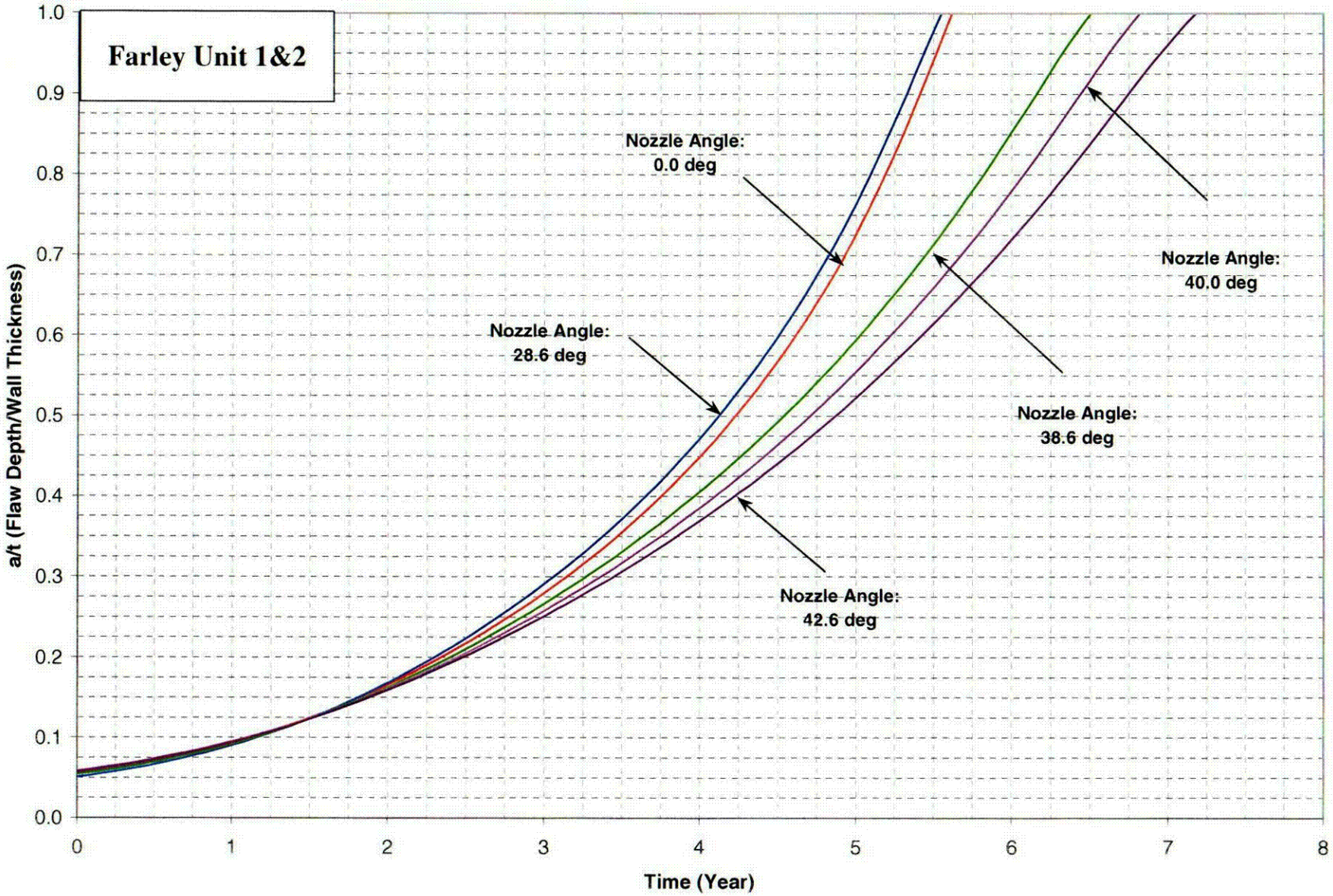

Figure 6-6 Crack Growth Predictions for Axial Inside Surface Flaws Above the Attachment Weld – Nozzle Uphill Side

C14

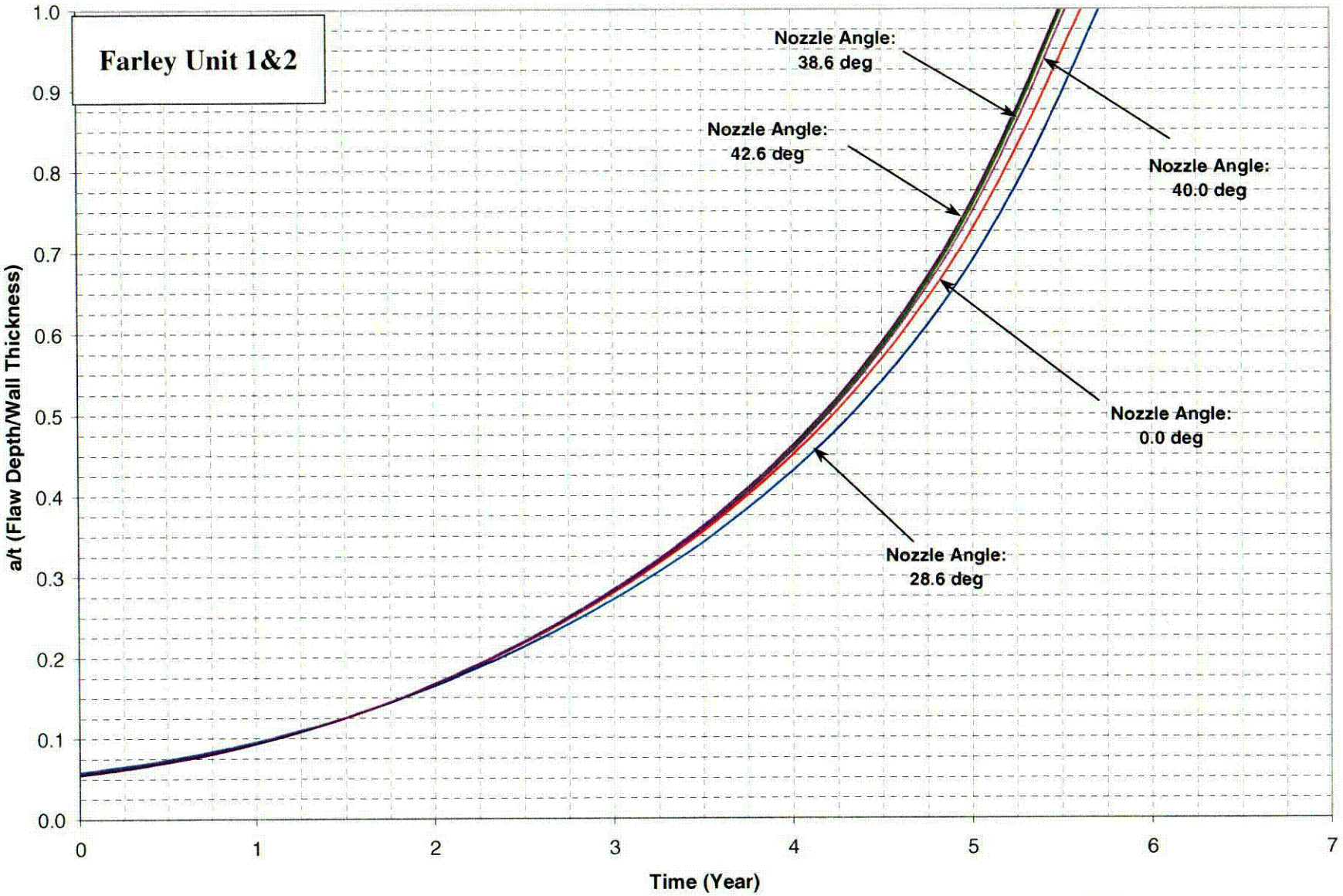

Figure 6-7 Crack Growth Predictions for Axial Inside Surface Flaws Above the Attachment Weld – Nozzle Downhill Side

C15

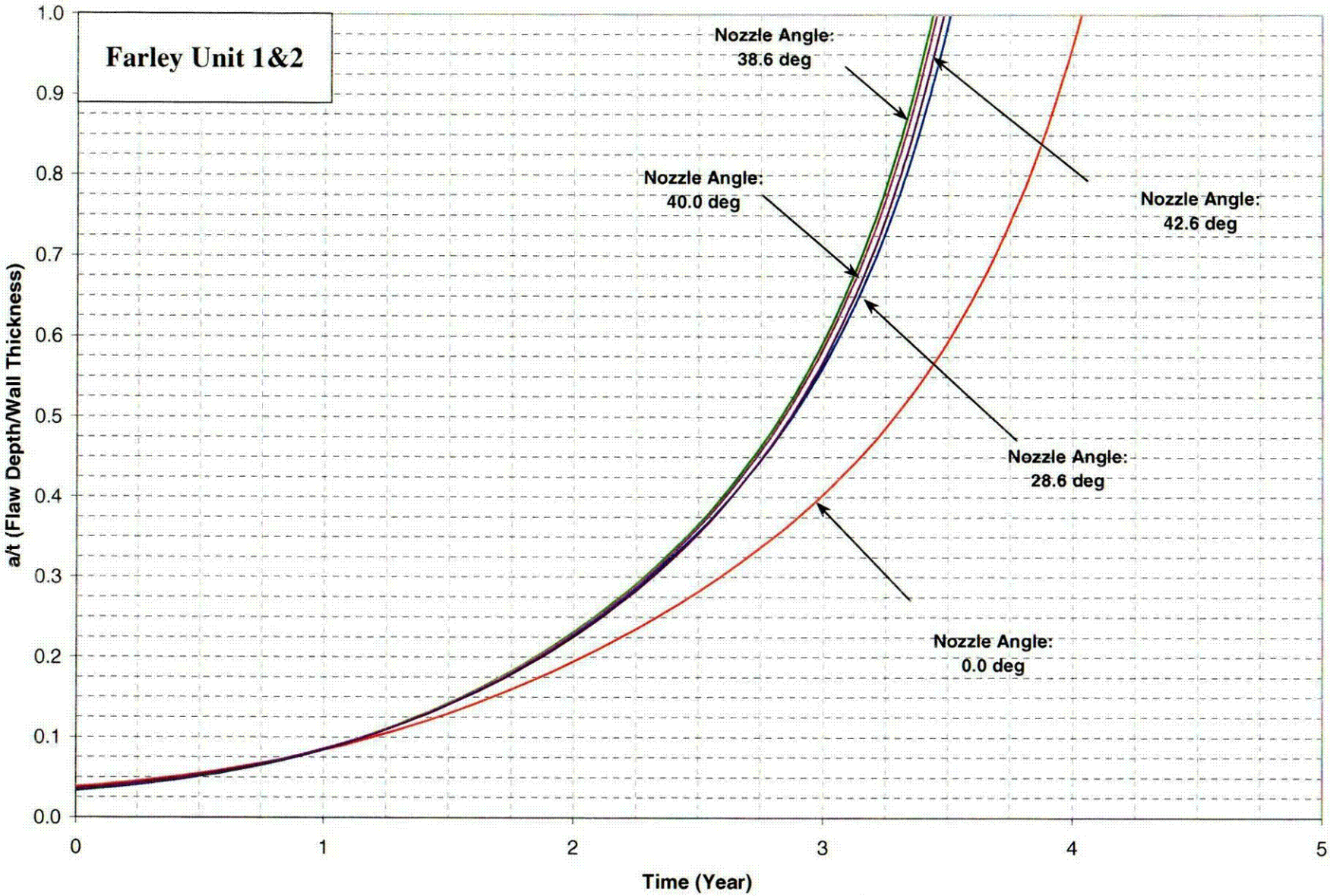

Figure 6-8 Crack Growth Predictions for Axial Outside Surface Flaws Below the Attachment Weld – Nozzle Uphill Side

C16

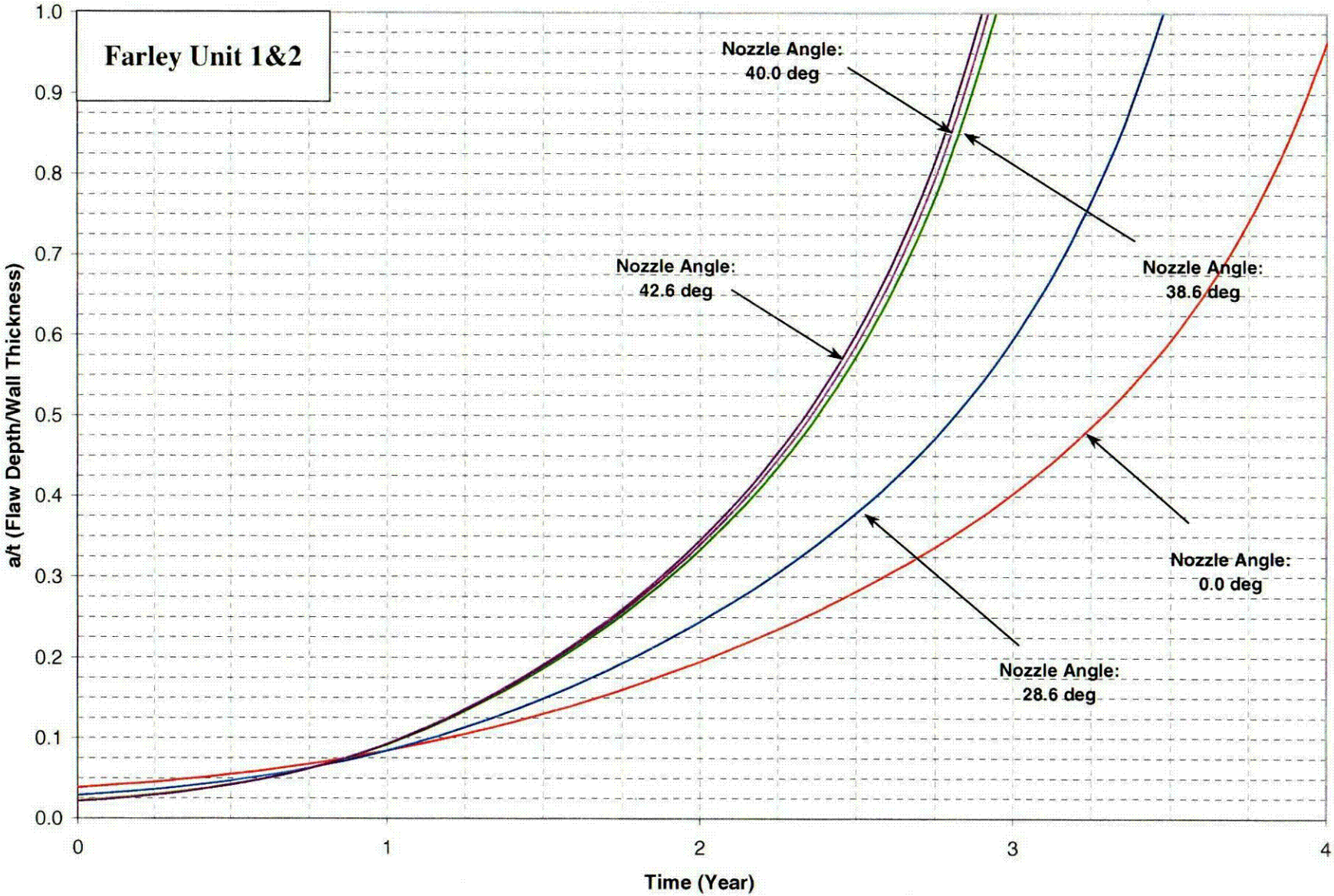

Figure 6-9 Crack Growth Predictions for Axial Outside Surface Flaws Below the Attachment Weld – Nozzle Downhill Side

C17

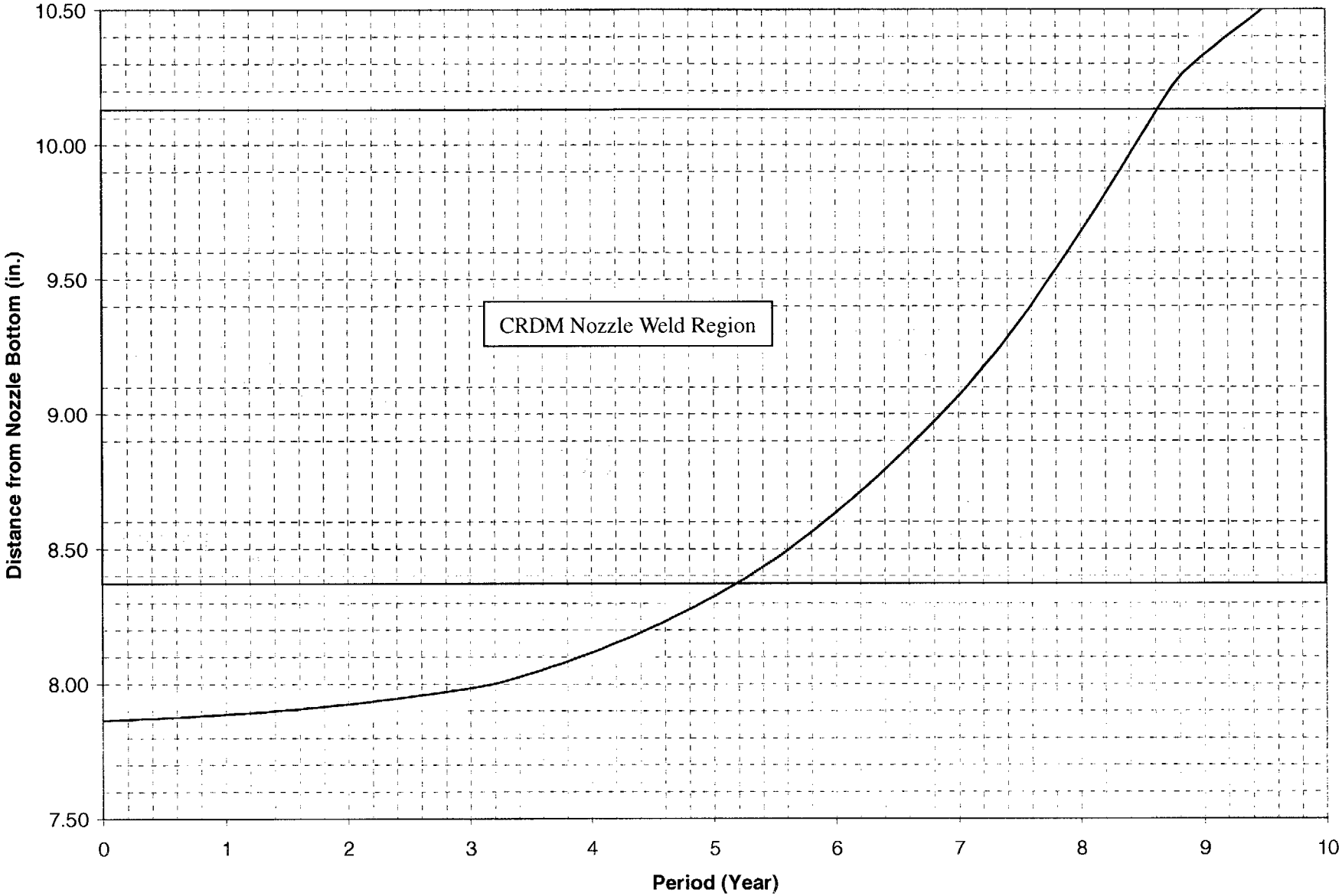

Figure 6-10 Crack Growth Predictions for Through-Wall Axial Flaws Located in the Outermost CRDM (42.6 Degrees) Row of Penetrations – Uphill Side

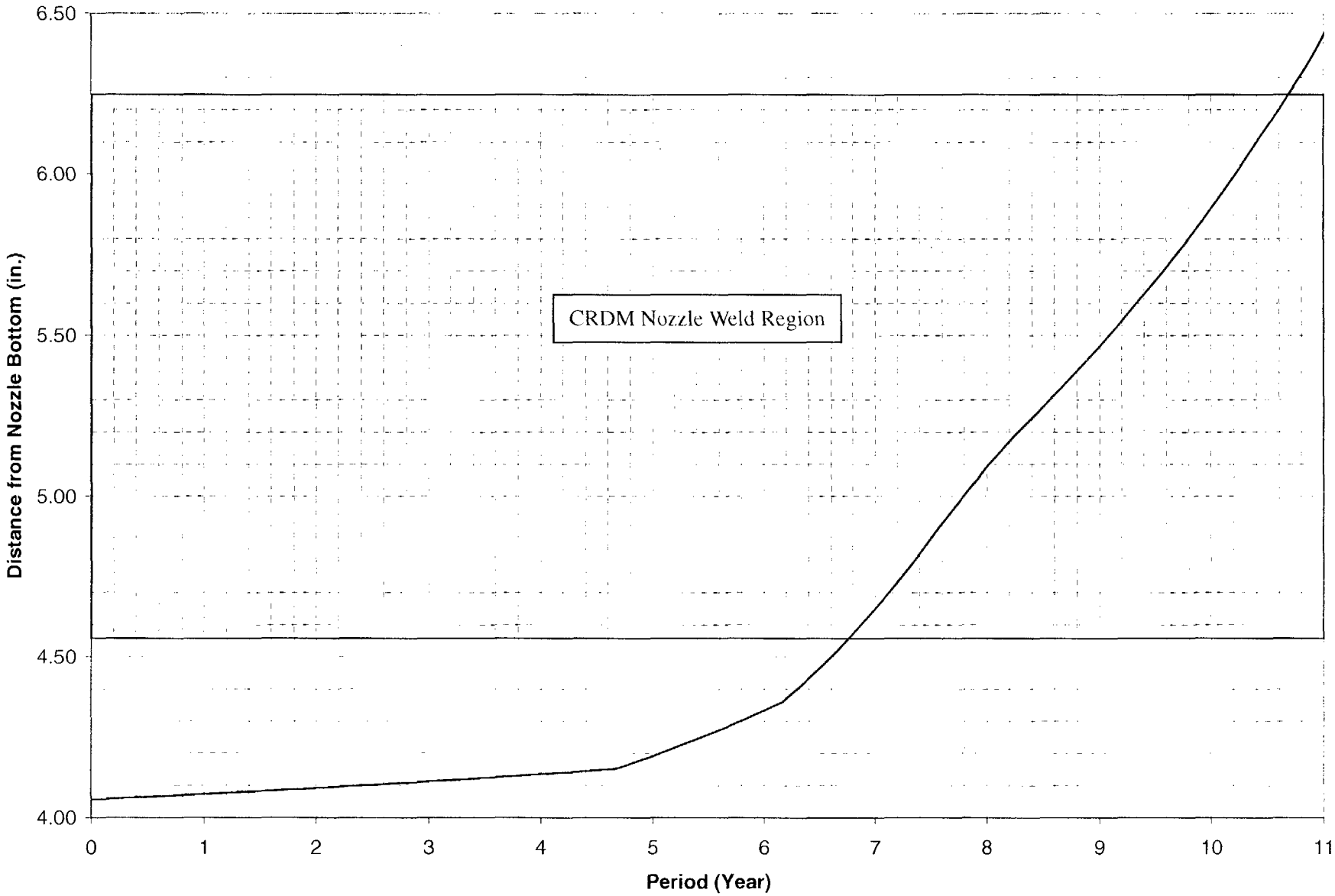

Figure 6-11 Crack Growth Predictions for Through-Wall Axial Flaws Located in the Outermost CRDM (42.6 Degrees) Row of Penetrations – Downhill Side

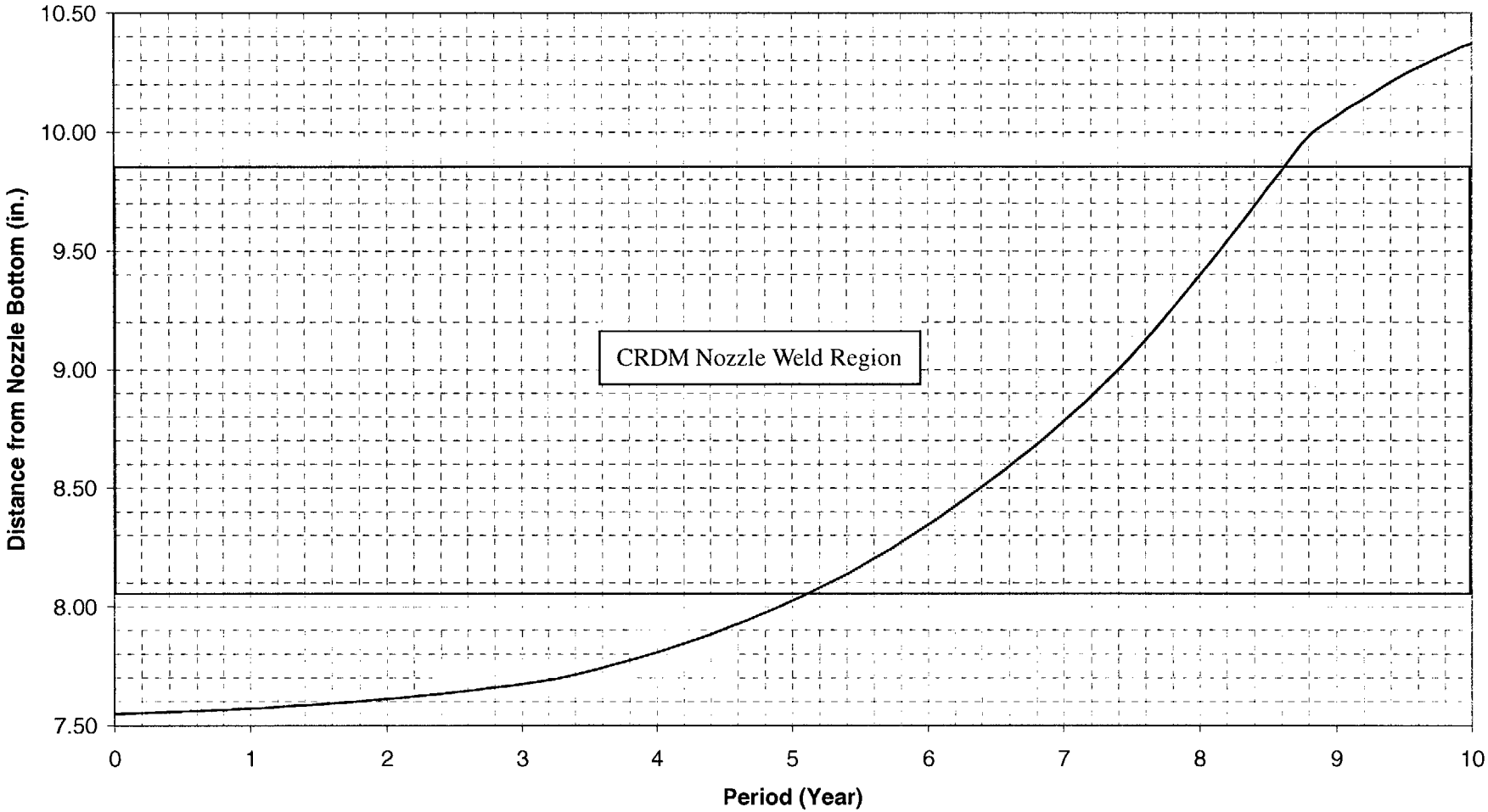

Figure 6-12 Crack Growth Predictions for Through-Wall Axial Flaws Located in the 40.0 Degrees Row of Penetrations – Uphill Side

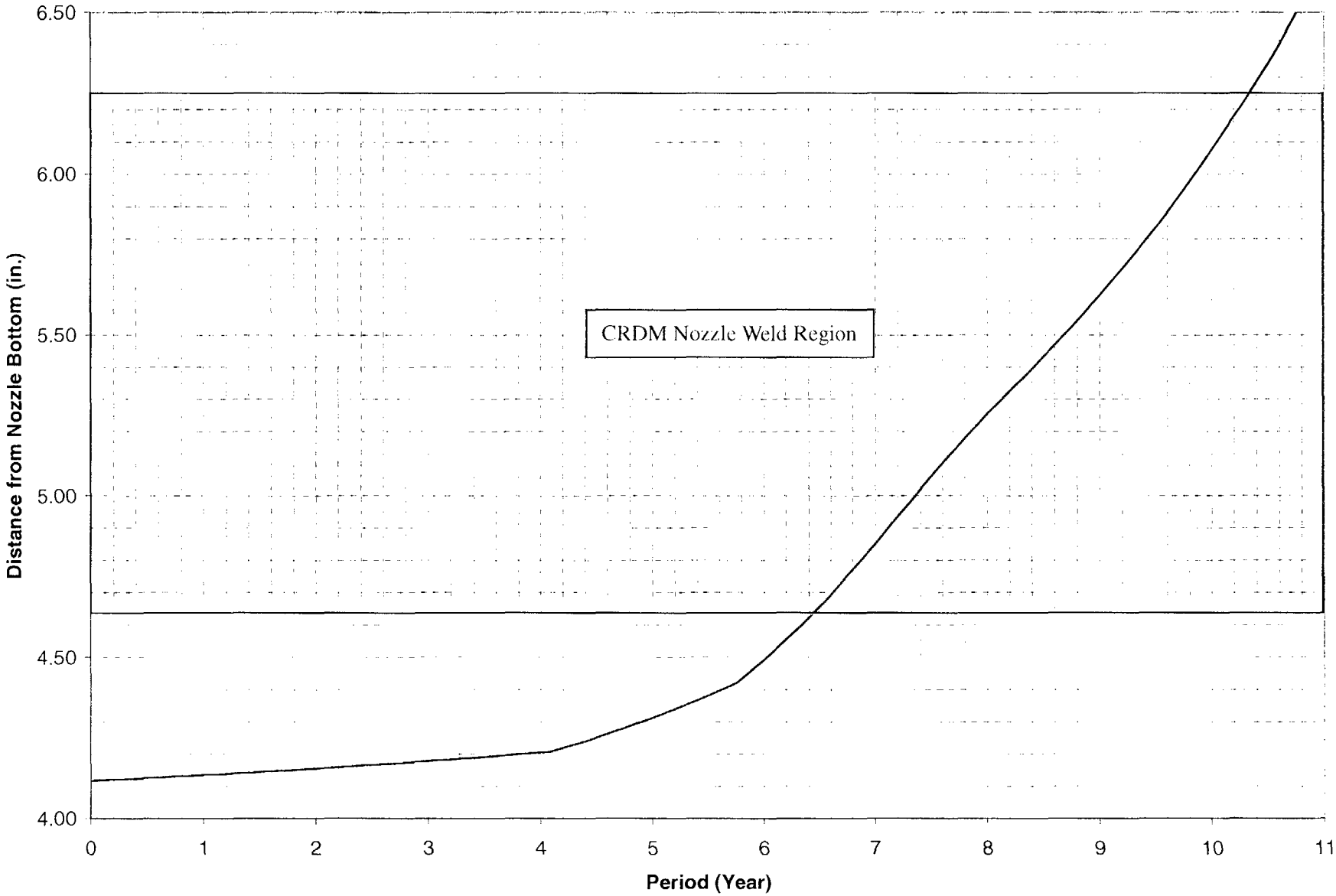

Figure 6-13 Crack Growth Predictions for Through-Wall Axial Flaws Located in the 40.0 Degrees Row of Penetrations – Downhill Side

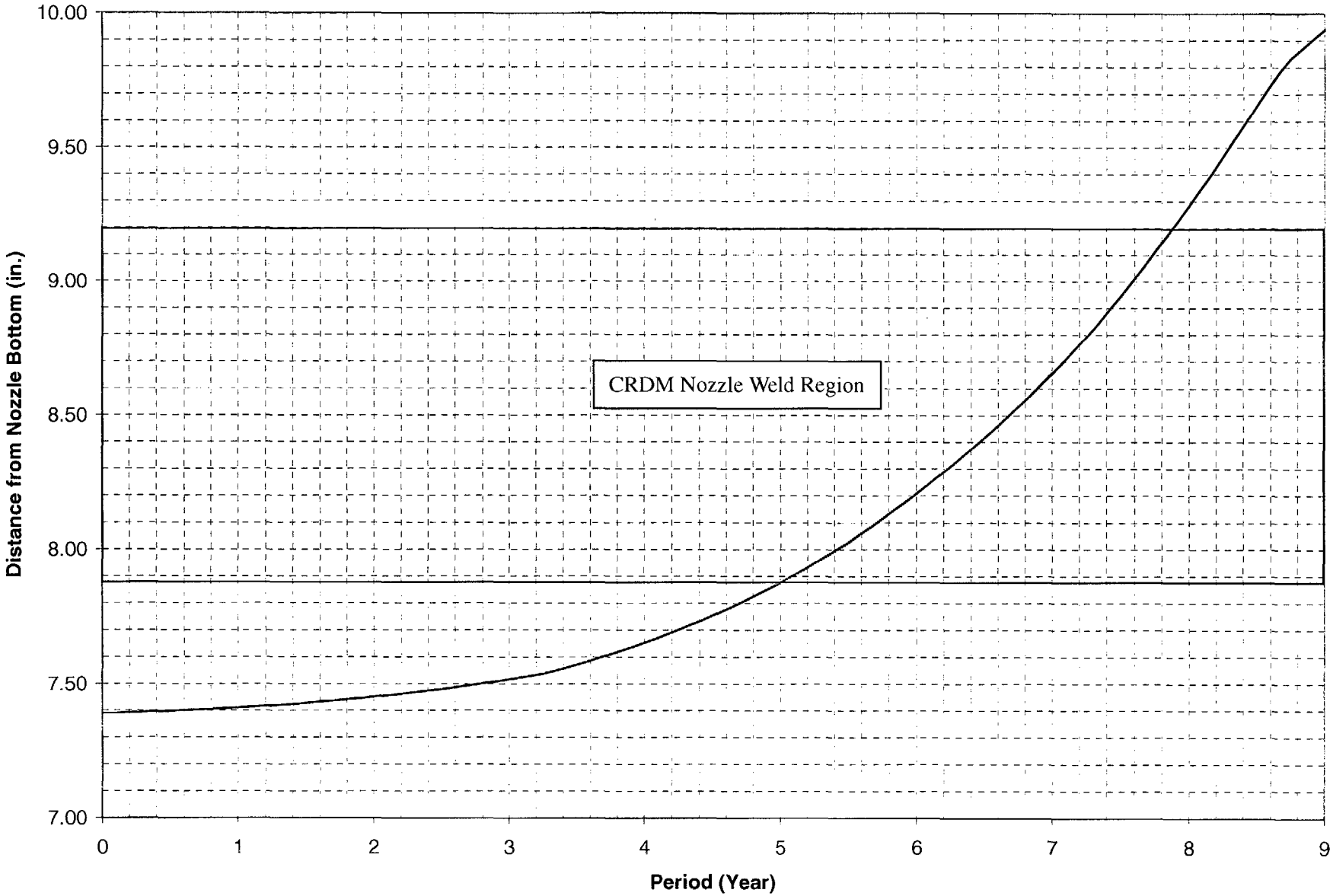

Figure 6-14 Crack Growth Predictions for Through-Wall Axial Flaws Located in the 38.6 Degrees Row of Penetrations – Uphill Side

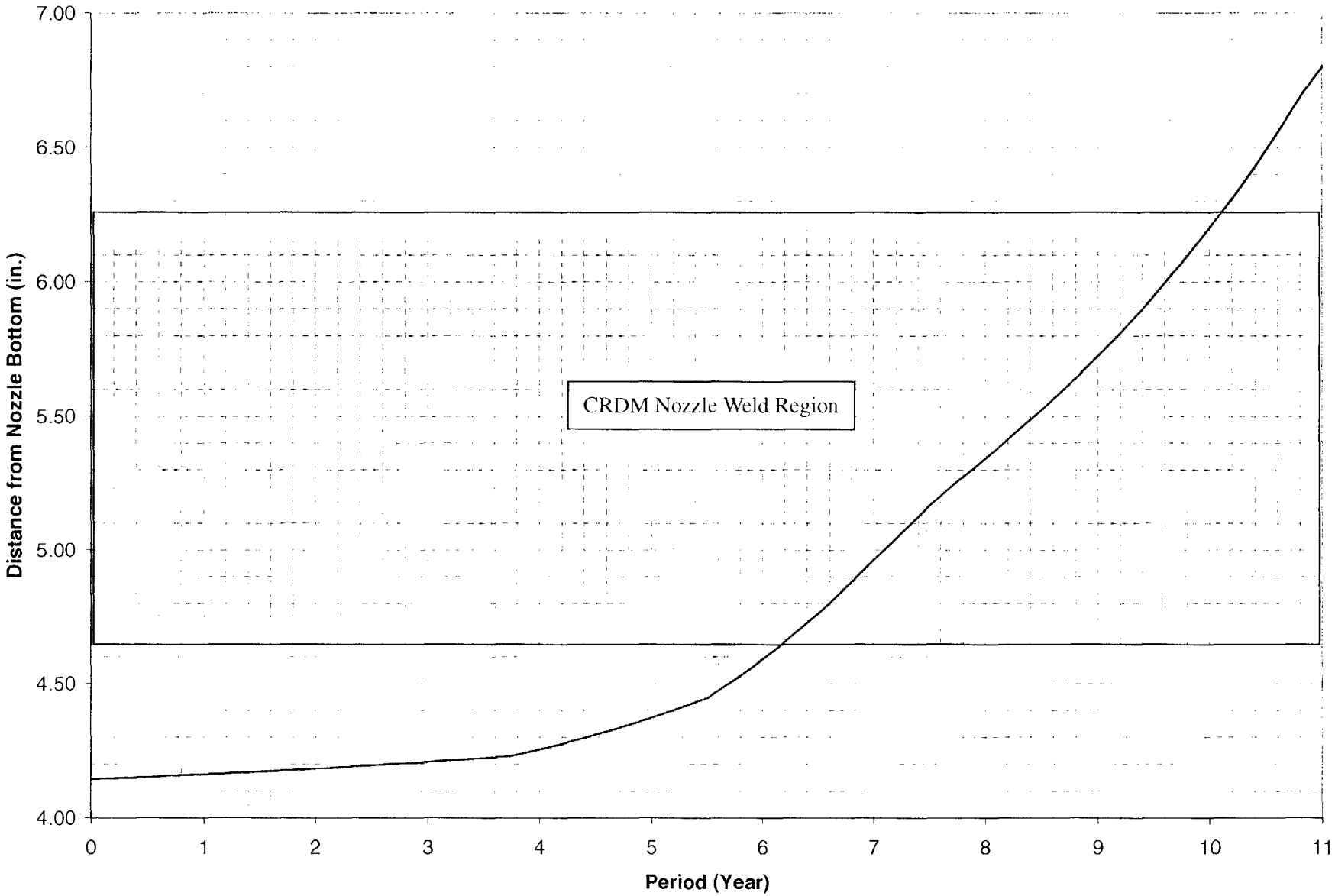

Figure 6-15 Crack Growth Predictions for Through-Wall Axial Flaws Located in the 38.6 Degrees Row of Penetrations - Downhill Side

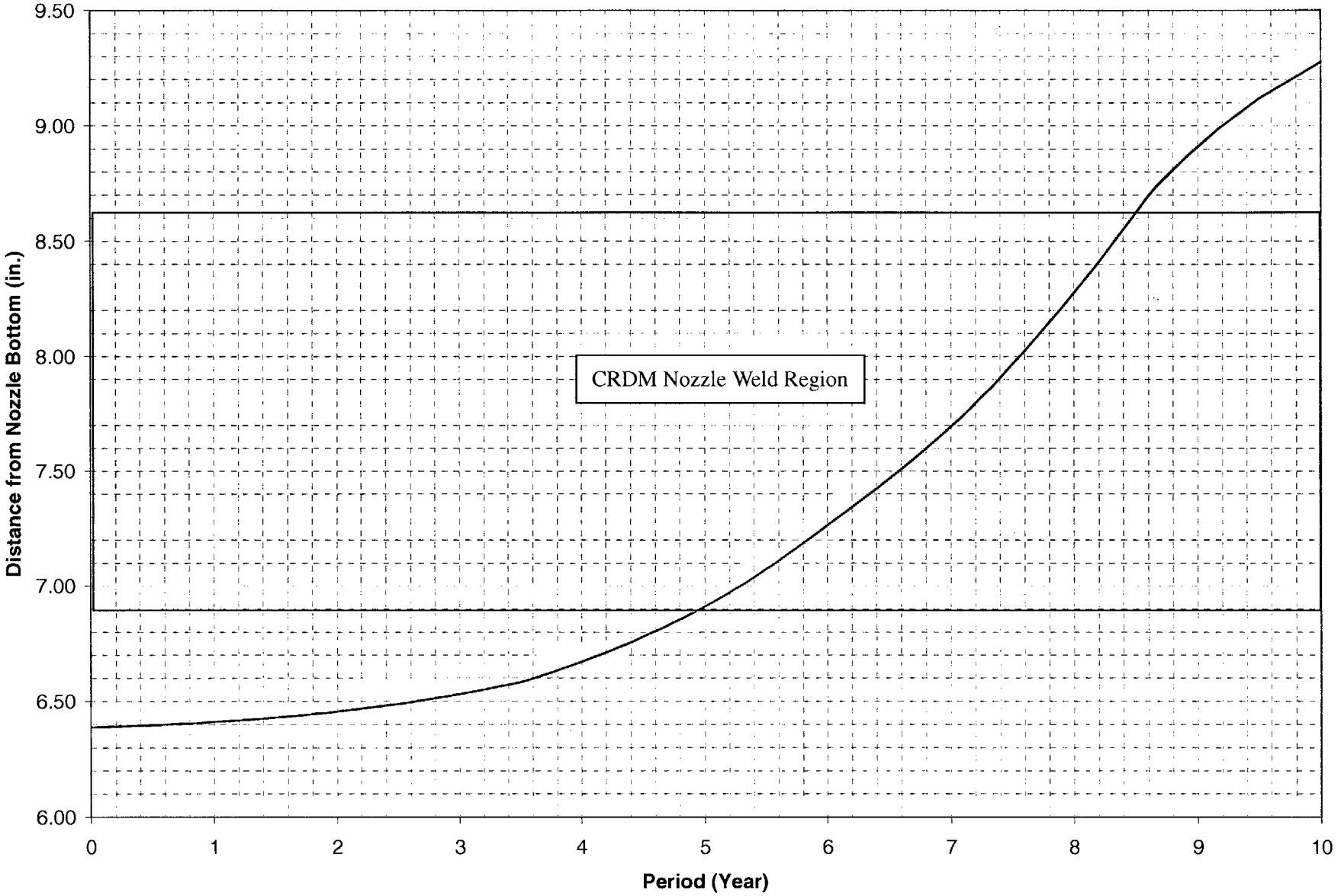

Figure 6-16 Crack Growth Predictions for Through-Wall Axial Flaws Located in the 28.6 Degrees Row of Penetrations – Uphill Side

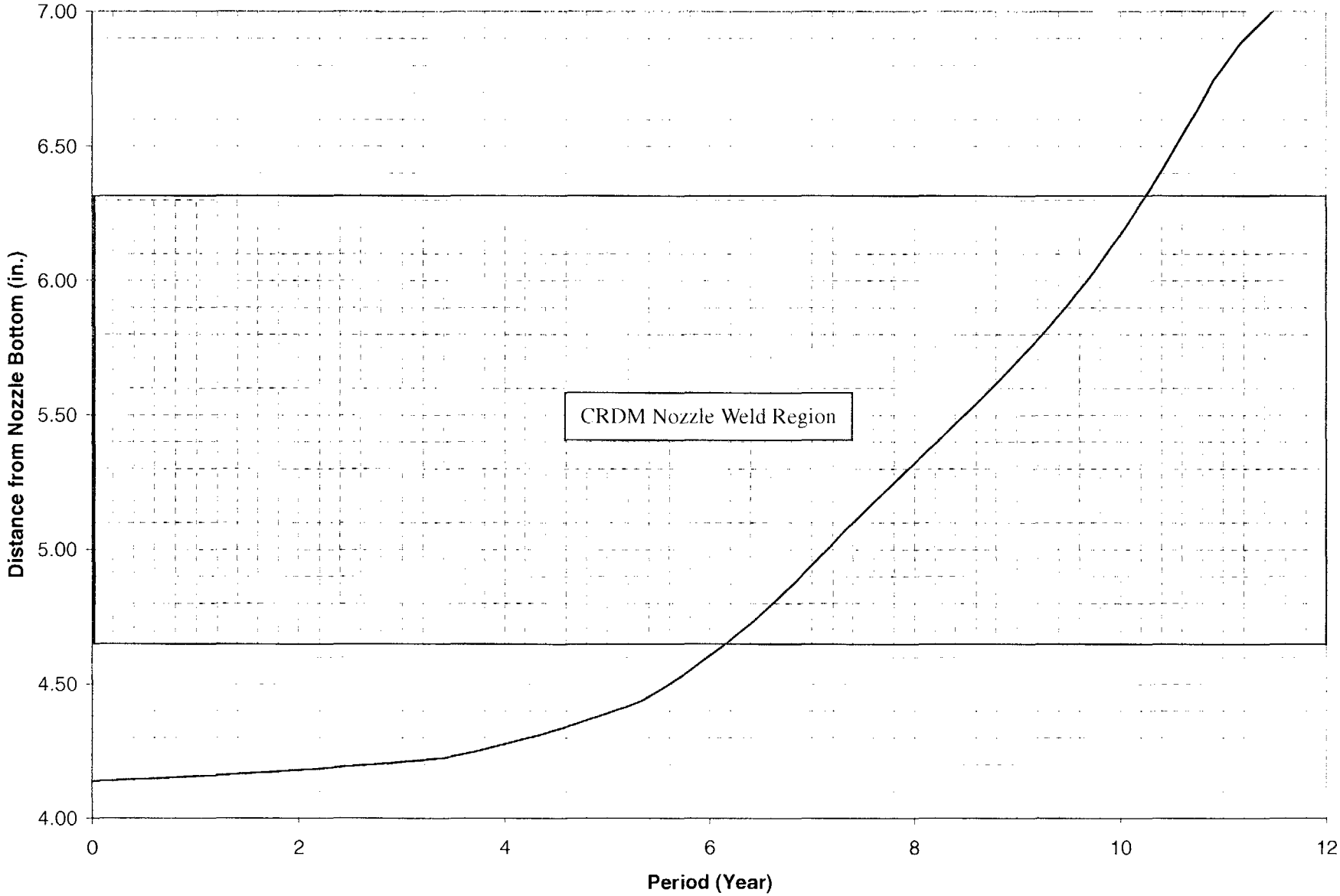

Figure 6-17 Crack Growth Predictions for Through-Wall Axial Flaws Located in the 28.6 Degrees Row of Penetrations – Downhill Side

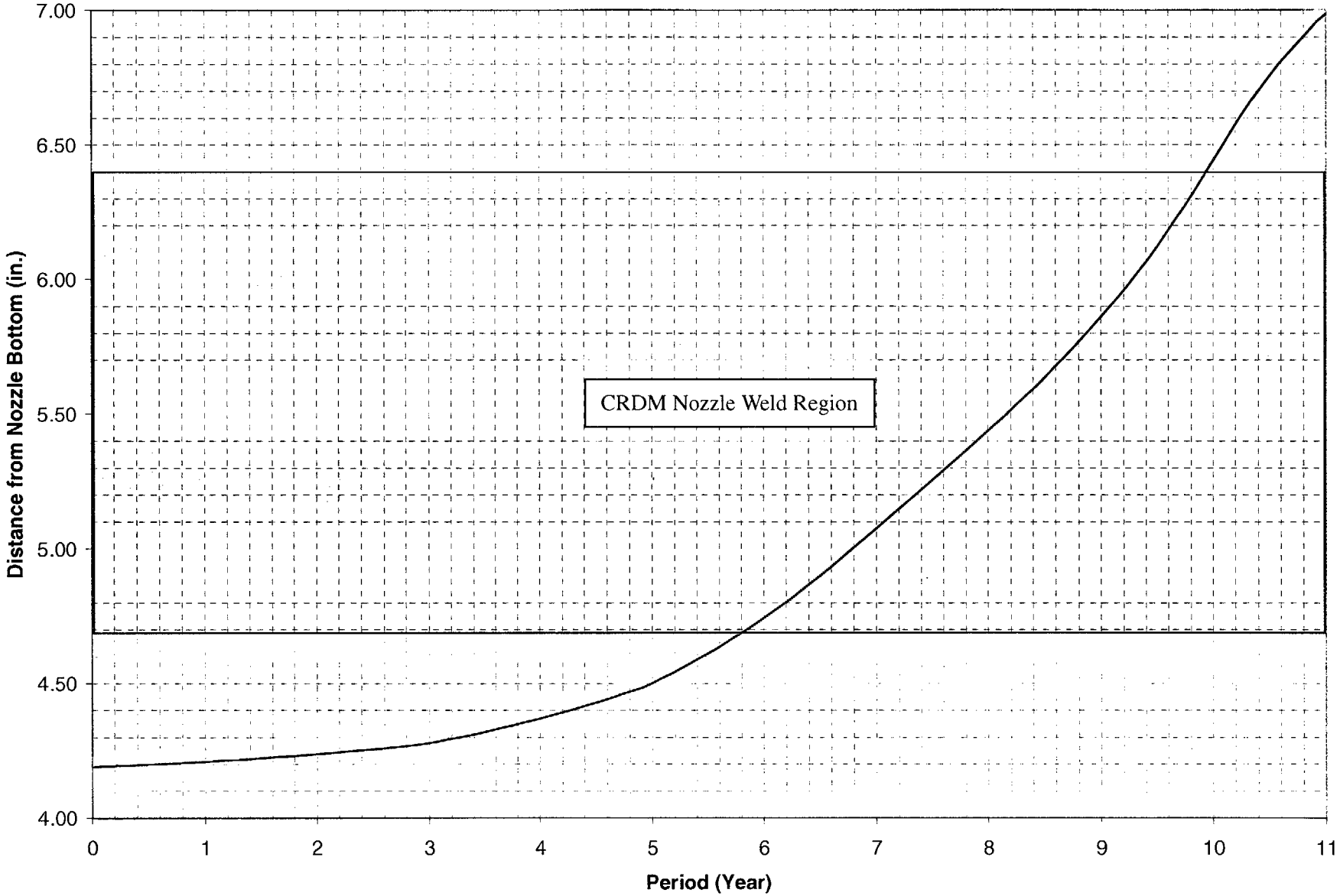

Figure 6-18 Crack Growth Predictions for Through-Wall Axial Flaws Located in the Center Penetration

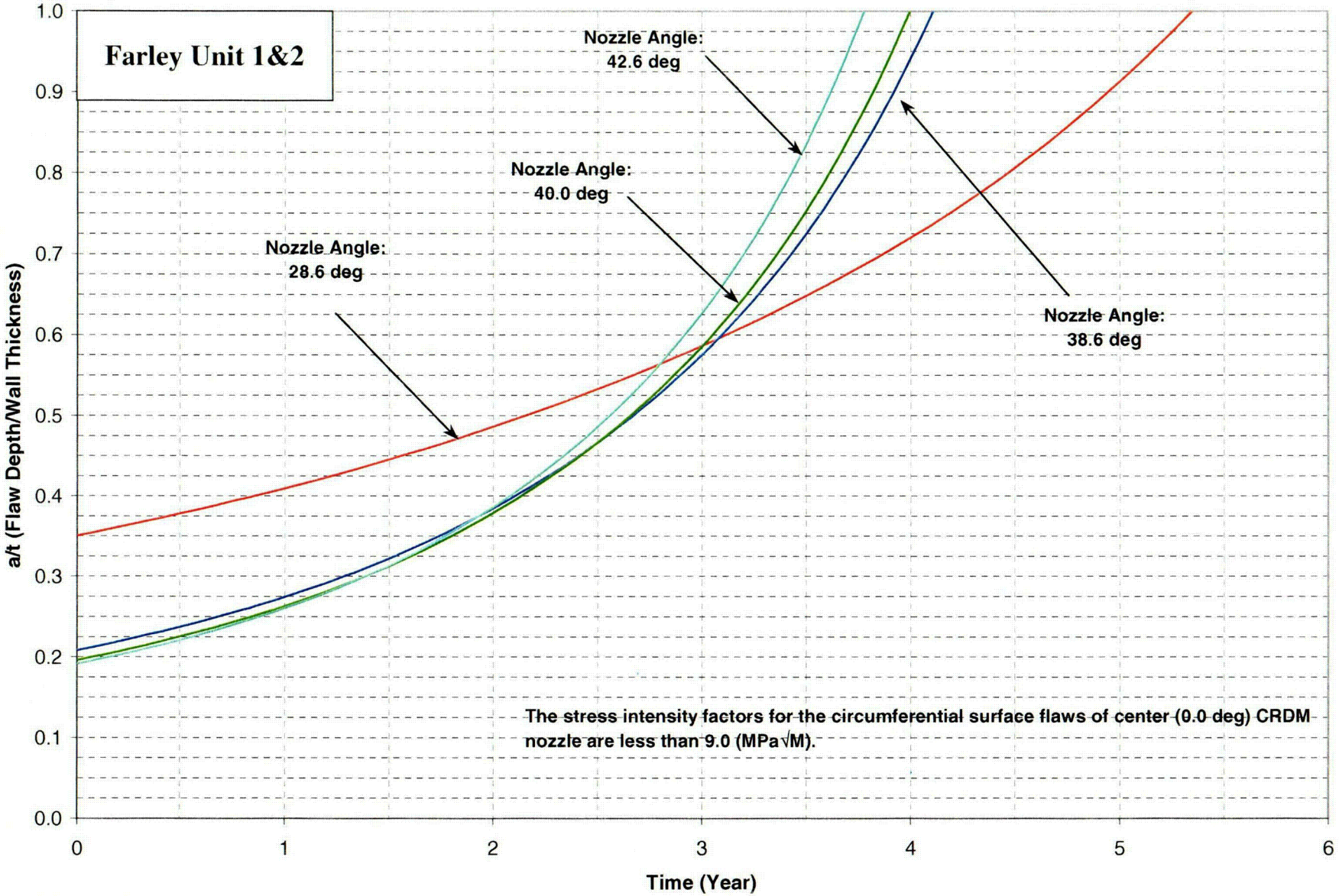

Figure 6-19 Crack Growth Predictions for Circumferential Outside Surface Flaws Near the Top of the Attachment Weld

C18

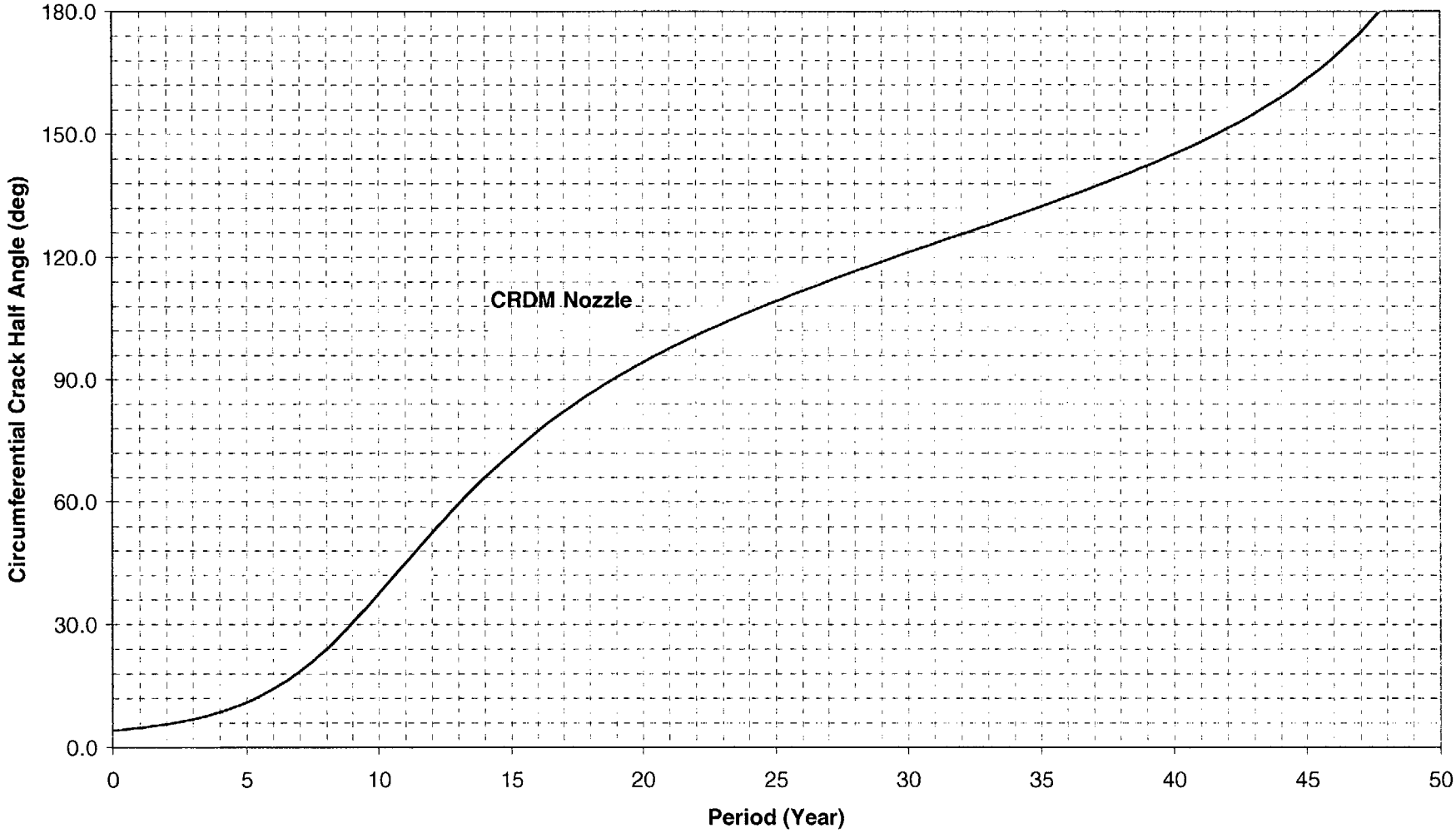

Figure 6-20 Crack Growth Predictions for Circumferential Through-Wall Cracks Near the Top of the Attachment Weld

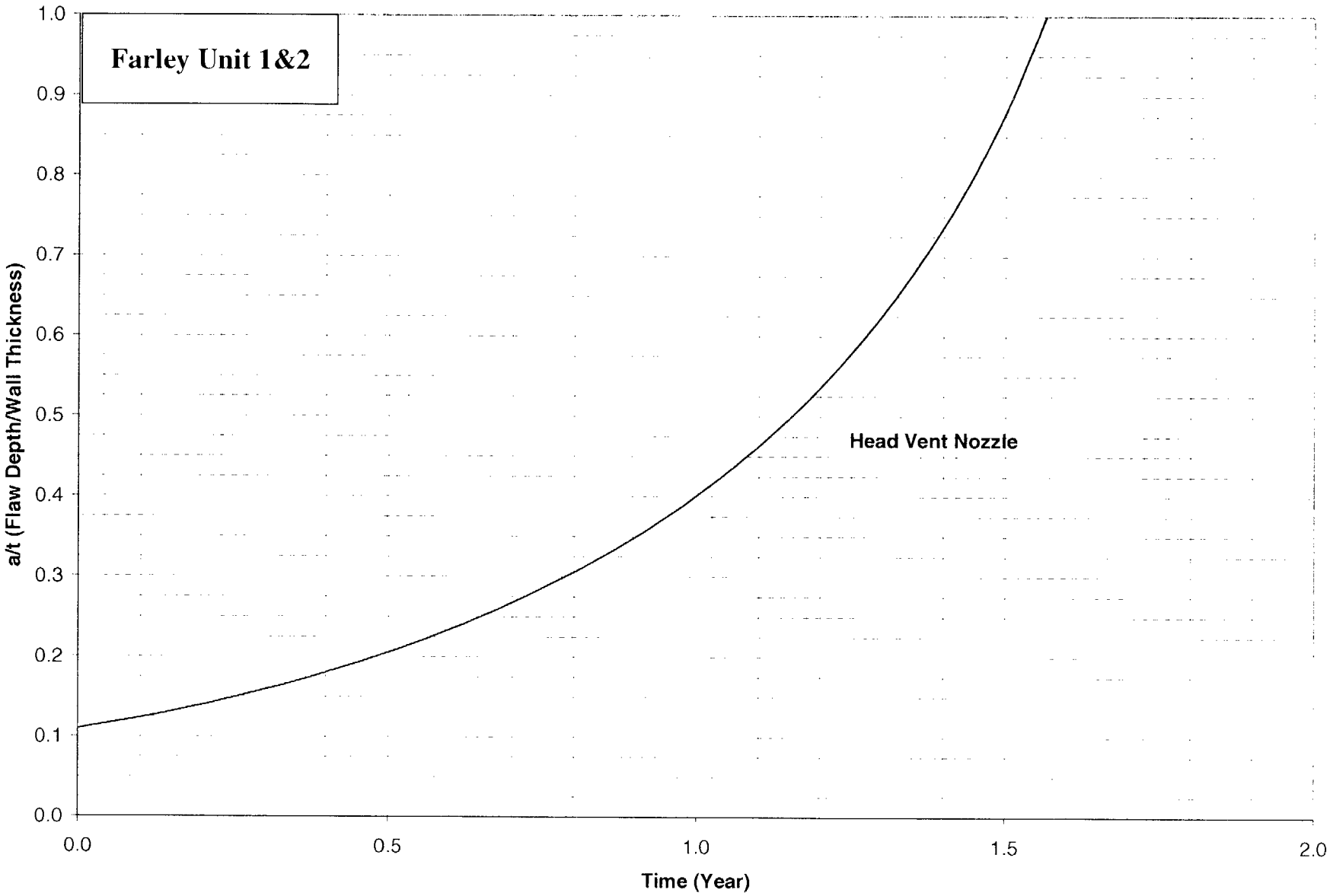

Figure 6-21 Crack Growth Predictions for Axial Inside Surface Flaws – Head Vent

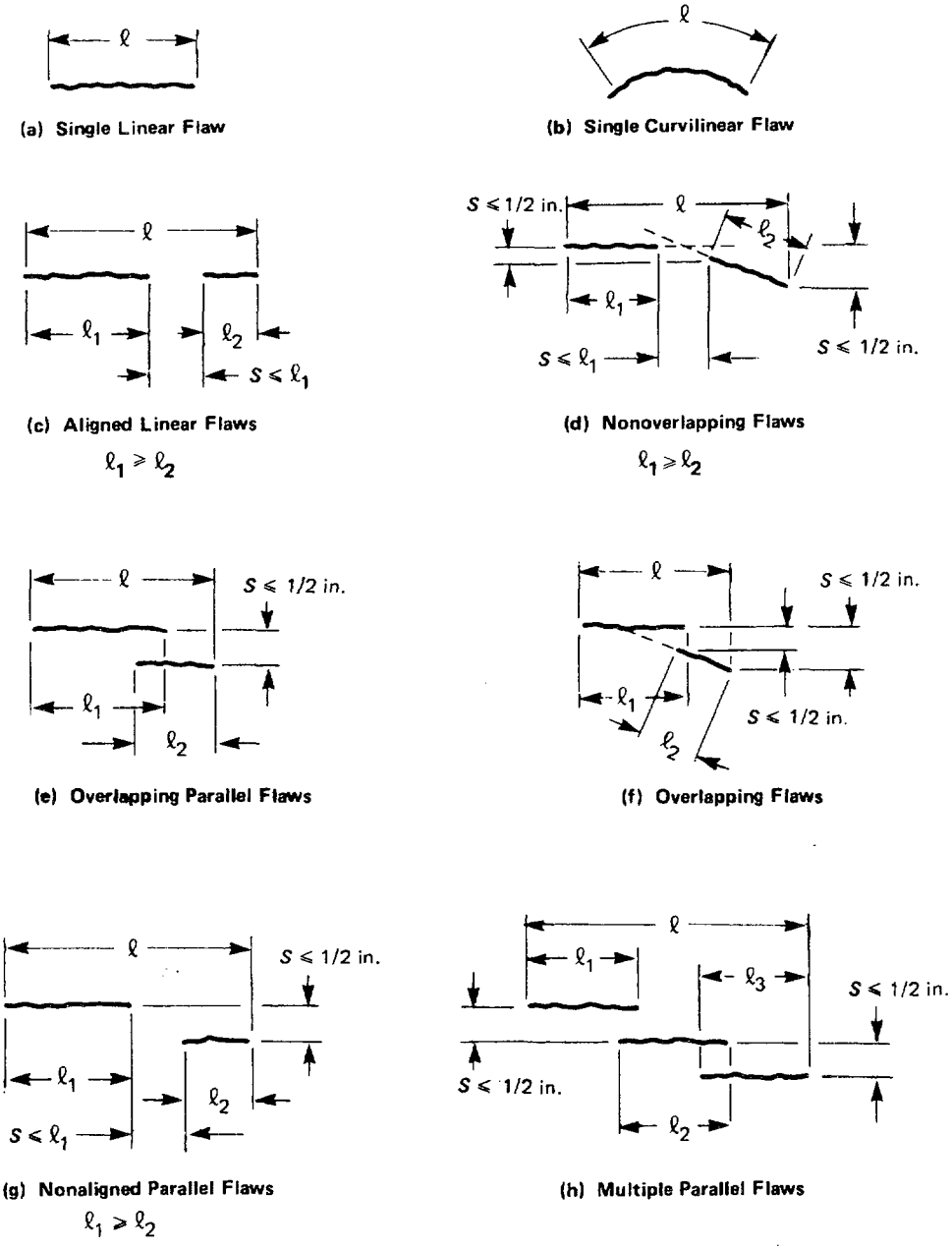

Figure 6-22 Section XI Flaw Proximity Rules for Surface Flaws (Figure IWA-3400-1)

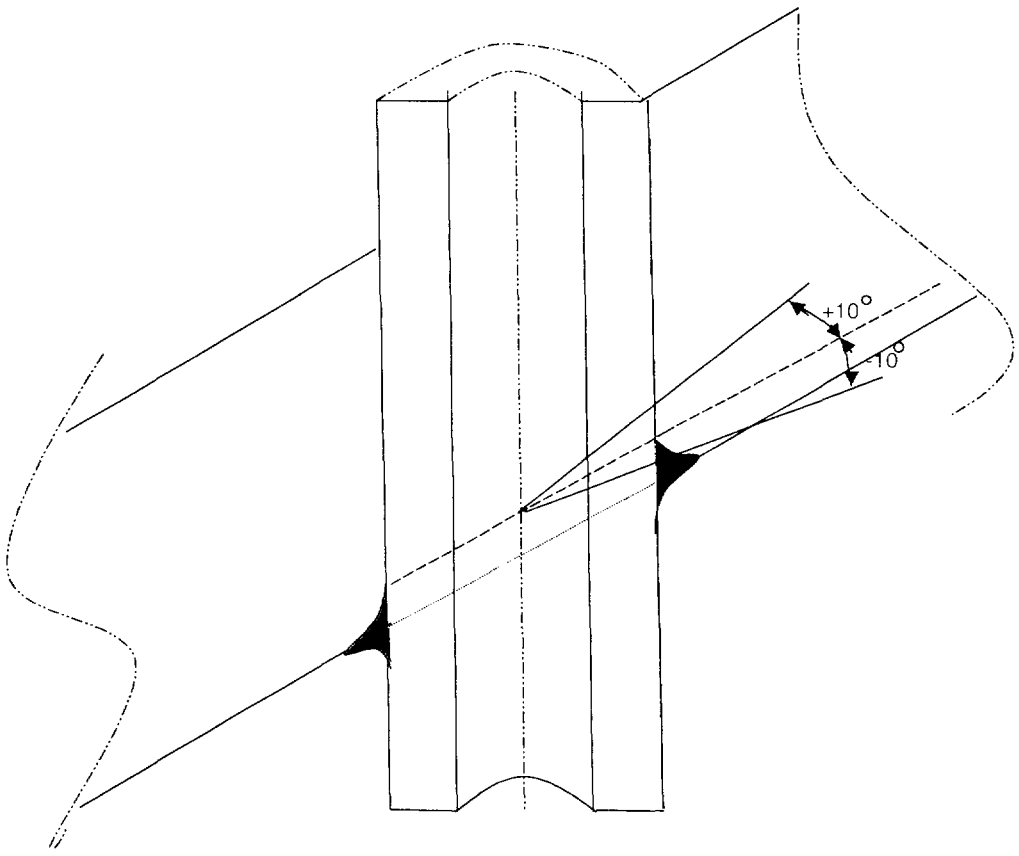

Figure 6-23 Definition of "Circumferential"

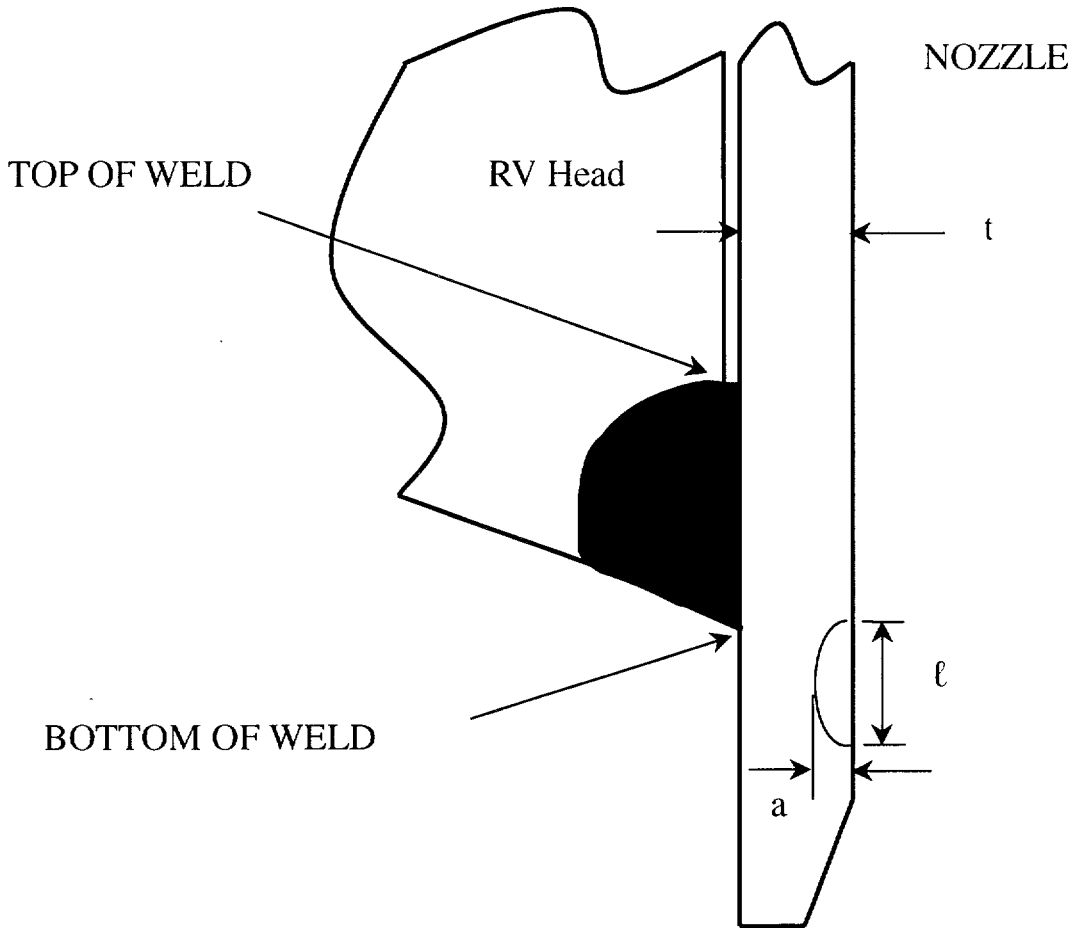

Figure 6-24 Schematic of Head Penetration Geometry

7 SUMMARY AND EXAMPLE PROBLEMS

An extensive evaluation has been carried out to characterize the loadings and stresses which exist in the head penetrations at Farley Units 1 and 2. Three-dimensional finite element models were constructed, and all pertinent loadings on the penetrations were analyzed [6]. These loadings included internal pressure and thermal expansion effects typical of steady state operation. In addition, residual stresses due to the welding of the penetrations to the vessel head were considered.

Results of the analyses reported here are consistent with the axial orientation and location of flaws which have been found in service in a number of plants and that the largest stress component is the hoop stress, and the maximum stresses were found to exist at the attachment weld. The most important loading conditions were found to be those which exist on the penetration for the majority of the time, which are the steady state loading and the residual stresses.

These stresses are important because the cracking which has been observed to date in operating plants has been determined to result from primary water stress corrosion cracking (PWSCC). These stresses were used in the fracture mechanics calculations to predict the future growth of flaws postulated to exist in the head penetrations. A crack growth law was developed specifically for the operating temperature of the vessel head at Farley Units 1 and 2 based on the EPRI recommendation, which is consistent with laboratory data as well as crack growth results for operating plants.

The crack growth predictions contained in Section 6 show that the future growth of cracks which might be found in the penetrations will be typically moderate, however, a number of effective full power years would be required for any significant extensions.

7.1 SAFETY ASSESSMENT

It is appropriate to examine the safety consequences of an indication which might be found. The indication, even if it were to propagate through the penetration nozzle wall, would have only minor consequences, since the pressure boundary would not be broken, unless it were to propagate above the weld.

Further propagation of the indication would not change its orientation, since the hoop stresses in the penetration nozzle are much larger than the axial stresses. Therefore, it is extremely unlikely that the head penetration would be severed.

If the indication were to propagate to a position above the weld, a leak could result, but the magnitude of such a leak would be very small, because the crack could not open significantly due to the tight fit between the penetration nozzle and the vessel head. Such a leak would have no immediate impact on the structural integrity of the system, but could lead to wastage in the ferritic steel of the vessel head, as the borated primary water concentrates due to evaporation. Davis Besse has demonstrated the consequence of ignoring such leaks.

Any indication is unlikely to propagate very far up the penetration nozzle above the weld, because the hoop stresses decrease in this direction, and this will cause it to slow down, and to stop before it reaches the outside surface of the head.

The high likelihood that the indication will not propagate up the penetration nozzle beyond the vessel head ensures that no catastrophic failure of the head penetration will occur, since the indication will be enveloped in the vessel head itself, which precludes the opening of the crack and limits leakage.

7.2 EXAMPLE PROBLEMS

The flaw tolerance charts in Figures 6-2 through 6-21 can be used with the acceptance criteria of Section 6.5 to determine the available service life. In this section, a few examples will be presented to illustrate the use of these figures. The example cases are listed in Table 7-1.

Example 1. For an axially oriented inside surface flaw located 1.2" below the weld and on the uphill side of penetration no. 30, the angle of this penetration must first be determined from Table 1-1. The angle for this penetration nozzle is 28.6 degrees. The crack growth curves of Figure 6-2 are applicable and Figure 6-2 has been reproduced as Figure 7-1. In this case, the initial flaw depth is 12.5 percent of the wall thickness. A straight line is then drawn horizontally at a/t=0.125 and intersecting the crack growth curve. Using the acceptance criteria in Table 6-1, the service life can then be determined as the remaining time for this flaw to grow to the limit of 100 percent of the wall thickness or approximately 3.5 years (labeled as Service Life in Figure 7-1). Assuming that the initial aspect ratio of 2.5:1 is maintained as the inside surface flaw becomes a through-wall flaw, the final length of the flaw is 1.5625 inch. The upper extremity of the flaw is now located 0.52 inch below the weld and validates the use of the crack growth curves of Figure 6-2.

Example 2. In this case, the flaw is identical in size to that used in Example 1, but located on the outside surface and on the uphill side of penetration no. 30. The applicable curve to use is Figure 6-8. Using the acceptance criteria in Table 6-1, the determination of service life is illustrated in Figure 7-2, where we can see that the result is approximately 2.1 years.

Example 3. The axial inside surface flaw is located at the weld and on the downhill side of penetration no. 62. From Table 1-1, the angle of this penetration nozzle is 42.6 degrees. The applicable curve is Figure 6-5 and used to determine the service life. In this case, the initial flaw depth is 7.5 percent of the wall thickness. Using the acceptance criteria in Table 6-1, the allowable service life can then be determined as the time for the flaw to reach a depth of 75 percent of the wall thickness by drawing a horizontal straight line at a/t=0.075 and intersecting the crack growth curve. As shown in Figure 7-3, the resulting service life is approximately 3.1 years.

Example 4. In this case, we have postulated an axial inside surface flaw that will require the use of two flaw charts for its evaluation because the upper extremity of this flaw will reach within 0.5 inch below the attachment weld as it propagates into the nozzle wall. The flaw has an initial depth of .078 inch and is located on the downhill side of penetration no. 30, which has an angle of 28.6 degrees. The length of the initial flaw is 0.394 inch long and its upper extremity is located 1.0 inch below the attachment weld. Assuming that the initial aspect ratio of 5:1 is maintained as the flaw propagates into the nozzle wall, the final length of a through-wall flaw would be 3.125 inches long. The location of the upper extremity of this flaw would have reached within 0.5 inch below the weld as it propagates into the nozzle wall.

For this postulated flaw, the first step is to estimate the time required for the initial flow to grow to within 0.5 inch of the weld. This can be accomplished with the use of Figure 6-3 and reproduced here as Figure

7-4A. The upper extremity of the flaw will grow to within 0.5 inch of the weld when its depth reaches 45 percent of the wall thickness and the required time to reach that size is estimated as 5.75 years in Figure 7-4A. The curves in Figure 6-5 for inside surface flaws near the weld is then used with the initial flaw depth being 45 percent of the wall thickness. Using the acceptance criteria in Table 6-1, Figure 7-4B shows an additional 0.7 year of service life for a total of 6.5 years.

Example 5. This case is an axial through-wall flaw with its upper extremity located 0.40 inches below the weld region on the uphill side of penetration no. 32. The angle of the penetration nozzle is 28.6 degrees as shown in Table 1-1. The crack growth curves of Figure 6-16 are applicable and Figure 6-16 has been reproduced as Figure 7-5. As illustrated in Figure 7-5, the service life is estimated to be approximately 2.3 years for the initial flaw to grow to the bottom of the attachment weld.

It is clear from these examples that the most important figures to use in evaluating the detected flaws in the head penetrations are Figures 6-2 through 6-9 for the axial surface flaws postulated on the CRDM nozzles. Figure 6-21 for axial surface flaws postulated on the head vent nozzle and Figure 6-19 for circumferential flaws postulated near the top of the attachment weld on the CRDM nozzles. The figures provided which project the growth of through-wall flaws are valuable, but may be of limited practical application with the current acceptance criteria. However, there is an important safety aspect to the through-wall flaw evaluation charts in that they demonstrate that flaw propagation above the weld will be very limited.

Several guidelines are important to understand when using these flaw evaluation charts.

1. If a flaw is found in a penetration nozzle for which no specific analysis was performed and there is a uniform trend as a function of penetration nozzle angle, interpolation between penetration nozzle is the best approach.

2. If a flaw is found in a penetration nozzle for which no specific analysis was performed and there is no apparent trend as a function of penetration nozzle angle, the result for the penetration nozzle with the closest angle should be used.

3. If a flaw is found which has a depth smaller than any depth shown for the penetration nozzle angle of interest, the initial flaw depth should be assumed to be the same as the smallest depth analyzed for that particular penetration nozzle.

Table 7-1 Example Problem Inputs: Initial Flaw Sizes and Locations

Example No.	Orientation	Vertical Location	Circumferential Location	Penetration Row	Length	Depth	Penetration No.	Source Figure
1	Axial - Inside Surface	1.2" Below Weld	Uphill	28.6°	0.197"	0.078"	30	6-2
2	Axial - Outside Surface	1.2" Below Weld	Uphill	28.6°	0.197"	0.078"	30	6-8
3	Axial - Inside Surface	At Weld	Downhill	42.6°	0.236"	0.047"	62	6-5
4	Axial - Inside Surface	1.0" Below Weld	Downhill	28.6°	0.394"	0.078"	30	6-3, 6-5
5	Axial Through-Wall	0.4" Below Weld	Uphill	28.6°	--	--	32	6-16

Example No.	Orientation	Vertical Location	Circumferential Location	Penetration Row	Length (2c)	Depth (a)	Wall Thickness (t)	a/t	Penetration No.	Source Figure
1	Axial - Inside Surface	1.2" Below Weld	Uphill	28.6°	0.197"	0.078"	0.625"	0.125	30	6-2

Table 1-1

Nozzle No.	Type	Angle (Degrees)
28	CRDM	27.0
29	CRDM	27.0
30	CRDM	28.6
31	CRDM	28.6
32	CRDM	28.6
33	CRDM	28.6

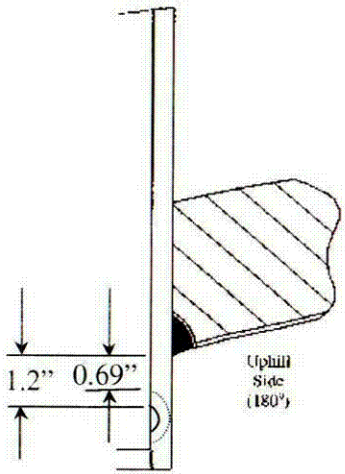

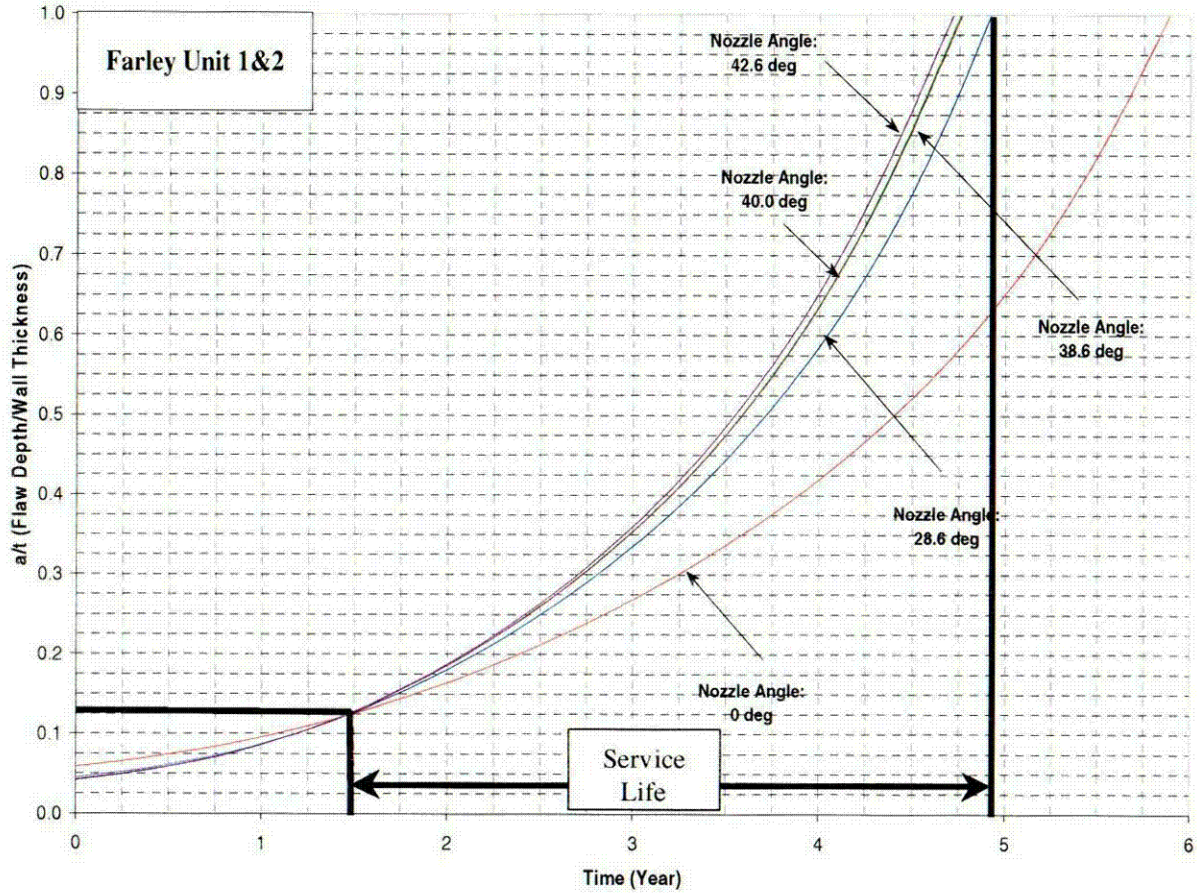

Figure 7-1 Example Problem 1

Example No.	Orientation	Vertical Location	Circumferential Location	Penetration Row	Length (2c)	Depth (a)	Wall Thickness (t)	a/t	Penetration No.	Source Figure
2	Axial - Outside Surface	1.2" Below Weld	Uphill	28.6°	0.197"	0.078"	0.625"	0.125	30	6-8

Table 1-1

Nozzle No.	Type	Angle (Degrees)
28	CRDM	27.0
29	CRDM	27.0
30	CRDM	28.6
31	CRDM	28.6
32	CRDM	28.6
33	CRDM	28.6

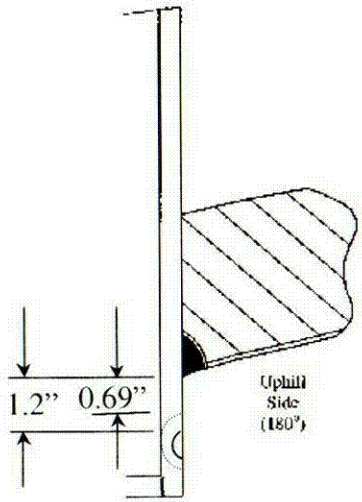

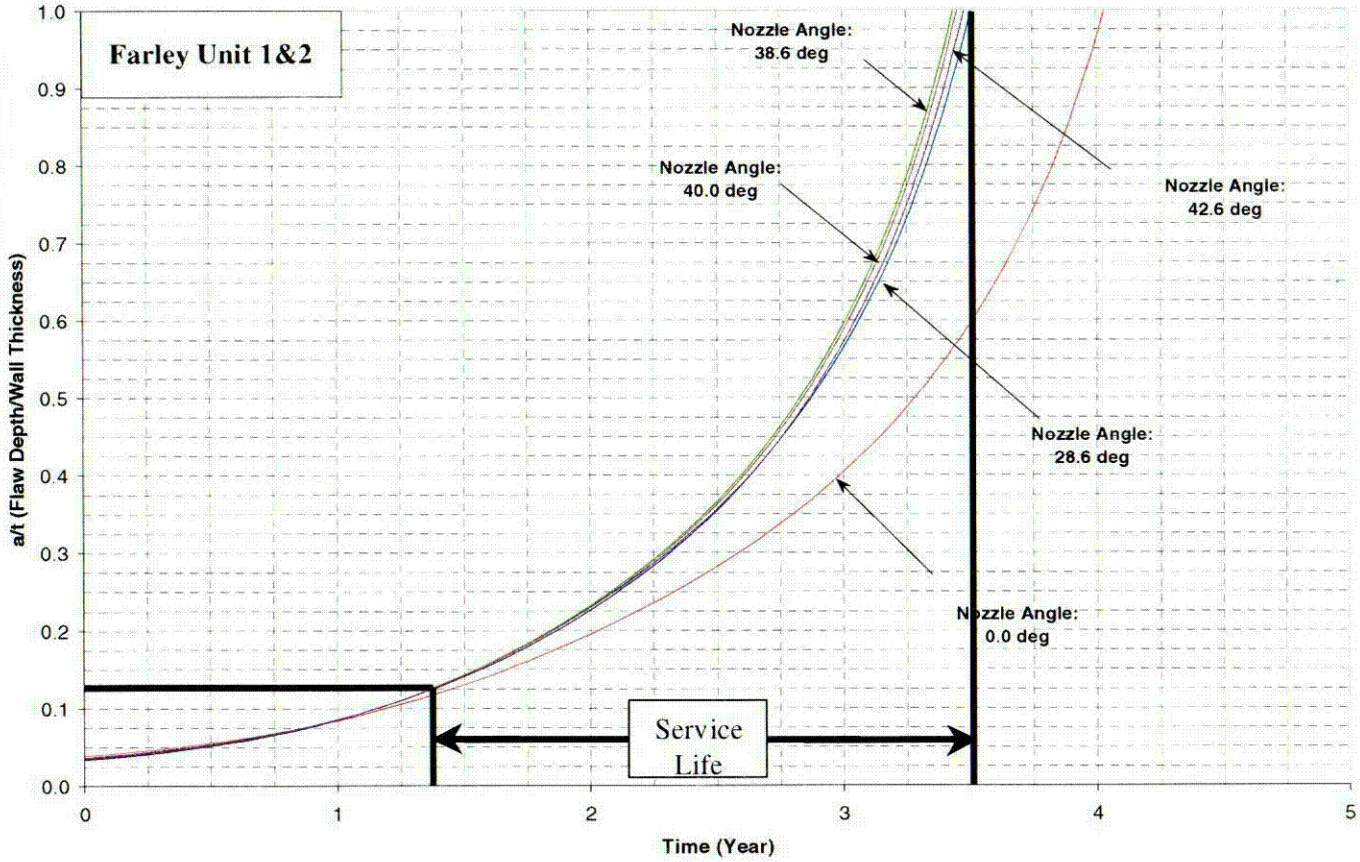

Figure 7-2 Example Problem 2

Example No.	Orientation	Vertical Location	Circumferential Location	Penetration Row	Length (2c)	Depth (a)	Wall Thickness (t)	a/t	Penetration No.	Source Figure
3	Axial - Inside Surface	At Weld	Downhill	42.6°	0.236"	0.047"	0.625"	0.075	62	6-5

Table 1-1

Nozzle No.	Type	Angle (Degrees)
60	CRDM	40.0
61	CRDM	40.0
62	CRDM	42.6
63	CRDM	42.6
64	CRDM	42.6

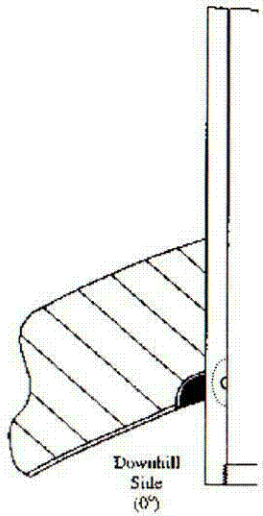

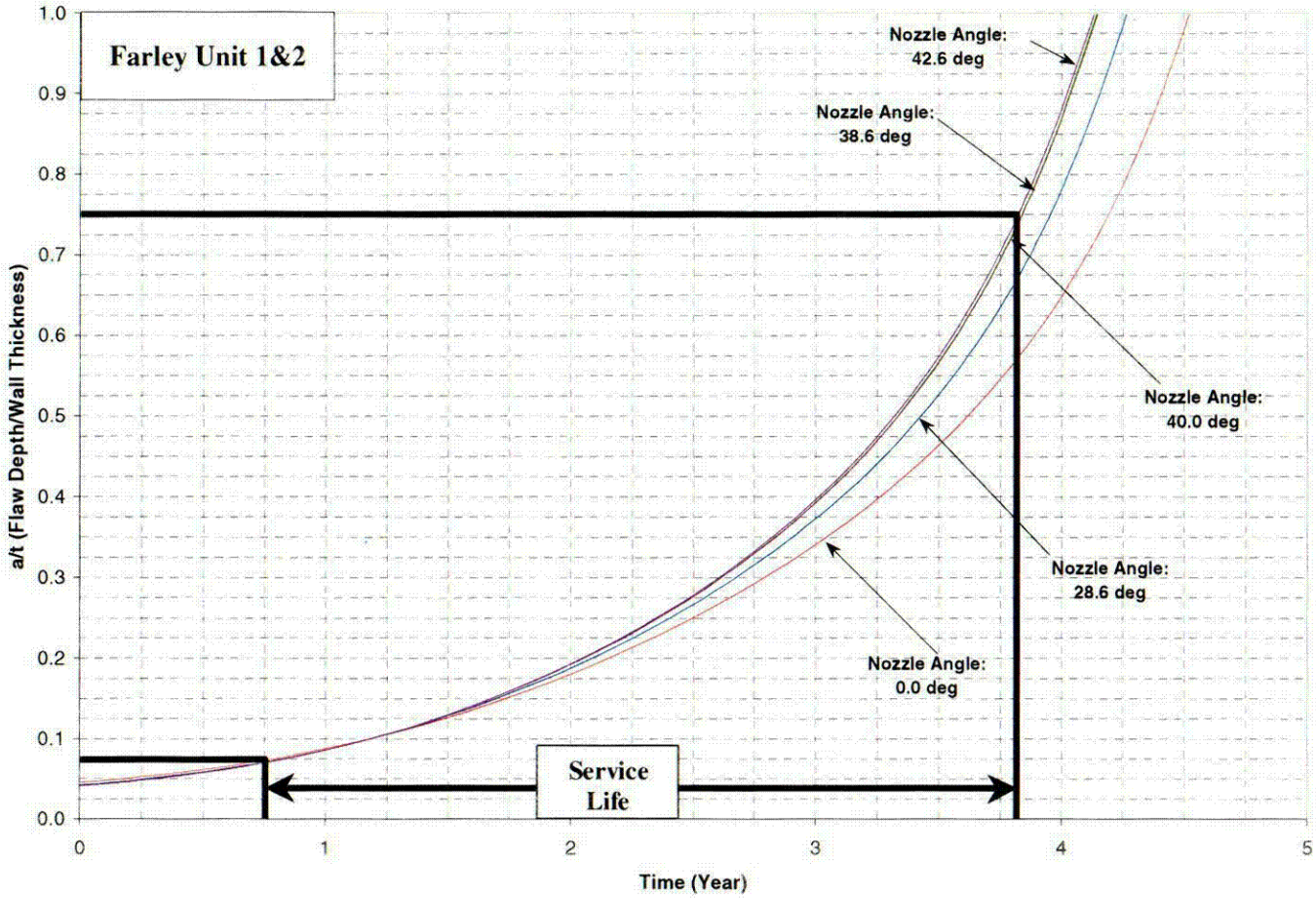

Figure 7-2 Example Problem 3

C21

Example No.	Orientation	Vertical Location	Circumferential Location	Penetration Row	Length (2c)	Depth (a)	Wall Thickness (t)	a/t	Penetration No.	Source Figure
4	Axial - Inside Surface	1.0" Below Weld	Downhill	28.6°	0.394"	0.078"	0.625"	0.125	30	6-3, 6-5

Table 1-1

Nozzle No.	Type	Angle (Degrees)
28	CRDM	27.0
29	CRDM	27.0
30	CRDM	28.6
31	CRDM	28.6
32	CRDM	28.6
33	CRDM	28.6

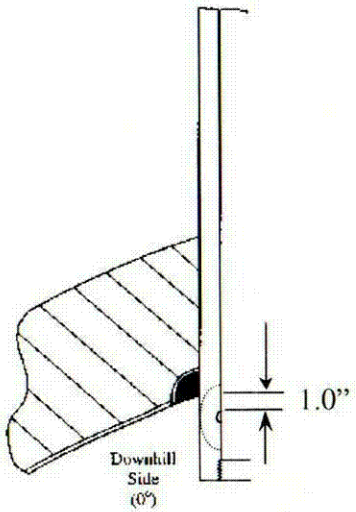

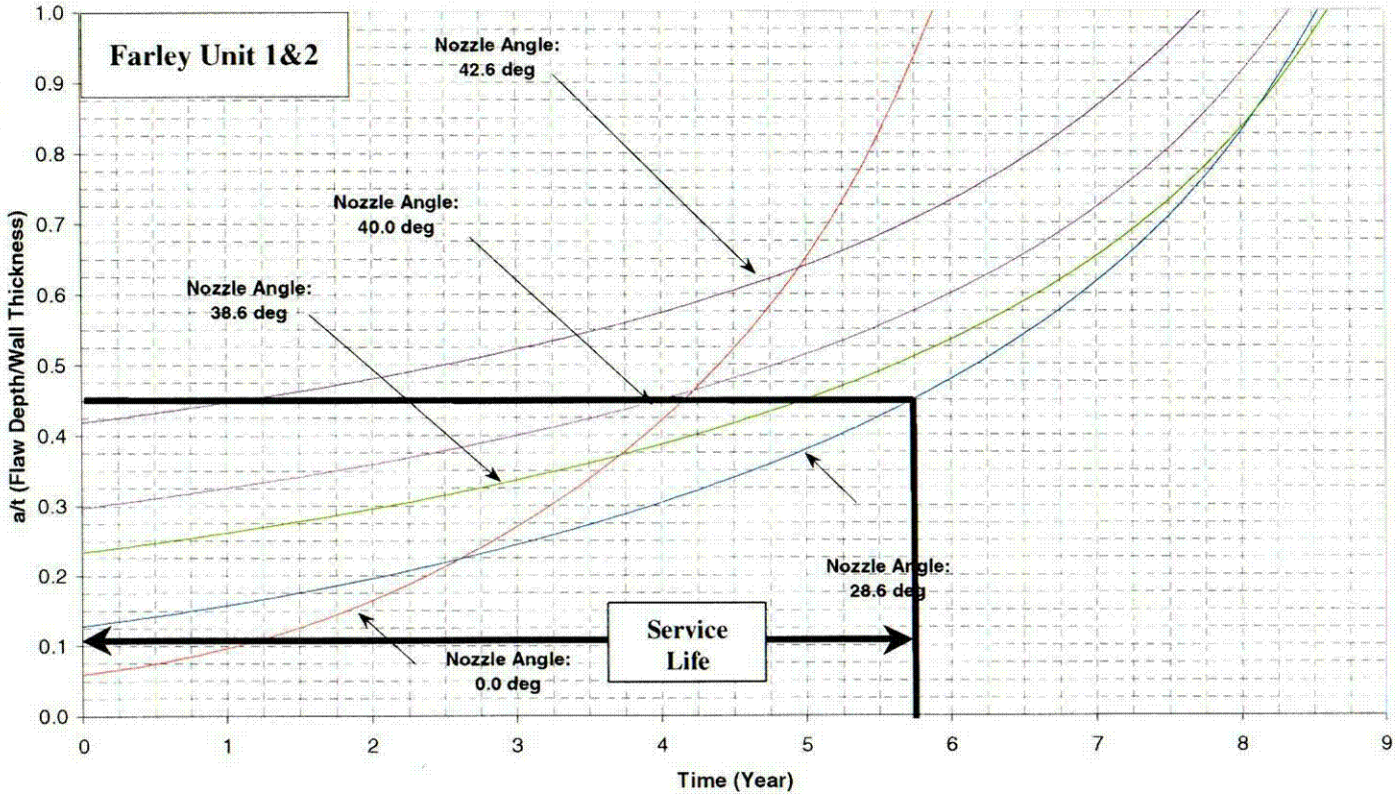

Figure 7-4A Example Problem 4 (See also Figure 7-4B)

Example No.	Orientation	Vertical Location	Circumferential Location	Penetration Row	Length (2c)	Depth (a)	Wall Thickness (t)	a/t	Penetration No.	Source Figure
4	Axial - Inside Surface	1.0" Below Weld	Downhill	28.6°	0.394"	0.078"	0.625"	0.125	30	6-3, 6-5

Table 1-1

Nozzle No.	Type	Angle (Degrees)
28	CRDM	27.0
29	CRDM	27.0
30	CRDM	28.6
31	CRDM	28.6
32	CRDM	28.6
33	CRDM	28.6

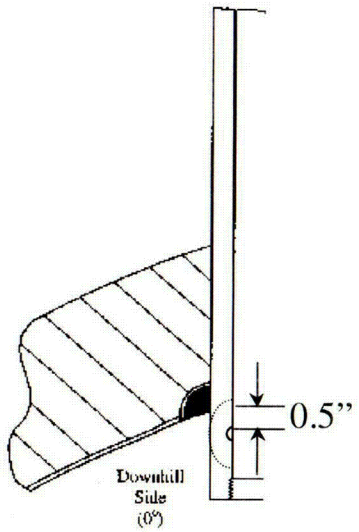

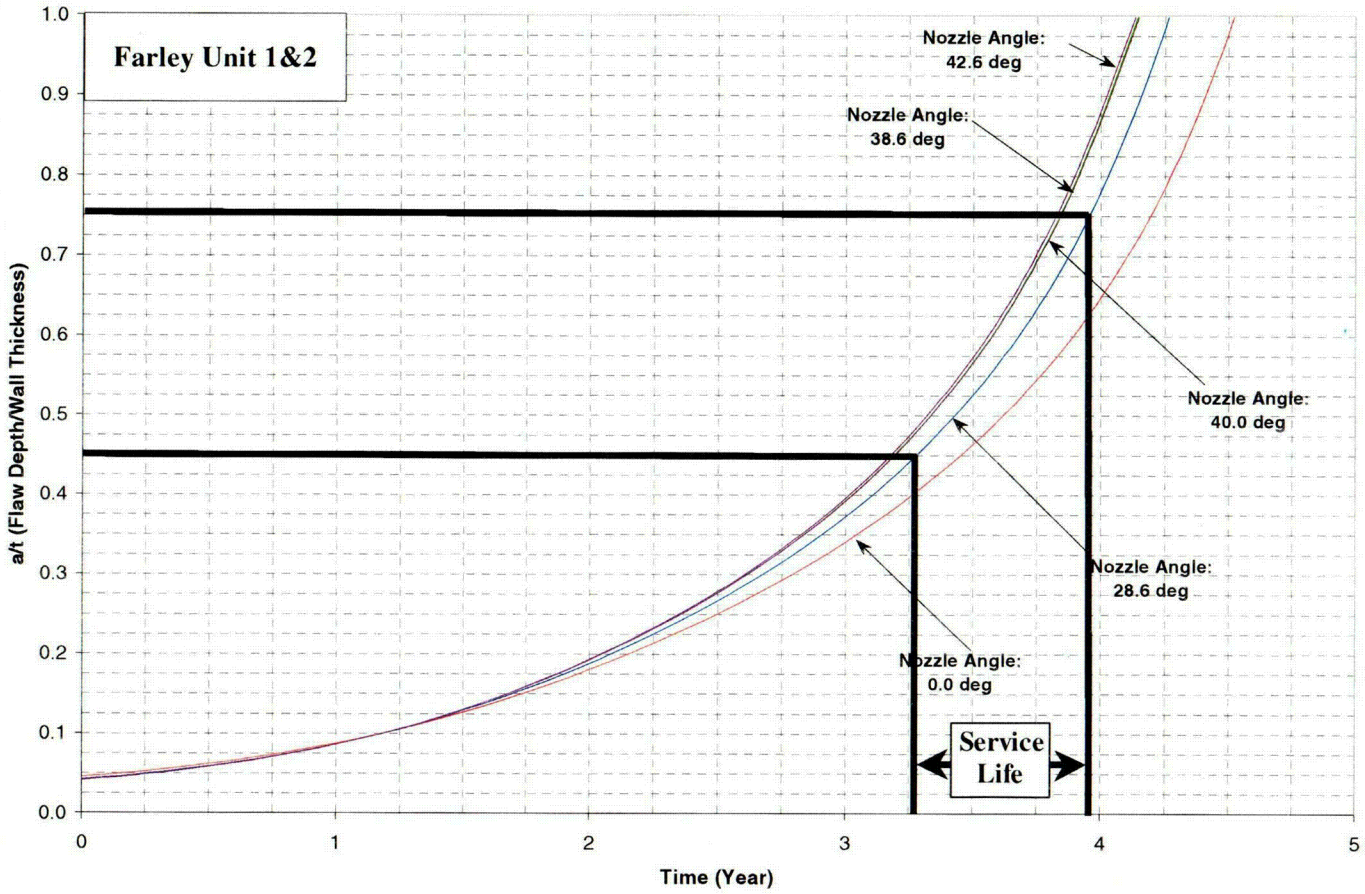

Figure 7-4B Example Problem 4 (See also Figure 7-4A)

C23

Example No.	Orientation	Vertical Location	Circumferential Location	Penetration Row	Length (2c)	Depth (a)	Penetration No.	Source Figure
5	Axial Through-Wall	0.4" Below Weld	Uphill	28.6°	--	--	32	6-16

Table 1-1

Nozzle No.	Type	Angle (Degrees)
28	CRDM	27.0
29	CRDM	27.0
30	CRDM	28.6
31	CRDM	28.6
32	CRDM	28.6
33	CRDM	28.6

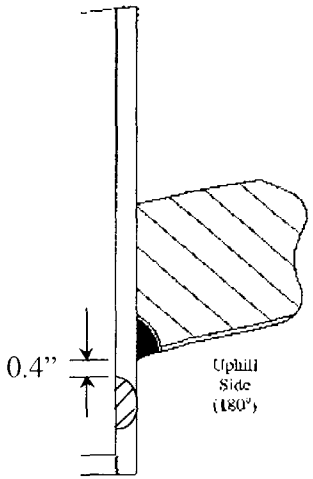

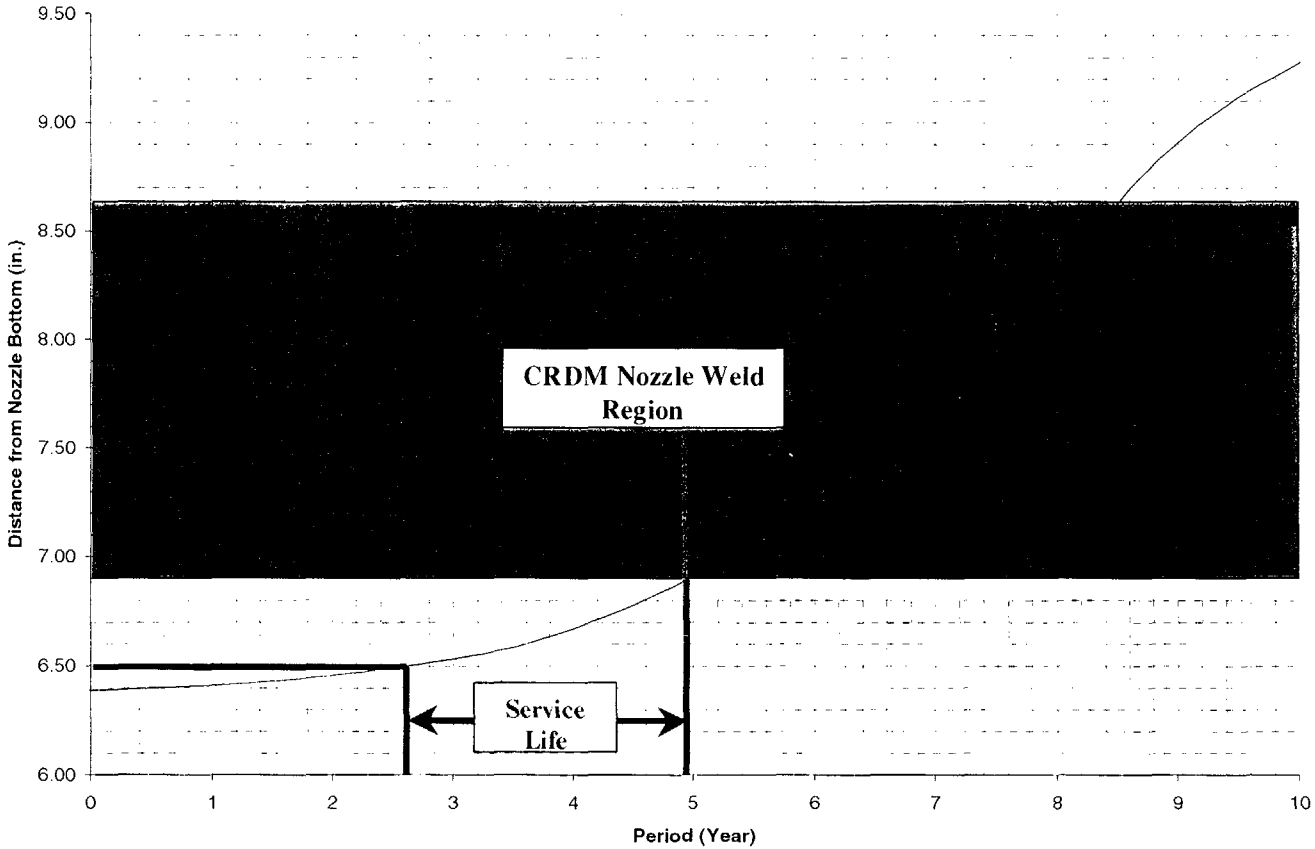

Figure 7-5 Example Problem 5

8 REFERENCES

1. Scott, P. M., "An Analysis of Primary Water Stress Corrosion Cracking in PWR Steam Generators," in Proceedings, Specialists Meeting on Operating Experience With Steam Generators, Brussels Belgium, Sept. 1991, pages 5, 6.

2. McIlree, A. R., Rebak, R. B., Smialowska, S., "Relationship of Stress Intensity to Crack Growth Rate of Alloy 600 in Primary Water," Proceedings International Symposium Fontevraud II, Vol, 1, p. 258-267, September 10-14, 1990.

3. Cassagne, T., Gelpi, A., "Measurements of Crack Propagation Rates on Alloy 600 Tubes in PWR Primary Water," in Proceedings of the 5th International Symposium on Environmental Degradation of Materials in Nuclear Power Systems-Water Reactors," August 25-29, 1991, Monterey, California.

4A. *Crack Growth and Microstructural Characterization of Alloy 600 PWR Vessel Head Penetration Materials,* EPRI, Palo Alto, CA. 1997. TR-109136.

4B. Vaillant, F. and C. Amzallag. "Crack Growth Rates of Alloy 600 in Primary Water," Presentation to the EPRI-MRP Crack Growth Rate (CGR) Review Team, Lake Tahoe, NV, presented August 10, 2001, and revised October 11, 2001

4C. Vaillant, F. and S. Le Hong. *Crack Growth Rate Measurements in Primary Water of Pressure Vessel Penetrations in Alloy 600 and Weld Metal 182,* EDF, April 1997. HT-44/96/024/A.

4D. Framatome laboratory data provided by C. Amzallag (EDF) to MRP Crack Growth Rate Review Team, October 4, 2001 (Proprietary to EDF).

4E. Cassagne, T., D. Caron, J. Daret, and Y. Lefevre. "Stress Corrosion Crack Growth Rate Measurements in Alloys 600 and 182 in Primary Water Loops Under Constant Load," *Ninth International Symposium on Environmental Degradation of Materials in Nuclear Power Systems-Water Reactors* (Newport Beach, CA, August 1-5, 1999), Edited by F. P. Ford, S. M. Bruemmer, and G. S. Was, The Minerals, Metals & Materials Society (TMS), Warrendale, PA, 1999.

4F. Studsvik laboratory data provided by Anders Jenssen (Studsvik) to MRP Crack Growth Rate Review Team, October 3, 2001 (Proprietary to Studsvik).

4G. [

]^{a,c,e}

4H. Materials Reliability Program (MRP) Crack Growth Rates for Evaluating Primary Water Stress Corrosion Cracking (PWSCC) of Thick Wall Alloy 600 Material," EPRI MRP Report MRP-55, May 30, 2002.

4I. "Crack Growth Rate Tests of Alloy 600 in Primary PWR Conditions," Communication from M. L. Castaño (CIEMAT) to J. Hickling (EPRI), March 25, 2002.

4J. G.:.mez-BriceZo, D., J. LapeZa, and F. Bl<zquez. "Crack Growth Rates in Vessel Head Penetration Materials." *Proceedings of the International Symposium Fontevraud III: Contribution of Materials Investigation to the Resolution of Problems Encountered in Pressurized Water Reactors* (Chinton, France, September 12-16, 1994), French Nuclear Energy Society, Paris, 1994, pp. 209-214.

4K. G.:.mez-BriceZo, D. and J. LapeZa. "Crack Growth Rates in Vessel Head Penetration Materials." *Proceedings: 1994 EPRI Workshop on PWSCC of Alloy 600 in PWRs* (Tampa, FL, November 15-17, 1994), EPRI, Palo Alto, CA, TR-105406, August 1995, pp. E4-1 through E4-15.

4L. G.:.mez-BriceZo, D., et al. "Crack Propagation in Inconel 600 Vessel Head Penetrations," Eurocorr 96, Nice, France, September 24-26, 1996.

4M. CastaZo, M. L., D. G.:.mez-BriceZo, M. Alvarez-de-Lara, F. Bl<zquez, M. S. Garcia, F. Hern<ndez, and A. Largares. "Effect of Cationic Resin Intrusions on IGA/SCC of Alloy 600 Under Primary Water Conditions," *Proceedings of the International Symposium Fontevraud IV: Contribution of Materials Investigation to the Resolution of Problems Encountered in Pressurized Water Reactors* (France, September 14-18, 1998), French Nuclear Energy Society, Paris, 1998, Volume 2, pp. 925-937.

5A. Newman, J. C. and Raju, I. S., "Stress Intensity Factor Influence Coefficients for Internal and External Surface Cracks in Cylindrical Vessels," in Aspects of Fracture Mechanics in Pressure Vessels and Piping, PVP Vol. 58, ASME, 1982, pp. 37-48.

5B. Hiser, Allen, "Deterministic and Probabilistic Assessments," presentation at NRC/Industry/ACRS meeting, November 8, 2001.

6. Fleming, Mark A., "Farley CRDM and Head Vent Stress Analysis," Dominion Engineering Inc. Calculation No. C-7744-02-1, Revision 0, July 2002.

7. USNRC Letter, W. T. Russell to W. Raisin, NUMARC, "Safety Evaluation for Potential Reactor Vessel Head Adapter Tube Cracking," November 19, 1993.

8. USNRC Letter, A. G. Hansen to R. E. Link, "Acceptance Criteria for Control Rod Drive Mechanism Penetrations at Point Beach Nuclear Plant, Unit 1," March 9, 1994.

9. Materials Reliability Program Response to NRC Bulletin 2001-01 EPRI MRP Report 48 (TP 1006284), August 2001.

10. Farley Plant Procedure FNP-1-STP-108 (Location of Upper Head Thermocouples)

11. Southern Company Email from Randy May to Mason Dove dated September 6, 2002 (Upper Head Fluid Temperature)

APPENDIX A

ALLOWABLE AREAS OF LACK OF FUSION: WELD FUSION ZONES

There are two fusion zones of interest for the head penetration nozzle attachment welds, the penetration nozzle itself (Alloy 600) and the reactor vessel head material (A533B ferritic steel). The operating temperature of the upper head region of the Farley Units 1 and 2 is 314°C (597°F) and the materials will be very ductile. The toughness of both materials is quite high and any flaw propagation along either of the fusion zones will be totally ductile.

Two calculations were completed for the fusion zones, one for the critical flaw size, and the second one for the allowable flaw size, which includes the margins required in the ASME code. The simpler case is the Alloy 600 fusion zone, where the potential failure will be a pure shearing of the penetration as the pressurized penetration nozzle is forced outward from the vessel head, as shown in Figure A-1.

The failure criterion will be that the average shear stress along the fusion line exceeds the limit shear stress. For the critical flaw size, the limiting shear stress is the shear flow stress, which is equal to half the tensile flow stress, according to the Tresca criterion. The tensile flow stress is the average of the yield stress and ultimate tensile stress of the material. The criterion for Alloy 600 tubes in the upper head region is:

$$\text{Average shear stress} < \text{shear flow stress} = 26.85 \text{ ksi}$$

This value was taken from the ASME Code, Section III, Appendix I, at 600°F.

For each penetration, the axial force which produces this shear stress results from the internal pressure. Since each penetration has the same outer diameter, the axial force is the same. The average shear stress increases as the load carrying area decreases (the area of lack of fusion increases). When this increasing lack of fusion area increases the stress to the point at which it equals the flow stress, failure occurs. This point may be termed the critical flaw size. This criterion is actually somewhat conservative. Alternatively, use of the Von Mises failure criterion would have set the shear flow stress equal to 60 percent of the axial flow stress, and would therefore have resulted in larger critical flaw sizes.

The allowable flaw size, as opposed to the critical flaw size discussed above, was calculated using the allowable limit of Section III of the ASME Code, paragraph NB 3227.2. The criterion for allowable shear stress then becomes:

$$\text{Average shear stress} < 0.6\ S_m = 13.98 \text{ ksi}$$

where S_m = the ASME Code limiting design stress from Section III, Appendix I.

The above approach was used to calculate the allowable flaw size and critical flaw size for the outermost and center penetrations. The results show that a very large area of lack of fusion can be tolerated by the head penetrations, regardless of their orientation. These results can be illustrated for the outermost CRDM penetration.

The total surface contact area for the fusion zone on the outermost head penetration is 17.4 in^2. The calculations above result in a required area to avoid failure of only 1.45 in^2, and using the ASME Code criteria, the area required is 2.79 in^2. These calculations show that as much as 83.9 percent of the weld may be unfused, and the code acceptance criteria can still be met.

To envision the extent of lack of fusion allowed, Figure A-2 was prepared. In this figure, the weld fusion region for the outermost penetration has been shown in an unwrapped, or developed view. The figure shows the extent of lack of fusion allowed in terms of limiting lengths for a range of circumferential lack of fusion. This figure shows that the allowable vertical length of lack of fusion for a full circumferential unfused region is 84 percent of the weld length. Conversely, for a region of lack of fusion extending the full vertical length of the weld, the circumferential extent is limited to 302 degrees. The extent of lack of fusion which would cause failure is labeled "critical" on this figure, and is even larger. The dimensions shown on this figure are based on an assumed rectangular area of lack of fusion.

The full extent of this allowable lack of fusion is shown in Figure A-3, where the axes have been expanded to show the full extent of the head penetration-weld fusion line. This figure shows that a very large area of lack of fusion is allowed for the outer most penetration. Similar results were found for the center penetration, where the weld fusion area is somewhat smaller at 16.1 in^2.

A similar calculation was also carried out for the fusion zone between the weld and the vessel head, and the result is shown in Figure A-4. The allowable area of unfused weld for this location is 84.8 percent of the total area. This approach to evaluating the fusion zone with the carbon steel vessel head is only approximate, but may provide a realistic estimate of the allowable. Note that even a complete lack of fusion in this region would not result in penetration nozzle ejection, because the weld to the head penetration would prevent the penetration nozzle from moving up through the vessel head.

The allowable lack of fusion for the weld fusion zone to the vessel head using the approximate approach may be somewhat in doubt, because of the different geometry, where one cannot ensure that the failure would be due to pure shear. To investigate this concern, additional finite element models were constructed with various degrees of lack of fusion discretely modeled, ranging from 30 to 65 percent. The stress intensities around the circumference of the penetration were calculated to provide for the effects of all the stresses, as opposed to the shear stress only, as used above. When the average stress intensity reaches the flow stress (53.7 ksi), failure is expected to occur. The code allowable stress intensity is 1.5 S_m, or 35 ksi, using the lower of the Alloy 600 and ferritic allowables at 316°C (600°F).

The results of this series of analyses are shown in Figure A-5, where it is clear that large areas of lack of fusion are allowed. As the area of lack of fusion increases, the stresses redistribute themselves, and that the stress intensity does not increase in proportion to the area lost. These results seem to confirm that shear stress is the only important stress governing the critical flaw size for the vessel head fusion zone as well.

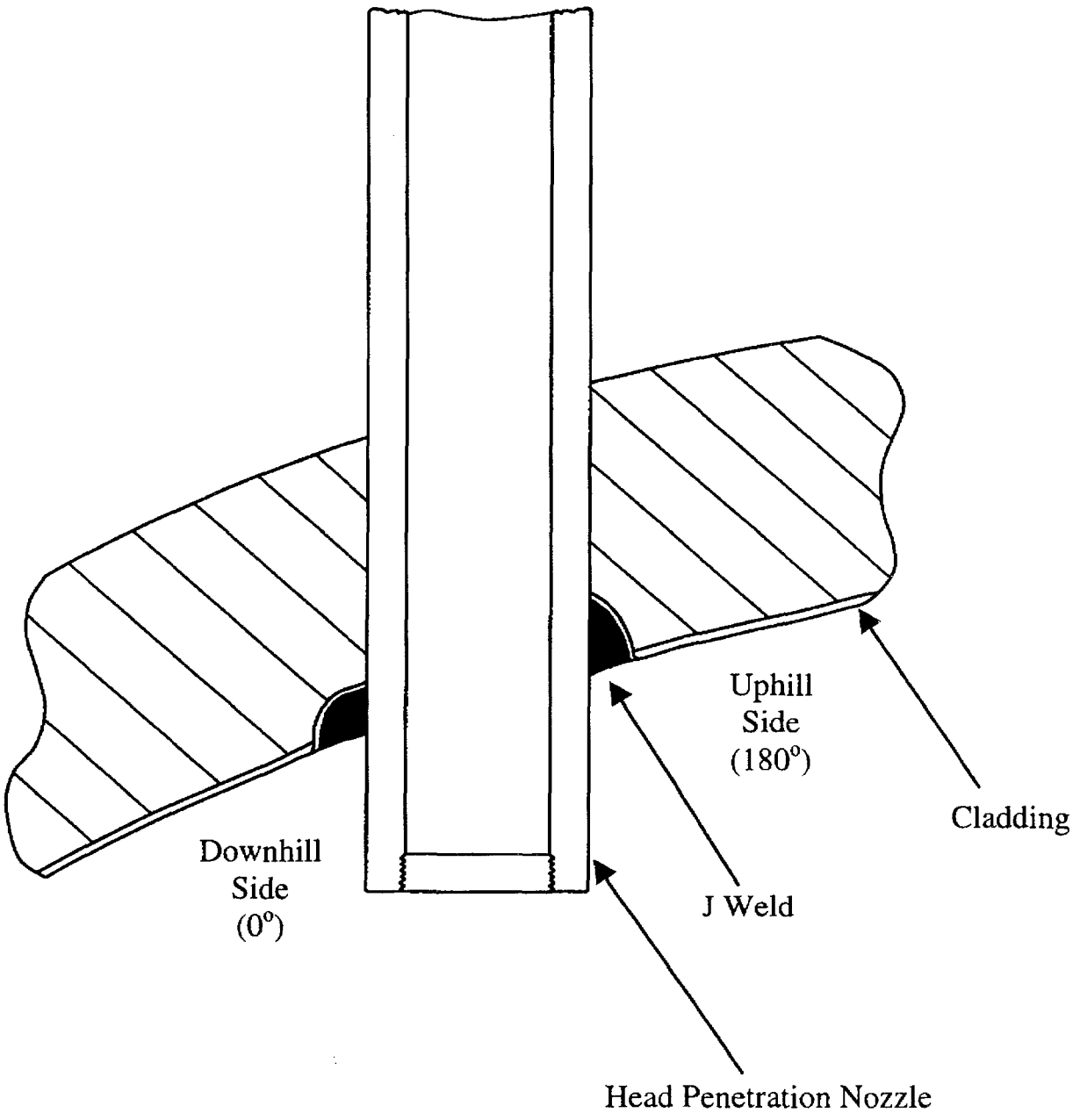

Figure A-1 Typical Head Penetration

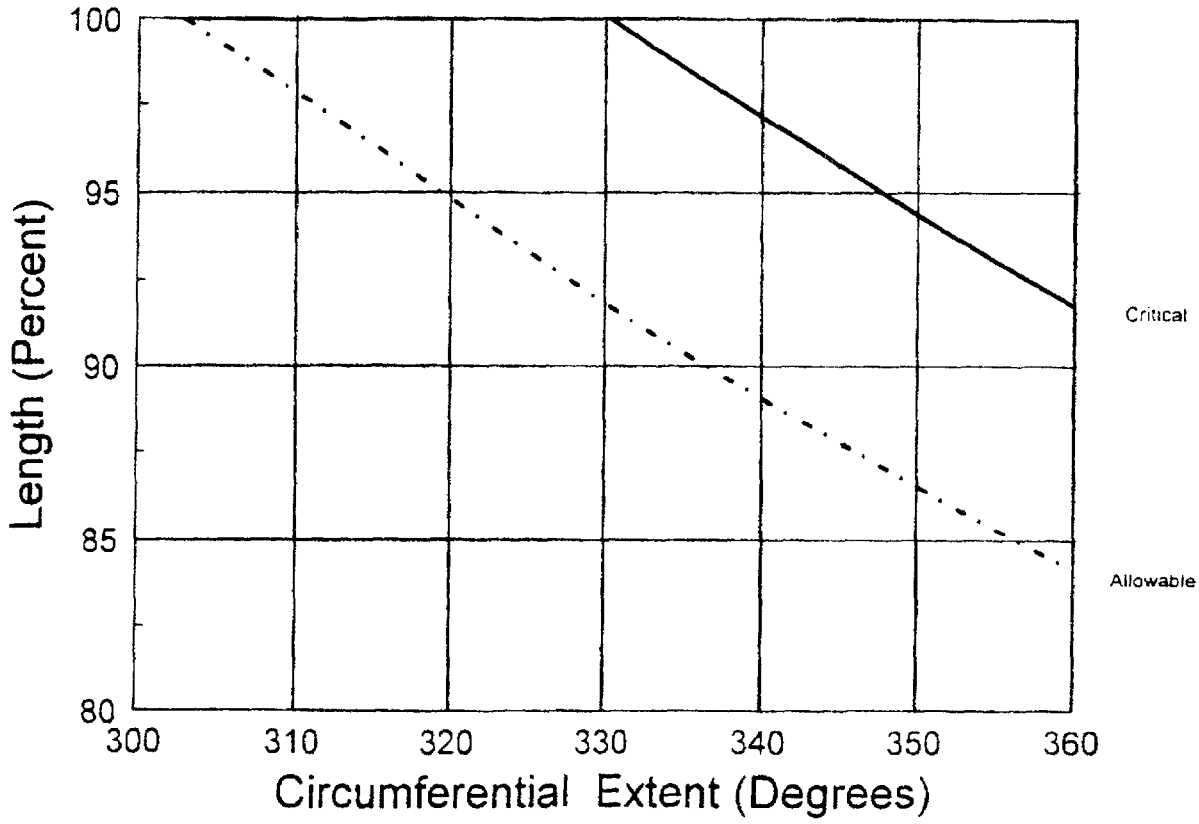

Figure A-2 **Allowable Regions of Lack of Fusion for the Outermost Penetration Tube to Weld Fusion Zone: Detailed View**

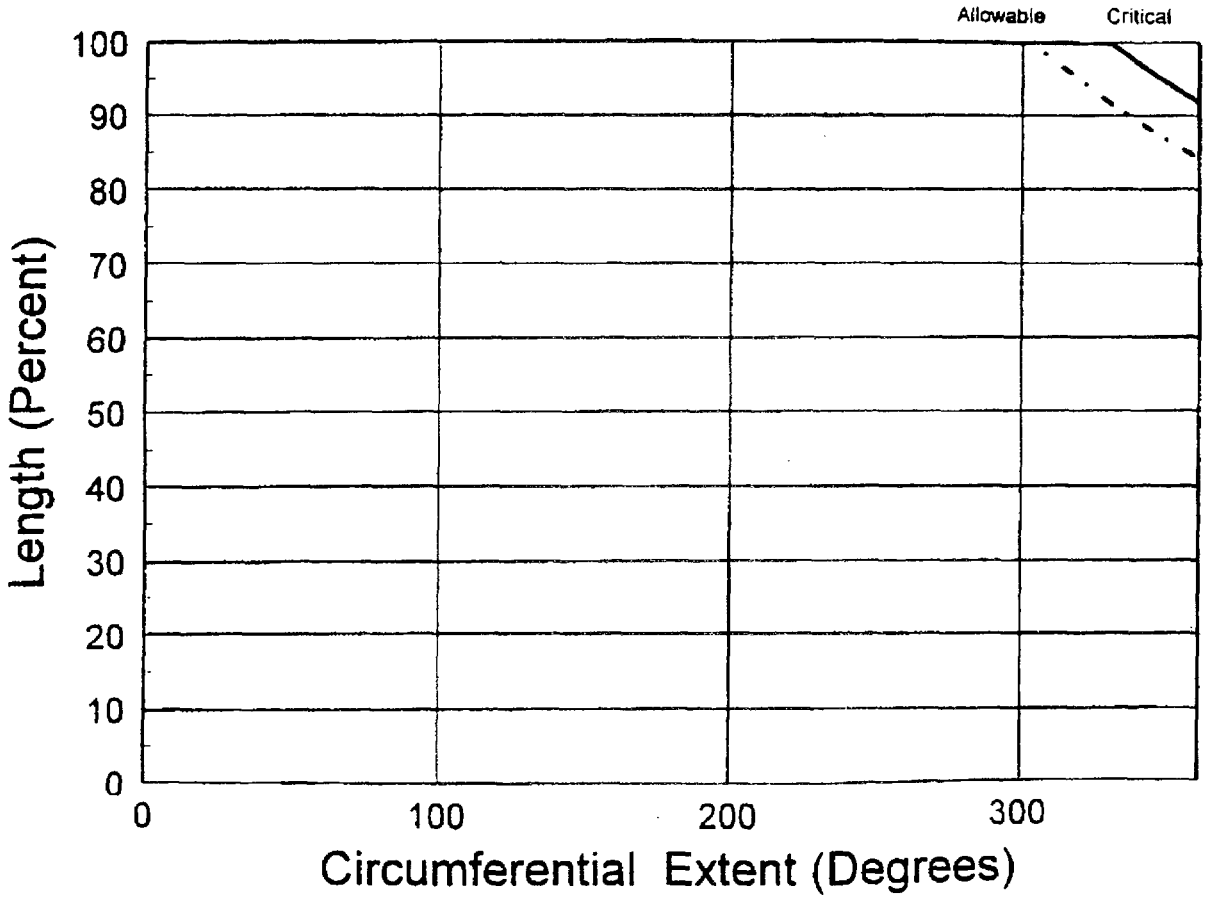

Figure A-3 Allowable Regions of Lack of Fusion for the Outermost Penetration Tube to Weld Fusion Zone

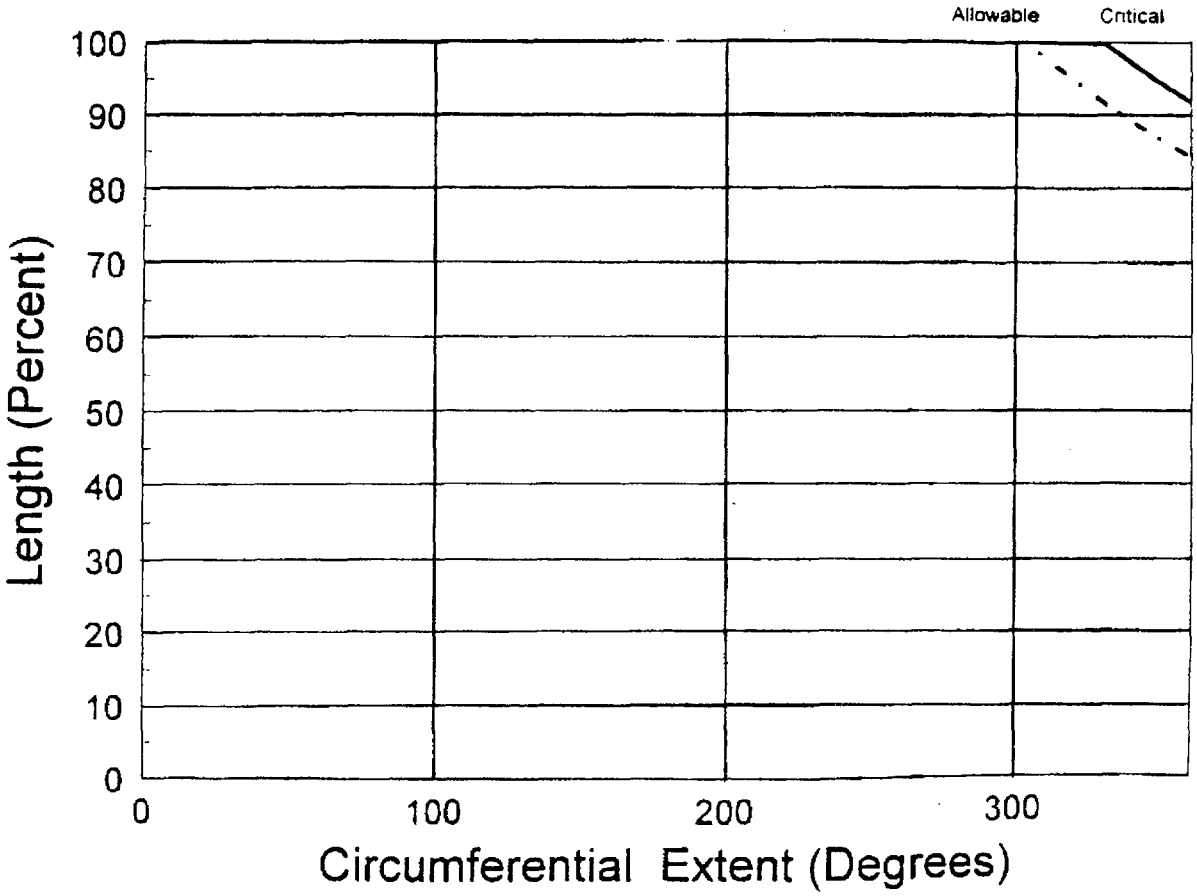

Figure A-4 Allowable Regions of Lack of Fusion for all Penetrations: Weld to Vessel Fusion Zone

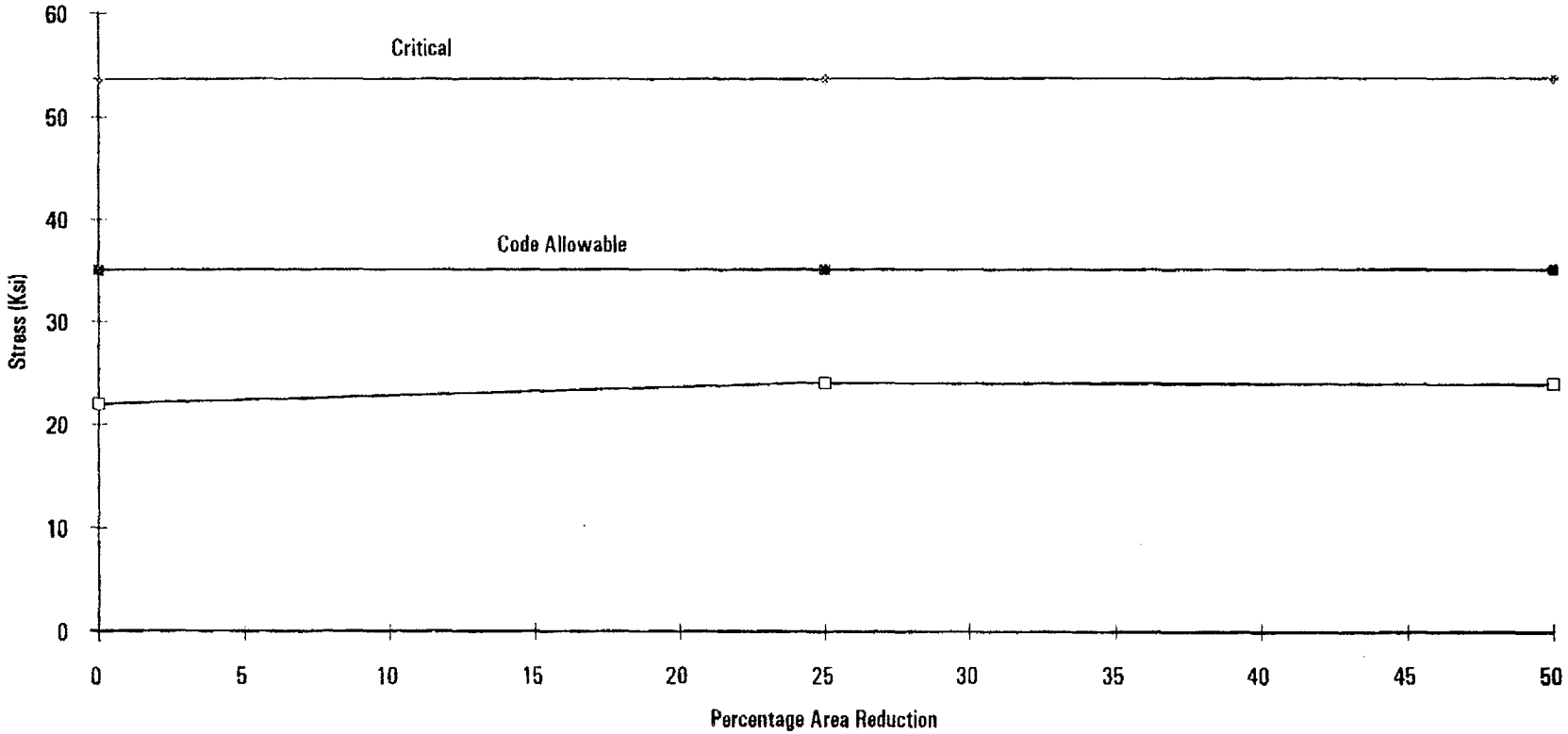

Figure A-5 Allowable Regions of Lack of Fusion for the Weld to Vessel Fusion Zone

Enclosure 4

Joseph M. Farley Nuclear Plant

Westinghouse Authorization Letter, CAW-03-1620, Affidavit, Proprietary Information Notice, and Copyright Notice

Westinghouse Electric Company
Nuclear Services
P.O. Box 355
Pittsburgh, Pennsylvania 15230-0355
USA

U.S. Nuclear Regulatory Commission
Document Control Desk
Washington, DC 20555-0001

Direct tel: (412) 374-5282
Direct fax: (412) 374-4011
e-mail: Sepp1ha@westinghouse.com

Attention: Mr. Samuel J. Collins

Our ref: CAW-03-1620

April 8, 2003

APPLICATION FOR WITHHOLDING PROPRIETARY INFORMATION FROM PUBLIC DISCLOSURE

Subject: WCAP-15925-P, "Structural Integrity Evaluation of Reactor Vessel Upper Head Penetrations to Support Continued Operation: - Farley Units 1 and 2" (Proprietary)

The proprietary information for which withholding is being requested in the above-referenced report is further identified in Affidavit CAW-03-1620 signed by the owner of the proprietary information, Westinghouse Electric Company LLC. The affidavit, which accompanies this letter, sets forth the basis on which the information may be withheld from public disclosure by the Commission and addresses with specificity the considerations listed in paragraph (b)(4) of 10 CFR Section 2.790 of the Commission's regulations.

Accordingly, this letter authorizes the utilization of the accompanying affidavit by Southern Nuclear Company.

Correspondence with respect to the proprietary aspects of the application for withholding or the Westinghouse affidavit should reference this letter, CAW-03-1620 and should be addressed to the undersigned.

Very truly yours,

H. A. Sepp, Manager
Regulatory and Licensing Engineering

Enclosures

cc: S. J. Collins
G. Shukla/NRR

bcc: H. A. Sepp (ECE 4-7A) 1L, 1A
R. Bastien, 1L, 1A (Nivelles, Belgium)
L. Ulloa (Madrid, Spain) 1L, 1A
C. Brinkman, 1L, 1A (Westinghouse Electric Co., 12300 Twinbrook Parkway, Suite 330, Rockville, MD 20852)
RLE Administrative Aide (ECE 4-7A) 1L, 1A (letters w/affidavits only)

CAW-03-1620

AFFIDAVIT

COMMONWEALTH OF PENNSYLVANIA:

ss

COUNTY OF ALLEGHENY:

Before me, the undersigned authority, personally appeared H. A. Sepp, who, being by me duly sworn according to law, deposes and says that he is authorized to execute this Affidavit on behalf of Westinghouse Electric Company LLC ("Westinghouse"), and that the averments of fact set forth in this Affidavit are true and correct to the best of his knowledge, information, and belief:

H. A. Sepp, Manager
Regulatory and Licensing Engineering

Sworn to and subscribed
before me this 8th day
of April, 2003

Sharon L. Fiori
Notary Public

SHARON L. FIORI
COMMONWEALTH OF PENNSYLVANIA
NOTARY PUBLIC

Notarial Seal
Sharon L. Fiori, Notary Public
Monroeville Boro, Allegheny County
My Commission Expires January 29, 2007
Member, Pennsylvania Association Of Notaries

(1) I am Manager, Regulatory and Licensing Engineering, in Nuclear Services, Westinghouse Electric Company LLC ("Westinghouse"), and as such, I have been specifically delegated the function of reviewing the proprietary information sought to be withheld from public disclosure in connection with nuclear power plant licensing and rule making proceedings, and am authorized to apply for its withholding on behalf of the Westinghouse Electric Company LLC.

(2) I am making this Affidavit in conformance with the provisions of 10 CFR Section 2.790 of the Commission's regulations and in conjunction with the Westinghouse application for withholding accompanying this Affidavit.

(3) I have personal knowledge of the criteria and procedures utilized by the Westinghouse Electric Company LLC in designating information as a trade secret, privileged or as confidential commercial or financial information.

(4) Pursuant to the provisions of paragraph (b)(4) of Section 2.790 of the Commission's regulations, the following is furnished for consideration by the Commission in determining whether the information sought to be withheld from public disclosure should be withheld.

(i) The information sought to be withheld from public disclosure is owned and has been held in confidence by Westinghouse.

(ii) The information is of a type customarily held in confidence by Westinghouse and not customarily disclosed to the public. Westinghouse has a rational basis for determining the types of information customarily held in confidence by it and, in that connection, utilizes a system to determine when and whether to hold certain types of information in confidence. The application of that system and the substance of that system constitutes Westinghouse policy and provides the rational basis required.

Under that system, information is held in confidence if it falls in one or more of several types, the release of which might result in the loss of an existing or potential competitive advantage, as follows:

(a) The information reveals the distinguishing aspects of a process (or component, structure, tool, method, etc.) where prevention of its use by any of

Westinghouse's competitors without license from Westinghouse constitutes a competitive economic advantage over other companies.

(b) It consists of supporting data, including test data, relative to a process (or component, structure, tool, method, etc.), the application of which data secures a competitive economic advantage, e.g., by optimization or improved marketability.

(c) Its use by a competitor would reduce his expenditure of resources or improve his competitive position in the design, manufacture, shipment, installation, assurance of quality, or licensing a similar product.

(d) It reveals cost or price information, production capacities, budget levels, or commercial strategies of Westinghouse, its customers or suppliers.

(e) It reveals aspects of past, present, or future Westinghouse or customer funded development plans and programs of potential commercial value to Westinghouse.

(f) It contains patentable ideas, for which patent protection may be desirable.

There are sound policy reasons behind the Westinghouse system which include the following:

(a) The use of such information by Westinghouse gives Westinghouse a competitive advantage over its competitors. It is, therefore, withheld from disclosure to protect the Westinghouse competitive position.

(b) It is information that is marketable in many ways. The extent to which such information is available to competitors diminishes the Westinghouse ability to sell products and services involving the use of the information.

(c) Use by our competitor would put Westinghouse at a competitive disadvantage by reducing his expenditure of resources at our expense.

(d) Each component of proprietary information pertinent to a particular competitive advantage is potentially as valuable as the total competitive advantage. If competitors acquire components of proprietary information, any one component may be the key to the entire puzzle, thereby depriving Westinghouse of a competitive advantage.

(e) Unrestricted disclosure would jeopardize the position of prominence of Westinghouse in the world market, and thereby give a market advantage to the competition of those countries.

(f) The Westinghouse capacity to invest corporate assets in research and development depends upon the success in obtaining and maintaining a competitive advantage.

(iii) The information is being transmitted to the Commission in confidence and, under the provisions of 10 CFR Section 2.790, it is to be received in confidence by the Commission.

(iv) The information sought to be protected is not available in public sources or available information has not been previously employed in the same original manner or method to the best of our knowledge and belief.

(v) The proprietary information sought to be withheld in this submittal is that which is appropriately marked in WCAP-15925-P, "Structural Integrity Evaluation of Reactor Vessel Upper Head Penetrations to Support Continued Operation: - Farley Units 1 and 2" (Proprietary), dated September 2002 , being transmitted by the Southern Nuclear Company letter and Application for Withholding Proprietary Information from Public Disclosure, to the Document Control Desk. The proprietary information as submitted for use by Southern Nuclear Company for Farley Units 1 and 2 is expected to be applicable for other licensee submittals in response to certain NRC requirements for justification of continued safe operation of Farley Units 1 and 2.

This information is part of that which will enable Westinghouse to:

(a) Determine the appropriate course of action in the event that indications of degradation are observed in Alloy 600 penetrations in the reactor vessel head.

(b) Develop a justification for continued safe operation.

(c) Assist the customer in obtaining NRC approval.

Further this information has substantial commercial value as follows:

(a) Westinghouse plans to sell the use of similar information to its customers for purposes of meeting NRC requirements for licensing documentation.

(b) Westinghouse can sell support and defense of continued safe operation.

(c) The information requested to be withheld reveals the distinguishing aspects of a methodology which was developed by Westinghouse.

Public disclosure of this proprietary information is likely to cause substantial harm to the competitive position of Westinghouse because it would enhance the ability of competitors to provide similar supporting documentation and licensing defense services for commercial power reactors without commensurate expenses. Also, public disclosure of the information would enable others to use the information to meet NRC requirements for licensing documentation without purchasing the right to use the information.

The development of the technology described in part by the information is the result of applying the results of many years of experience in an intensive Westinghouse effort and the expenditure of a considerable sum of money.

In order for competitors of Westinghouse to duplicate this information, similar technical programs would have to be performed and a significant manpower effort, having the requisite talent and experience, would have to be expended.

Further the deponent sayeth not.